



Norwegian University of  
Science and Technology

# Evaluation of Cyanobacteria Removal in an Integrated Process of Electroflotation and Rapid Filtration Using Plastic Filter Media

Vivian Palani

Civil and Environmental Engineering

Submission date: March 2019

Supervisor: Thomas Meyn, IBM

Co-supervisor: Maurício Luiz Sens, Universidade Federal de Santa Catarina

Norwegian University of Science and Technology

Department of Civil and Environmental Engineering

*(This page is left blank intentionally)*

## Abstract

Cyanobacteria is one of the Earth's oldest oxygen-producing organisms and can be found in a variety of water bodies. The main problem associated with cyanobacteria is their ability to release cyanotoxins that may cause damages to the liver, the neuromuscular system and the skin. In the water treatment plant located near Lake Peri in Florianopolis (Brazil), high cyanobacteria levels are causing high energy demands due to frequently required backwashing, resulting in high sludge production. In addition, there is a risk of cyanotoxins being released and ending up in the water distribution system. As cyanobacteria are often light, flotation technologies are a good substitute for sedimentation basins. Within flotation technologies, electroflotation (EF) has proved to be a promising alternative due to simplicity of operation and its ability to generate small bubbles. In this study, a pilot plant with an integrated system of electroflotation using dimensionally stable anodes (DSA<sup>®</sup>) followed by rapid filtration with polyvinyl chloride (PVC) spheres as filter media was used to evaluate the performance on cyanobacteria removal from the water of Lake Peri. Its' performance on turbidity and colour removal was also evaluated. Different electrical current densities were used to identify the optimal removal rate. NaCl was used to improve the electrical conductivity of raw water. For the highest current density applied, the polarity was inverted to avoid further corrosion on the DSA<sup>®</sup>s. The results gave the highest cyanobacteria removal rate of 92,3% at a current density of 89,2 A/m<sup>2</sup> after EF. With regards to cyanobacteria removal, the filtration step did not contribute significantly. The maximal cyanobacteria removal rate after the integrated process was 96,7%. Corrosion on the DSA<sup>®</sup> was shown to have a large impact on the results, among other effects, it increased the turbidity and partly affected the flotation performance. The turbidity increased less during polarity inversion and high amounts of chlorine was generated. The filter removed up to 76,4% of the turbidity relative to the values after EF. However, the integrated process as a whole did not remove a significantly large amount of turbidity, the highest removal rate being 52%. Although EF was shown to be efficient in the removal of cyanobacteria, the turbidity increase, thought to be caused by the corrosion, is crucial as the cyanobacteria can be retained in the particles. Regarding PVC spheres used as filter media, the need for long backwash duration resulted in a non-cost-effective solution.

**Keywords:** Electroflotation, Cyanobacteria, Dimensionally stable anodes, Corrosion, Chlorine, Filtration, Polyvinyl chloride

*(This page is left blank intentionally)*

## Sammendrag

Cyanobakterier er en av jordens eldste oksygenproduserende organismer og finnes i en rekke vann. Hovedproblemet forbundet med cyanobakterier er deres evne til å frigjøre cyanotoksiner som kan forårsake skader på leveren, det nevromuskulære systemet og huden. I vannbehandlingsanlegget i nærheten av innsjøen Peri i Florianopolis (Brasil) forårsaker høye cyanobakterienivåer høye energibehov grunnet ofte nødvendig filterspyling, noe som resulterer i høy slamproduksjon. I tillegg er det fare for at cyanotoksiner slippes ut og ender opp i vandistribusjonssystemet. Siden cyanobakterier ofte er lette, er flotasjonsteknologier en god erstatning for sedimenteringsbassenger. Innen flotasjonsteknologier har elektroflotasjon (EF) vist seg å være et lovende alternativ på grunn av enkel drift og evne til å generere små bobler. I denne studien ble et pilotanlegg med et integrert system med elektroflotering ved hjelp av dimensjonelt stabile anoder (DSA<sup>®</sup>) etterfulgt av filtrering med polyvinylklorid (PVC) kuler som filter materiale brukt til å evaluere ytelsen ved fjerning av cyanobakterier fra vannet fra innsjøen Peri. Pilotens ytelse på fjerning av turbiditet og farge ble også evaluert. Forskjellige elektriske strømtettheter ble brukt til å identifisere optimal fjerningsgrad. NaCl ble brukt til å forbedre konduktiviteten av råvannet. For den høyeste strømtettheten som ble påført, ble polariteten invertert for å unngå ytterligere korrosjon av DSA<sup>®</sup>-ene. Resultatene ga høyest reduksjon av cyanobakterier på 92,3% med en strømtetthet på 89,2 A / m<sup>2</sup> etter EF. Med hensyn til fjerning av cyanobakterier bidro ikke filtrering betydelig. Maksimal reduksjon av cyanobakterier etter den integrerte prosessen var på 96,7%. Korrosjon på DSA<sup>®</sup> ble påvist å ha stor innvirkning på resultatene, blant annet ved å økte turbiditeten og delvis påvirke flotasjonsytelsen. Turbiditeten økte mindre da polariteten var invertert og store mengder klor ble generert. Filteret fjernet opptil 76,4% av turbiditeten i forhold til verdiene etter EF. Imidlertid fjernet den integrerte prosessen som helhet ikke en signifikant stor mengde turbiditet, da den høyeste reduksjonen var på 52%. Selv om EF ble påvist å være effektivt ved fjerning av cyanobakterier, er turbiditetsøkningen, som antas å være forårsaket av korrosjonen, avgjørende da cyanobakteriene kan knytte seg til partiklene. Når det gjelder PVC-kuler som brukes som filter materiale, resulterte behovet for lang filterspylingstid i en ikke-kostnadseffektiv løsning.

**Nøkkelord:** Elektroflotasjon, Cyanobakterier, Dimensjonalt stabile anoder, Korrosjon, Klor, Filtrering, Polyvinylklorid

*(This page is left blank intentionally)*

## Resumo

As cianobactérias estão entre os organismos produtores de oxigênio mais antigos da Terra, e podem ser encontradas em diversos corpos d'água. O principal problema associado às cianobactérias é a liberação de cianotoxinas que podem causar lesões no fígado, no sistema neuromuscular e na pele. Na planta de tratamento localizada próximo à Lagoa do Peri, em Florianópolis, o alto nível de cianobactérias tem causado um excesso de demanda de energia – necessária para retrolavagem -, resultando numa alta produção de resíduos. Além disso, há o risco de as cianotoxinas serem liberadas na água e seguirem para o sistema de distribuição. Como cianobactérias são leves, processos de flotação são uma boa alternativa às bacias de sedimentação. Dentre as tecnologias de flotação, a eletroflotação (EF) tem se mostrado promissora por gerar pequenas bolhas e ser de fácil operação. Nesse estudo, uma planta piloto com um sistema integrado de eletroflotação utilizando ânodos dimensionalmente estáveis (DSA<sup>®</sup>) seguido por filtração rápida com esferas de policloreto de vinil (PVC) foi utilizada para avaliar a performance da remoção de cianobactérias de água da Lagoa do Peri. A performance na remoção de cor e turbidez também foi avaliada. Diferentes densidades de corrente foram testadas para identificar qual propiciava um maior índice de remoção. NaCl foi adicionado para melhorar a condutividade da água. Para a maior densidade de corrente aplicada, a polaridade foi invertida para evitar corrosão nos DSA<sup>®</sup>s. Os resultados mostraram a maior taxa de remoção de cianobactérias sendo 92,3% numa densidade de corrente de 89,2 A/m<sup>2</sup> após a EF. Concernente à remoção de cianobactérias, a filtração não contribuiu significativamente. A taxa máxima de remoção de cianobactérias após o processo inteiro foi 96,7%. A corrosão no DSA<sup>®</sup> impactou os resultados significativamente, aumentando a turbidez e inibindo parcialmente a flotação. A turbidez aumentou menos quando a polaridade estava invertida e um alto nível de cloro foi gerado. O filtro removeu até 76,4% da turbidez em relação aos valores após a EF. No entanto, o processo como um todo não reduziu a turbidez significativamente, com taxa máxima 52%. Apesar de a eletroflotação ter se mostrado eficiente na remoção de cianobactérias, o aumento na turbidez (provavelmente causado por corrosão) é um fator crucial, pois as cianobactérias podem ser retidas nas partículas. Quanto ao uso das esferas de PVC como filtro, a necessidade de longa retrolavagem acarretou em um baixo custo-benefício.

**Palavras-chaves:** Eletroflotação, Cianobactéria, Ânodos dimensionalmente estáveis, Corrosão, Cloro, Filtração, Policloreto de vinil

*(This page is left blank intentionally)*

## Acknowledgements

Firstly, I would like to thank my supervisor professor Thomas Meyn and professor Sveinung Sægrov from the Department of Civil and Environmental Engineering at NTNU, who made this journey in Brazil possible. Thank you for believing in me and for putting in the effort to facilitate the process. I would like to thank my co-supervisor professor Maurício Luiz Sens from the Department of Sanitary and Environmental Engineering at UFSC for giving me the opportunity to write my thesis under his supervision in Brazil.

To Thyara Campos Martins Nonato and Tiago Burgardt at UFSC, for their enormous amount of guidance and patience throughout this period. The finalization of this project was in great parts thanks to you. A huge thank you to Willian for helping me collect water and all the fun conversations we had while doing so.

To my dear friends Shian and Frida, for your patience with me throughout my thesis and generally in life. I am forever grateful for your encouragement whenever I try something different. To Kristina, for calming me during the stressful periods.

There simply is not enough room to thank this next person, who has been with me throughout this whole project. Rodrigo, thank you for the immense amount of help and support you provided me with from the beginning to the end of this journey. I am eternally grateful the coincidences of life made you a part of mine. My memories of Brazil will forever include you.

To my family, for everything.

Deu tudo certo.

Florianopolis 5<sup>th</sup> of March 2019



---

Vivian Palani

*(This page is left blank intentionally)*

# Table of Content

<b>1</b>	<b>INTRODUCTION .....</b>	<b>1</b>
1.1	Background.....	1
1.2	Lagoa do Peri.....	2
1.3	Thesis description.....	5
<b>2</b>	<b>LITERATURE REVIEW .....</b>	<b>7</b>
<b>2.1</b>	<b>Cyanobacteria.....</b>	<b>7</b>
2.1.1	Cyanotoxins.....	8
2.1.1.1	Hepatotoxins.....	8
2.1.1.1.1	<i>Microcystin</i> .....	8
2.1.1.1.2	<i>Nodularins</i> .....	9
2.1.1.1.3	<i>Cylindrospermopsin</i> .....	9
2.1.1.2	Neurotoxins .....	9
2.1.1.2.1	<i>Anatoxin-a</i> .....	10
2.1.1.2.2	<i>Anatoxin-a(s)</i> .....	10
2.1.1.2.3	<i>Saxitoxins</i> .....	10
2.1.1.2.4	<i><math>\beta</math>-N-methylamino-L-alanine</i> .....	11
2.1.1.3	Dermatotoxins .....	11
2.1.2	Taste and odour compounds.....	11
2.1.3	Harmful cyanobacteria blooms and their challenges .....	12
2.1.4	Conventional treatment methods.....	12
2.1.4.1	Inlet.....	13
2.1.4.2	Effect of pre-treatment on cyanobacteria and cyanotoxins.....	13
2.1.4.3	Effect of particle separation treatment.....	14
2.1.4.3.1	<i>Effect of coagulation-flocculation-sedimentation</i> .....	14
2.1.4.3.2	<i>Effect of filtration</i> .....	14
2.1.4.3.3	<i>Effect of activated carbon</i> .....	15
2.1.4.4	Effect of degradation treatments.....	16
<b>2.2</b>	<b>Flotation processes .....</b>	<b>16</b>
2.2.1	Theory of flotation .....	17
2.2.2	Electrochemical treatment methods .....	19
2.2.3	Electroflotation.....	20
2.2.3.1	Electroflotation reactor.....	22
2.2.3.1.1	<i>Electrode materials</i> .....	22
2.2.3.1.2	<i>Electrode arrangement</i> .....	24
2.2.3.1.3	<i>Reactor design</i> .....	27
2.2.3.2	Variables.....	29
2.2.3.2.1	<i>Effect of pH</i> .....	30
2.2.3.2.2	<i>Effect of temperature</i> .....	30
2.2.3.2.3	<i>Effect of conductivity</i> .....	31
2.2.3.2.4	<i>Effect of inter-electrode spacing</i> .....	31
2.2.3.2.5	<i>Effect of current density</i> .....	31
2.2.3.2.6	<i>Electrode deactivation, passivation and polarity inversion</i> .....	32
2.2.3.2.7	<i>Energy consumption</i> .....	33

2.2.3.3	Gas volume and bubble/particle ratio .....	34
2.2.3.4	Particle charge .....	35
2.2.3.5	Advantages and disadvantages of electroflotation .....	35
2.2.3.6	Application of EF .....	36
<b>2.3</b>	<b>Filtration .....</b>	<b>37</b>
2.3.1	Rapid filtration .....	38
2.3.1.1	Classifications of rapid filtration .....	38
2.3.1.2	Filtration stage .....	39
2.3.1.3	Clean bed head loss .....	40
2.3.2	Filter media .....	43
2.3.2.1	Grain size and distribution .....	44
2.3.2.2	Grain shape .....	44
2.3.2.3	Grain density and hardness .....	45
2.3.2.4	Specific surface area and filter porosity .....	45
2.3.2.5	Arrangement of filter media .....	46
2.3.3	Filtration backwash .....	47
2.3.3.1	Factors determining the frequency of backwash .....	47
2.3.3.2	Mechanism .....	48
2.3.3.3	Backwash rate and filter bed expansion .....	49
2.3.4	Process challenges with filtration .....	51
2.3.4.1	Chemical treatment .....	51
2.3.4.2	Control of filter flow rate .....	51
2.3.4.3	Problems related to backwashing .....	52
2.3.4.3.1	<i>Mudball formation</i> .....	52
2.3.4.3.2	<i>Shrinkage of filter</i> .....	52
2.3.4.3.3	<i>Gravel displacement</i> .....	52
2.3.4.4	Media loss .....	53
2.3.4.5	Air binding .....	53
2.3.5	Plastic grains used as filter media .....	53
<b>3</b>	<b>METHODOLOGY .....</b>	<b>55</b>
<b>3.1</b>	<b>Raw water collection .....</b>	<b>55</b>
<b>3.2</b>	<b>Pilot system .....</b>	<b>55</b>
3.2.1	Electrochemical reactor .....	57
3.2.2	Filtration .....	57
<b>3.3</b>	<b>Experimental procedure .....</b>	<b>59</b>
3.3.1	Experiments .....	59
3.3.1.1	Addition of salt .....	60
3.3.1.2	Sample collection and measurements .....	61
3.3.1.3	Water column height, head losses and effluent rate .....	61
3.3.1.4	Fotoslugde removal and filter backwash .....	62
3.3.2	Additional experiments and measurements .....	62
3.3.2.1	Retention time and sample outtake .....	63
3.3.2.2	Polarity inversion .....	63
<b>3.4</b>	<b>Analysis .....</b>	<b>64</b>
3.4.1	Parameters .....	64

3.4.2	Cyanobacteria cell count .....	65
3.4.3	Removal rate .....	66
<b>4</b>	<b>RESULTS AND DISCUSSION .....</b>	<b>69</b>
<b>4.1</b>	<b>Electroflotation performance .....</b>	<b>69</b>
4.1.1	Parameters after electroflotation .....	69
4.1.1.1	Turbidity .....	69
4.1.1.2	Colour .....	76
4.1.1.3	pH, conductivity, temperature and free/total chlorine .....	78
4.1.2	Removal of cyanobacteria .....	81
4.1.3	Effect of retention time and sample outtake .....	84
4.1.4	Effect of polarity inversion .....	86
4.1.4.1	Free and total chlorine .....	86
4.1.4.2	Separation capacity .....	88
4.1.5	Cost of operation .....	90
<b>4.2</b>	<b>Integrated process .....</b>	<b>90</b>
4.2.1	Parameters after filtration .....	91
4.2.1.1	Turbidity .....	91
4.2.1.2	Colour .....	95
4.2.2	Removal of cyanobacteria .....	97
4.2.3	Water column height and head losses .....	99
4.2.4	Effluent rate .....	102
4.2.5	Filter backwash .....	103
<b>4.3</b>	<b>Challenges with conducting the experiments .....</b>	<b>105</b>
<b>5</b>	<b>CONCLUSION .....</b>	<b>107</b>
<b>6</b>	<b>REFERENCES .....</b>	<b>109</b>

**APPENDIX A – Parameters**

**APPENDIX B – Cyanobacteria cell density**

**APPENDIX C – Water column height, piezometer and effluent rate**

**APPENDIX D – Backwash turbidity**

## List of tables

Table 2.1: Comparison of slow sand filtration and rapid filtration design criteria* .....	38
Table 3.1: Depth of piezometers .....	59
Table 3.2: Overview of experiments conducted.....	60
Table 3.3: Overview of experiments for polarity comparison .....	64
Table 3.4: Overview of analysis conducted .....	65
Table 4.1: Average removal rate of experiments .....	83

## List of Figures

Figure 1.1: General location of Lake Peri .....	3
Figure 1.2: Detailed location of the water treatment plant at Lake Peri .....	4
Figure 2.1: Bubble-particle collision mechanisms: a) inertia, b) gravity, c) interception and d) Brownian diffusion.....	17
Figure 2.2: Schematic illustration of the formation of TPCL. ....	18
Figure 2.3: Classification of electrochemical treatment methods. ....	20
Figure 2.4: Conventional electrode arrangement. ....	25
Figure 2.5: Vertical electrodes arrangement .....	26
Figure 2.6: Open electrodes arrangement .....	26
Figure 2.7: Alternative open electrodes arrangement .....	27
Figure 2.8: Single-stage EF with a horizontal flow .....	28
Figure 2.9: Single-stage EF with a vertical flow.....	28
Figure 2.10: Single-stage EF with a contacting chamber and a separation chamber.....	28
Figure 2.11: Two-stage electroflotation .....	29
Figure 2.12: Head loss versus time during filtration.....	40
Figure 2.13: Effluent turbidity versus time during filtration.....	40
Figure 2.14: Effect of filtration rate, media size and bed porosity on clean bed head loss.....	43
Figure 3.1: Schematic of pilot.....	56
Figure 3.2 Electrode set up seen from the side (left) and above (right). ....	57
Figure 3.3 Total filter column (left) and two layers of gravel support (right) .....	58
Figure 4.1: Turbidity level after EF .....	70
Figure 4.2: Turbidity removal rates after EF.....	71
Figure 4.3: Corrosion on the anodes after Experiment 6 .....	72
Figure 4.4: Proposed schematic on the deactivation mechanism of Ti/RuO <sub>2</sub> -IrO <sub>2</sub> -TiO <sub>2</sub> .....	73
Figure 4.5: Turbidity and colour removal from a previous study (a) Removal rates (b) Turbidity and colour level .....	73
Figure 4.6: Sludge accumulation in Experiment 4 (left) and 6 (right).....	75
Figure 4.7: Floccs trapped in the electrochemical reactor. From Experiment 5 .....	76
Figure 4.8: Colour level after EF .....	77
Figure 4.9: Colour removal rates after EF.....	78
Figure 4.10: pH (left) and conductivity (right) after EF .....	79

Figure 4.11: Temperature after EF .....	80
Figure 4.12: Cyanobacteria cell density after EF .....	81
Figure 4.13: Cyanobacteria removal rates after EF.....	82
Figure 4.14: Cyanobacteria removal in previous study.....	83
Figure 4.15: Turbidity and colour level without flux through filter without salt.....	85
Figure 4.16: Turbidity and colour level without flux through filter with NaCl.....	85
Figure 4.17: Comparison of total chlorine from Experiment I (left) and Experiment II (right) .....	87
Figure 4.18: Comparison of sludge after Experiment I after 60 min. (left) and Experiment II after 25 min. (right) .....	88
Figure 4.19: Comparison of sludge after Experiment I after 60 min. (left) and Experiment II after 25 min. (right) .....	88
Figure 4.20: Turbidity level (left) and colour level (right) .....	89
Figure 4.21: Cyanobacteria cell density (left) and removal rate (right).....	89
Figure 4.22: Turbidity removal rate from filtration relative to EF.....	92
Figure 4.23: Overall turbidity level after integrated process .....	93
Figure 4.24: Overall turbidity removal rates after integrated process.....	93
Figure 4.25: Retained particles in filter after Experiment 4.....	94
Figure 4.26: Colour removal rate after filtration relative to EF .....	95
Figure 4.27: Overall colour level after integrated process .....	96
Figure 4.28: Overall colour removal rate after integrated process.....	96
Figure 4.29: Overall cyanobacteria cell density after integrated process .....	97
Figure 4.30: Overall cyanobacteria removal rates after integrated process .....	98
Figure 4.31: Average cyanobacteria removal rates after EF and integrated process .....	99
Figure 4.32: Change in water column height .....	100
Figure 4.33: Head loss in piezometers .....	101
Figure 4.34: Effluent rate of experiments .....	102
Figure 4.35: Turbidity backwash .....	103
Figure 4.36: Accumulated sand and particles in the intersection between PVC spheres and gravel after Experiment 6.....	104
Figure 4.37: Start of filter backwash (left) and end of filter backwash (right). .....	105

## Abbreviations

<b>2-MIB/MIB</b>	2-methylisoborneol
<b>ANTX-a</b>	Anatoxin-a
<b>ANTX-a(s)</b>	Anatoxin-a(s)
<b>APHA</b>	American Public Health Association
<b>APT</b>	Aplysiatoxin
<b>AWWA</b>	American Water Works Association
<b>BMAA</b>	$\beta$ -N-methylamino-L-alanine
<b>CASAN</b>	Companhia Catarinense de Águas e Saneamento
<b>CD</b>	Current density
<b>CyanoHAB</b>	Harmful cyanobacteria bloom
<b>CYL</b>	Cylindrospermopsin
<b>DAF</b>	Dissolved air flotation
<b>DSA<sup>®</sup></b>	Dimensionally Stable Anodes
<b>EC</b>	Electrocoagulation
<b>ED</b>	Electrodesinfection
<b>EF</b>	Electroflotation
<b>EO</b>	Electrooxidation
<b>FTC</b>	Free and total chlorine
<b>IBM</b>	Institutt for Bygg- og Miljøteknikk
<b>LAPOA</b>	Laboratório de Potabilização das Águas
<b>LTX</b>	Lyngyatoxin
<b>MC</b>	Microcystin
<b>NOD</b>	Nodularin
<b>PVC</b>	Polyvinyl chloride
<b>STX</b>	Saxitoxin
<b>TPCL</b>	Three-phase contact line
<b>UFSC</b>	Universidade Federal de Santa Catarina

## Symbols

$\mu$	Dynamic viscosity of fluid, kg/m s
$A_{\text{anode}}$	Area of cross-section of current direction, m <sup>2</sup>
$C_0$	Concentration in raw water
$CD$	Current density, A/m <sup>2</sup>
$C_t$	Concentration in treated water after hour t
$C_t^{\text{EF}}$	Concentration after EF after hour t
$C_t^{\text{F}}$	Concentration after filtration after hour t
$d$	Media grain diameter, m
$ES$	Effective size, dimensionless
$F$	Faraday's constant, 96 500 C/mol
$g$	Acceleration due to gravity, 9,81 m/s <sup>2</sup>
$h_L$	Head loss across media bed, m
$I$	Electric current, A
$k_p$	Hydraulic permeability, m/s
$L$	Depth of granular media, m
$L_E$	Depth of expanded bed, m
$L_F$	Depth of bed at rest (fixed bed), m
$n_{\text{H/O}}$	Electron transfer number for the respective reactions of H <sub>2</sub> and O <sub>2</sub>
$Q_{\text{H/O}}$	Gas generation rate for H <sub>2</sub> and O <sub>2</sub> respectively, L/s
$Q_W$	Water flow rate, m <sup>3</sup> /h
$R$	Removal rate, %
$Re$	Reynolds number for flow around a sphere, dimensionless
$R_{\text{Rel}}$	Removal rate after filtration relative to EF, %
$S$	Specific surface area, m <sup>-1</sup>
$U$	Electrolysis voltage, V
$U$	Uniformity, dimensionless
$v$	Superficial velocity (filtration rate), m/s
$V_0$	Molar volume of gases at normal state, 22,4 L/mol
$v_b$	Backwash velocity, m/h
$V_M$	Volume of media, m <sup>3</sup>
$V_T$	Total volume of media med, m <sup>3</sup>

$V_V$	Void volume in media, $m^3$
$W$	Specific energy consumption, $kWh/m^3$
$\beta$	Backwash calculation factor, dimensionless
$\epsilon$	Filter bed porosity, dimensionless
$\epsilon_E$	Porosity of bed at rest (fixed bed), dimensionless
$\epsilon_F$	Porosity of expanded bed, dimensionless
$\theta_C$	Contact angle
$\kappa_I$	Head loss coefficient due to inertial forces, unitless
$\kappa_I$	Head loss coefficient due to inertial forces, unitless
$\kappa_k$	Kozeny coefficient, unitless
$\kappa_V$	Head loss coefficient due to viscous forces, unitless
$\kappa_V$	Head loss coefficient due to viscous forces, unitless
$\xi$	Shape factor, dimensionless
$\rho_p$	Density of particle, $kg/m^3$
$\rho_w$	Density of air, $kg/m^3$
$\rho_w$	Density of water, $kg/m^3$
$\Phi_g$	Minimum volume of gas required for flotation, mL/L, ppm
$\Phi_p$	Volume of particle, mL/L, ppm
$\Psi$	Sphericity, dimensionless

*(This page is left blank intentionally)*

# 1 Introduction

## 1.1 Background

Cyanobacteria, often referred to as blue-green algae are the oldest known oxygen producing organism (Paerl and Paul, 2012) and plays an important part in the ecosystem. Bloom formation of cyanobacteria occur naturally when the conditions are favorable, and the blooms come periodically. Many cyanobacteria are capable of producing toxins, known as cyanotoxins, that may be released depending on different factors (Svrcek and Smith, 2004; Westrick *et al.*, 2010; Merel *et al.*, 2013).

An increase in distribution and frequency of cyanobacteria blooms has led to concern within the water treatment industry (Paerl and Paul, 2012; Merel *et al.*, 2013). Among the causing factors are higher discharges of nutrients, nitrogen and phosphorous, that reaches water sources (O'Neil *et al.*, 2012; Paerl and Paul, 2012). The main concern related to the bloom formation is if the cyanobacteria will release cyanotoxins and that can potentially reach consumers and induce liver, neuromuscular and skin damages (Merel *et al.*, 2013).

Aside from human health problems, an abundance in cyanobacteria in the can cause operation problems in the treatment plant. Among the most common problems are clogging of filters, requiring frequent backwashing which is energy inefficient and can cause high water losses and high sludge production (Romero *et al.*, 2014; Almuhtaram *et al.*, 2018).

As there is also a risk of toxin release from the long filter run causing cell death and therefore lysis (Svrcek and Smith, 2004; Almuhtaram *et al.*, 2018) and possibly as a result of agitation in the filtration processes, other removal methods should be considered. Several studies have identified flotation as an efficient process to remove cyanobacteria, as they often are light, and therefore float easily (Merel *et al.*, 2013; EPA, 2014). Flotation could be used as a substitute for sedimentation. The most common flotation technology within potable water is dissolved air flotation (DAF). A few studies have recently tried using electroflotation as a possible technology within drinking water treatment (Ghernaout, Benblidia and Khemici, 2015; Campos *et al.*, 2018). Electroflotation is a technology using electrolysis of water to generate bubbles that floats the pollutants to the surface of the water. The technology was initially used to separate valuable minerals from ores, but is today among others applied in treatment of

wastewater and industrial effluent (Sillanpa and Shestakova, 2017; Martínez-Huitle, Rodrigo and Scialdone, 2018)

One of the main benefits of using electroflotation is the ability to generate very small bubbles, creating a larger surface area, which increases the flotation efficiency. In addition, the system is compact and easy to operate (Comninellis and Chen, 2010). However, electrolysis requires a certain conductivity in order to be economically beneficial, as a low conductivity will require a higher applied current.

An integrated processes of electroflotation processes followed by rapid filtration have previously been studied with good results (Campos *et al.*, 2017, 2018). A costly feature of filters are the water and energy consumption during backwash processes. As the most common filter media used is sand, being a dense material, looking at alternative solutions to materials would be of interest. In addition, with customized filter media grains the uniformity can be improved. For this reason plastic filter media could be considered as an alternative, although there has been made very little study on this field (Schöntag and Sens, 2015).

## **1.2 Lagoa do Peri**

Lagoa do Peri is a natural lake located in the island of Florianopolis in the south of Brazil and is used as drinking water source, see Figure 1.1.

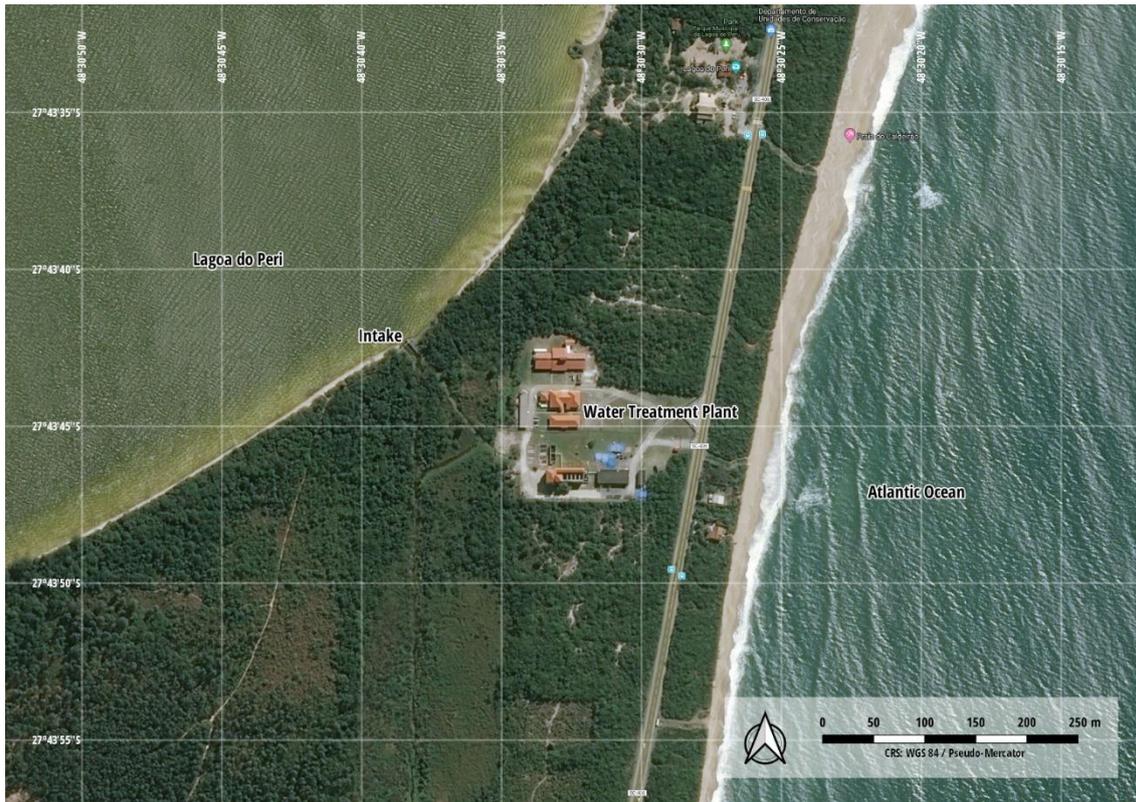
**Figure 1.1: General location of Lake Peri**



Source: Basemap by ESRI

The lake is subtropical with an average temperature in the summer of 24,3°C and 16,4°C during winter (Romero *et al.*, 2014) and most of the precipitation falls during the spring and summer, from October to March, with an average around 1,519 mm/year (Simonassi cited in Romero *et al.*, 2014; Mondardo cited in Romero *et al.*, 2014). The lake area is 5,2 km<sup>2</sup> and has a catchment area of 20,1 km<sup>2</sup>. The approximate perimeter of the lake is 11 km, the length of lake 4 km and a minimum width of 1,5 km. The maximum depth is 11 m and the medium depth is 7 m (Oliveira, 2002). The vegetation surrounding the lake is typical of the Atlantic Rain Forest and protected by national park status (Romero *et al.*, 2014).

**Figure 1.2: Detailed location of the water treatment plant at Lake Peri**



*Source: Satellite imagery by Bing*

In this lake, cyanobacteria formation occurs throughout the year (Romero *et al.*, 2014). The cyanobacteria species that have been identified in the lake are *Cylindrospermopsis raciborskii*, being the dominant specie in the lake, *Limnothrix* and *Planktolyngbya limnetica*. Other species *Chroococcus*, *Apahanotece* and *Pseudanabaena* have also been identified, but they are benthic and rare (Sylvéus, 2012). The dominant genera occurring in the lake is *Cylindrospermopsis raciborskii*, and has been identified in potencies of  $10^5$ - $10^6$  cells/ml (Sylvéus, 2012; Romero *et al.*, 2014). According to Annex XI and XII of the Brazilian Ministry of Health's guidelines N° 2.914, a monthly monitoring is required when the cell density is  $\leq 10\ 000$  cells/ml and weekly monitoring is required when the cell density exceeds 10 000 cells/ml. If the cell density is  $\geq 20\ 000$  cells/mL, weekly monitoring of cyanotoxins, after the water has passed through the water treatment plant, becomes mandatory (MS, 2012).

The water treatment plant was built in 2000 and is operated by Santa Catarina's Sanitation Company (CASAN in Portuguese). It operates by using direct filtration system and can supply 100 000 consumers at peak demand. Due to the high levels of cyanobacteria, the treatment plant

experiences challenges such as frequently required backwashing, requiring high manpower, problems with sludge disposal and high energy demands as a result of the high concentration of phytoplankton in the water. The risk of cyanobacteria and cyanotoxin breakthrough is also present (Romero *et al.*, 2014).

### **1.3 Thesis description**

The objective of this thesis is to look at the performance of an integrated system of electroflotation prior to filtration using polyvinyl chloride as filter media in treating drinking water with high cyanobacteria concentration.

The experiments were performed in a pilot scale study and the technical aspects that were evaluated were the following:

1. The performance of an integrated system of electroflotation and filtration used in drinking water treatment, with a focus on cyanobacteria removal
2. The performance of polyvinyl chloride spheres used as filter media grains

*(This page is left blank intentionally)*

## 2 Literature review

This chapter is divided in three parts to provide a better background understanding. The first chapter is dedicated to cyanobacteria, their toxins and the affects of conventional treatments on them. The second part is dedicated to the flotation, aside from a short intro, only focusing on electroflotation, The chapter also consists of a small section that gives an overview over the available electrochemical treatment methods. The third part is dedicated to filtration, focusing on rapid filtration, filter backwash and filter media.

### 2.1 Cyanobacteria

Cyanobacteria, also known as blue-green algae, are photosynthetic prokaryotes and the Earth's oldest known oxygen producers (Svrcek and Smith, 2004; Paerl and Paul, 2012). Cyanobacterias are known for their abilities to perform nitrogen fixation, that is uptake atmospheric N<sub>2</sub> and convert it to NH<sub>3</sub>, although not all cyanobacteria have this ability (Svrcek and Smith, 2004; Osswald *et al.*, 2007). The cyanobacteria are found worldwide and take part in the ecosystems in freshwater, brackish water, marine water (O'Neil *et al.*, 2012; Paerl and Paul, 2012; Preece *et al.*, 2017), and have also been detected in groundwater (Yang, Kong and Zhang, 2016).

Cyanobacteria blooms occur naturally when the conditions are favorable, generally in euphoric waters because of their nutrient abundance (Svrcek and Smith, 2004; Paerl and Paul, 2012). These microorganisms consists of many species with a variety in morphology, ranging from spherical and ovoid to cylindrical and filamentous forms (Coute and Bernard cited in Humbert, 2009; Newcombe, 2009) with individual cell sizes between 0,5 to 60 µm (*Blue-green algae - organism*, 2017). Cyanobacterias do not always occur as single-celled organisms in the water, but may aggregate to irregular colonies (Svrcek and Smith, 2004; Newcombe, 2009). In the drinking water industry, removal of cyanobacteria is wanted as they are related to production of harmful toxic compounds, in addition to 2-methylisoborneol (2-MIB, in some literature referred to as MIB) and geosmin that cause unpleasant taste and odors in the water (Merel *et al.*, 2013).

### 2.1.1 Cyanotoxins

Cyanobacterias can produce toxic secondary metabolites, known as cyanotoxins. Secondary metabolites are compounds produced by the organism that is not used for cell division or energy consumption (Svrcek and Smith, 2004). Cyanotoxins can be classified into three groups, according to their target organ: hepatotoxins, neurotoxins and dermatotoxins (Merel *et al.*, 2013). An important notion is that a single specie bloom may be having toxic and non-toxic strains (Svrcek and Smith, 2004). The cyanotoxins can be intracellular and extracellular material in the cyanobacteria cell. However, usually the majority of the toxins are intercellular (Chorus and Bartram, 2000; Merel *et al.*, 2013). Some cyanotoxins are more hydrophilic than others and in priority from most hydrophilic to most hydrophobic the cyanotoxins are saxitoxins, cylindrosperopsin, anatoxin-a and microcystin RR, YR, LR, LA (Westrick *et al.*, 2010).

#### 2.1.1.1 Hepatotoxins

The hepatotoxins mainly induce liver damages (Merel *et al.*, 2013), but some of the toxins have shown to affect other organs as well (Chorus and Bartram, 2000).

##### 2.1.1.1.1 Microcystin

Microcystins (MCs) are the main and most widespread type of cyanotoxins and are for the same reason the most studied cyanotoxin, with over 80 variants of the toxin that have been identified (Humbert, 2009). They have been shown to be produced by the cyanobacteria generas *Microcystis*, *Oscillatoria (Planktothrix)*, *Nostoc*, *Anabaena* and *Anabaenopsis* (Chorus and Bartram, 2000; Westrick *et al.*, 2010; Merel *et al.*, 2013). Microcystins are in most cases water soluble (Chorus and Bartram, 2000) and stable as they can withstand many hours of boiling and may persist for years when stored dry in room temperature (Svrcek and Smith, 2004). Microcystins have caused several animal poisonings (Stewart, Seawright and Shaw, 2008) in addition to several reported human poisonings (Hillborn *et al.*, 2007). In Caruaru, Brazil, the death of over 50 patients came as a result of use of MCs containing water for hemodialysis (Jochimsen *et al.*, 1998). WHO has consequently set a guideline of a maximum value of 1 µg/L for MC-LR for drinking water (World Health Organization, no date).

#### 2.1.1.1.2 *Nodularins*

Nodularins (NODs) are primarily found in brackish water and have mainly been reported in Australia, New Zealand and the Baltic sea (Chorus and Bartram, 2000; Svrcek and Smith, 2004; Humbert, 2009). They are associated only with the genera *Nodularia spumigena* and so far only six variants of NODs have been identified (Chorus and Bartram, 2000; Humbert, 2009). They work similar as MCs and are tumor promoters. Because the lack of reported intoxication of humans, there are have not been set guidelines for the concentration of NODs (Merel *et al.*, 2013).

#### 2.1.1.1.3 *Cylindrospermopsin*

Cylindrospermopsin (CYL) was considered a tropical cyanotoxin as it was initially reported in Thailand, Australia and New Zealand (Chiswell *et al.*, 1999; Li *et al.*, 2001; Stirling and Quilliam, 2001). However, it has been reported in temperate areas also, such as Germany (Fastner *et al.*, 2003). *Cylindrospermopsis raciborskii*, *Aphanizomenon ovalisporum*, *Raphidiopsis curvata* and *Umazakia natans* can all perform biosynthesis of the toxin (Banker *et al.*, 1997; Fristachi *et al.*, 2008; Westrick *et al.*, 2010). The toxin is reported to be about 50% intracellular and 50% extracellular (Westrick *et al.*, 2010). CYL is highly water soluble and has been shown to have a half-life of up to ten days in highly pure water (Chiswell *et al.*, 1999). Although CYL mainly attacks the liver, it can also affect other organs such as the kidneys, thymus and the heart (Humbert, 2009). The Palm Island mystery in 1979 in Australia is the most famous case of human intoxication from CYL, causing over 100 admissions of children to the hospital as a result of consumption of contaminated drinking water (Bourke *et al.*, 1983). Based on an experiment on mice, a guideline for a maximum concentration of 1 µg/L in drinking water has been proposed (Humpage and Falconer, 2003).

#### 2.1.1.2 Neurotoxins

The neurotoxins target the neuromuscular system and can result in paralyzation of the peripheral nerve system, the skeletal muscle and the respiratory muscles. Respiratory arrest have resulted in death within a few minutes or hours (Humbert, 2009). Most neurotoxins are acute acting, meaning that they cause act quickly after a small dose (Svrcek and Smith, 2004).

#### 2.1.1.2.1 *Anatoxin-a*

Anatoxin-a (ANTX-a) has occurred in USA, Asia, Africa and Europe (Ballot *et al.*, 2003; Namikoshi *et al.*, 2003; Carrasco *et al.*, 2007; Osswald *et al.*, 2007), and is the smallest reported toxin among the cyanotoxins with a molecular mass of 165 Da (Westrick *et al.*, 2010). The specie that mainly produce the toxin is *Anabaena*, but it can also be produced by other species such as *Aphanizomenon*, *Planktothrix* and *Cylindrospermum* (Van Apeldoorn *et al.*, 2007; Fristachi *et al.*, 2008; Westrick *et al.*, 2010). Various animal poisonings have been reported as a result of ANTX-a, resulting in vomiting and respiratory arrest, resulting in death (Gugger *et al.*, 2005; Wood *et al.*, 2007). No human poisonings have been reported so far, and no official guideline is set for drinking water as the results for the toxicity have not been similar. However, a guideline of 3 µg/L has been suggested (Svrcek and Smith, 2004).

#### 2.1.1.2.2 *Anatoxin-a(s)*

Anatoxin-a(s) (ANTX-a(s)) have been reported in restricted areas such as USA, Scotland, Denmark and Brazil (Onodera *et al.*, 1997; Molica *et al.*, 2005; Merel *et al.*, 2013). The toxin is found to be produced by *Anabaena* species. No guideline has been proposed for drinking water as there exists very few studies on ANTX-a(s) (Van Apeldoorn *et al.*, 2007; Merel *et al.*, 2013).

#### 2.1.1.2.3 *Saxitoxins*

Saxitoxins (STXs) have been found in freshwater in Australia, Denmark and USA (Chorus and Bartram, 2000; Van Apeldoorn *et al.*, 2007), and are commonly associated with “red tides” (Westrick *et al.*, 2010) because of their red colour during blooms.. They are known marine toxins produced by *Alexandrium spp.* and *Gymnodinium spp* (Humbert, 2009) and sixteen variants of saxitoxins have been reported (Westrick *et al.*, 2010). However, STXs have been identified in freshwater species, mainly *Anabaena circinalis* and *Aphanizomenon flos-aque*, but also in *Lyngya wollei* and *C. raciborskii*. STXs occurrences are mostly known for animal deaths and are also referred to as paralytic shellfish poison (Westrick *et al.*, 2010). They may induce nerve dysfunction, paralysis and death due to respiration failure (Van Apeldoorn *et al.*, 2007) and several human intoxications have occurred caused by consumption of marine shellfish, resulting in numbness, complete paralysis and death (Humbert, 2009; Merel *et al.*, 2013). However, none av these have been due to drinking water, and no drinking water guideline have

been set, with the exception of Australia having a guideline of 3 µg /L of STX equivalence (Westrick *et al.*, 2010).

#### 2.1.1.2.4 *β-N-methylamino-L-alanine*

β-N-methylamino-L-alanine (BMAA) has been detected in England, Peru, South Africa, China and USA (Esterhuizen and Downing, 2008; Johnson *et al.*, 2008; Metcalf *et al.*, 2008; Brand *et al.*, 2010; Li *et al.*, 2010). Although lack of extensive studies, it has been indicated that BMAA is produced by all known groups of cyanobacteria (Cox *et al.*, 2005). No guideline is set for drinking due to lack of toxicological data (Merel *et al.*, 2013).

#### 2.1.1.3 Dermatotoxins

The dermatotoxins include aplysiatoxins (APTxs) and lyngbyatoxins (LTXs) and are mainly produced by *Lynbya majuscula* (Van Apeldoorn *et al.*, 2007). They have so far only been found in marine water (Merel *et al.*, 2013). The effects after exposure can include dermatitis, oral and gastronomic inflammation resulting in diarrhea, in addition to being potential tumor promoters. However, there is not a lot of data available on them (Van Apeldoorn *et al.*, 2007; Merel *et al.*, 2013).

### 2.1.2 Taste and odour compounds

Cyanobacteria are also related to production of secondary metabolites that induces odour and a musty, earthy taste to the water. The most common types of secondary metabolites to induce this is geosmin and 2-methylisoborneol (2-MIB, in some literature referred to as MIB). A variety of cyanobacteria genera's are associated with the production of geosmin and/or 2-MIB, among others *Anabeana*, *Aphanizomenon*, *Oscillatoria* and *Microcystis* (Chorus and Bartram, 2000; Graham *et al.*, 2008). As these are known as toxin-producing genera, smell or taste can be used as an early warning of a potential toxin production. However, there has not been found to be any correlation between odour and taste producing compounds and toxins. An important notion is that lack of taste and odour does not indicate that cyanobacteria is not present in the water (Chorus and Bartram, 2000).

### **2.1.3 Harmful cyanobacteria blooms and their challenges**

Although playing an important role in the ecosystem, the increase of harmful cyanobacteria blooms (cyanoHABs) and their distribution worldwide comes with concern regarding ecosystems, water used for recreation and drinking water (O'Neil *et al.*, 2012; Paerl and Paul, 2012; Merel *et al.*, 2013). A combination of climate change causing higher temperatures and change in hydrological patterns, population growth causing higher nutrient rich discharges in water bodies and urbanization causing higher runoffs is the leading causes of this expansion (O'Neil *et al.*, 2012; Paerl and Paul, 2012).

The driver that has received the most attention with regards to bloom formation is the nutrient pollution, phosphorous and nitrogen, making the waters more eutrophic. Growth is also increased when the water is stagnant with little wind. Other favorable conditions for bloom formation is waters that are neutral or slightly alkaline with temperatures between 15-30 degrees (Svrcek and Smith, 2004). The bloom may be dominated by a single specie of cyanobacteria or have several. Even in a single specie bloom there may be strains of cyanobacteria that are not toxic. The toxins are formed in all stages during the cyanobacteria growth, until cell lysis is reached during the decline of the bloom and the cyanobacteria is degraded.

There are two main concerns associated with cyanoHABs in the water treatment sector one being a reduction of efficiency, often related to clogging of the filters and the second being the release of cyanotoxins in the drinking water. Filter clogging will require more frequent backwashing and demanding more energy. In addition, the agitation from the backwashing process might rupture the cells, causing intracellular toxins to be released in the water.

### **2.1.4 Conventional treatment methods**

For drinking water treatment with regards to removal of cyanobacteria, one has to take into consideration the agitation the cyanobacteria cell maybe exposed to. The cyanobacteria should be removed without compromising the cell integrity (Merel *et al.*, 2013), as the intracellular cyanotoxins may be released if the cell is ruptured.

It is firstly important to know what type of cyanobacteria and cyanotoxins the raw water can obtain, and secondly whether the cyanotoxin is intracellular or extracellular (Westrick *et al.*, 2010). For the process of removing the cells it can be done mainly in the separation step of the treatment and this will remove the intracellular toxins given that the cell will not rupture in the process. The removal of extracellular toxins is more difficult, but follows the same processes that are applied for removal of natural organic matter (NOM). This can be done by physical removal, such as active carbon or membrane filtration, or by chemical or biological inactivation, such as UV and oxidation or degradation by bacteria (Svrcek and Smith, 2004; Westrick *et al.*, 2010).

#### 2.1.4.1 Inlet

Three management strategies to avoid cyanobacteria into the treatment plant is to (1) use an alternative source, (2) adjust the intake depth and (3) treat the water at the intake. The first step may be difficult to apply as many treatment plants do not have access to more than one source. It is possible to adjust the intake depth as some cyanobacteria blooms occur at specific depths. However, this area lacks research (Westrick *et al.*, 2010; Merel *et al.*, 2013). Treatment of the water at intake will be discussed in the next section about pre-treatment.

#### 2.1.4.2 Effect of pre-treatment on cyanobacteria and cyanotoxins

The effect of pre-treatment by coarse filtration has little effect on the cyanobacteria and cyanotoxins, as is mainly to remove macro-contaminants that may disturb the following treatment processes or the treatment facilities. Pre-oxidation on the other hand may impact the cells. The pre-oxidation is done by ozone or chlorine in order to improve the efficiency for the following treatment steps. This process induces cell lysis, resulting in release of intracellular toxins. In addition, the chlorine and ozone are rapidly consumed by the high concentration of dissolved organic carbon on the water, meaning the cyanotoxins will not be significantly oxidized. For this reason, although pre-oxidation is becoming less common because of the potential harmful by-products produced, it should be avoided during high blooms in the drinking water source (Westrick *et al.*, 2010; Merel *et al.*, 2013).

### 2.1.4.3 Effect of particle separation treatment

#### 2.1.4.3.1 *Effect of coagulation-flocculation-sedimentation*

The coagulation/flocculation process aims to agglomerate the colloidal material in the water to make the separation step move efficient. When iron or aluminum salts are added as coagulant the negatively charged colloids are neutralized and prevents electrostatic repulsion between the particles, resulting in formation of flocs that can removed by sedimentation, filtration or flotation (Merel *et al.*, 2013).

Cyanobacteria have a negative charge on the cell membrane and may roughly be considered as colloids as they can be removed by coagulation-flocculation-sedimentation. The removal of cyanobacteria through coagulation-flocculation-sedimentation has been shown to be efficient. The coagulant dose required is dependent on how much cyanobacteria there is in the water and the age of the cells. An important notion is that the processes of coagulation-flocculation-sedimentation remove the intracellular cyanotoxin, not the extracellular cyanotoxins (Merel *et al.*, 2013).

As certain types of species have gas vacuoles, they might prevent the flocs from settling in the sedimentation tank. To avoid this flotation may be implemented instead of sedimentation, dissolved air flotation (DAF) have been shown to be efficient in the removal of cyanobacteria and could be used as an alternative. For clarifiers, cell lysis has been shown to happen rapidly in the sludge accumulated. For that reason, sludge should be quickly extracted on order to avoid cyanotoxin release and back contamination of water (Svrcek and Smith, 2004; Merel *et al.*, 2013).

#### 2.1.4.3.2 *Effect of filtration*

Slow sand filtration has been efficient in removal of cyanobacteria without rupturing the cells, and hence removing their intracellular toxins as well (Grützmacher *et al.*, 2002). Also, slow sand filtration removed extracellular toxins as they were biodegraded by bacteria that grow on the upper layer of the filter. On the other hand, not every sand filter may favor the growth of toxin-degrading microorganisms and the degradation has only been observed with MCs (Svrcek and Smith, 2004; Merel *et al.*, 2013).

Rapid sand filters are the most common filters used. They are generally found to be insufficient in removal of cyanobacterial cells without using multimedia filters and adequate chemical pretreatment. In general, sand filters should be ineffective in removing dissolved cyanotoxins, with the exception of filters using granular activated carbon. The filter runs should not be long as it may lead to toxins entering the filtered water from cells lysis conducted by the cells that have been retained in the filter (Svrcek and Smith, 2004).

Membrane filtration covers the processes of microfiltration (0,1-10  $\mu\text{m}$ ), ultrafiltration (1-100 nm), nanofiltration (around 1 nm) and reverse osmosis (0,1 nm). Microfiltration and ultrafiltration have shown to be good in removal of cyanobacteria without inducing cell lysis. Clogging may however occur frequently. In addition, the microfiltration is not expected to remove extracellular toxins as the pore size is too big. Ultrafiltration membranes has shown to remove MCs, but might not be able to remove smaller toxins. Nanofiltration and reverse osmosis should preferable not be used to remove cyanobacteria cells as they will quickly clog (Merel *et al.*, 2013). However, they have shown to be efficient in removal of extracellular toxins such as MC-LR, ANTX-a, CYL and NODs (Vuori *et al.*, 1997; Ribau Teixeira and Rosa, 2006; Dixon *et al.*, 2011).

#### 2.1.4.3.3 *Effect of activated carbon*

Powdered activated carbon (PAC) and granular activated carbon (GAC) can be used to perform adsorption. Activated carbon does not have an impact on cyanobacteria and intracellular toxins, but are efficient in removal of extracellular MCs, CYL, ANTX-a and STXs. The removal depends on the size of the pores of the absorbent. MCs have shown to be adsorbed efficiently with mesopores (2-50 nm), whereas micropores are recommended for the smaller STXs (Merel *et al.*, 2013). Activated carbon can also work eliminate cyanotoxins through biodegradation when growth of certain microorganisms occur on the GAC (Westrick *et al.*, 2010; Merel *et al.*, 2013). However, the removal of cyanotoxins with activated carbon depends on the concentration of the natural organic matter (NOM) in the water, as a higher concentration of NOM will result in competition in adsorption (Huang, Cheng and Cheng, 2007).

#### 2.1.4.4 Effect of degradation treatments

The cyanotoxins can also be inactivated or degraded in the disinfection step. UV irradiation have proven to potentially remove MCs, ANTX-a and CYL, but the effect on other toxins have not been investigated. The efficiency of UV radiation depends on intensity of radiation, lamp type and design and the turbidity of the water. Ozone has shown to react well with the common cyanotoxins, but is less efficient against STXs. The NOM-concentration also affects the removal as there will be competition for the O<sub>3</sub> (Merel *et al.*, 2013). Chlorination is shown to quickly transform the MCs, NODs, CYL and STX, and less efficient towards ANTX-a (Merel *et al.*, 2013).

## 2.2 Flotation processes

Flotation is a separation process where the particles in the suspension attach to bubbles generated (usually air). The particles that are most effectively removed in flotation processes are in the size range 10-200 µm. The three most important factors in order to evaluate the success of flotation are solid hydrophobicity, the ratio of bubble to particle size and the amount of turbulence in the fluid (Wakeman, 2011).

There are generally three method of generating gas bubbles. The three are given below with an estimate of the diameter of the bubble size generated (Wakeman, 2011):

1. Mechanical (0,2-2 mm):

Air injection combined with an agitator to disperse the bubbles or pumping the air through a porous plate (mechanical flotation or froth flotation).

2. Nucleation (40-70 µm):

The suspension is supersaturated under pressure before relieving the pressure (microflotation). The suspension is saturated with air, before vacuum is applied and create a bubble formation (vacuum flotation). Saturation of water under pressure before injecting it to into the suspension (dissolved air flotation).

3. Electrolysis (< 50 µm with minimal turbulence):

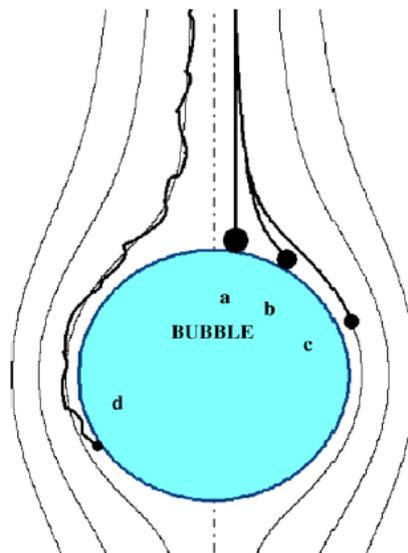
Use of electrolysis to generate bubbles (electroflotation).

The most common technology in drinking water treatment is dissolved air flotation (DAF) (Wakeman, 2011).

### 2.2.1 Theory of flotation

Several studies have been conducted in order to understand the interaction between bubbles and particles in a suspension, but the results show that it is difficult to set a general theory of how the interaction really occurs and what forces are predominating (Miettinen, Ralston and Fornasiero, 2010; Lecrivain *et al.*, 2015; Xing *et al.*, 2017). Usually the bubble-particle encounter happens in three stages; the particle approach, the collision between the bubble and particle, and the sliding down of the particle to the bottom of the bubble. The four main collision mechanisms are shown in Figure 2.1, illustrating capture of particle by inertia (an objects resistance to change in its velocity or direction), gravity, interception and Brownian diffusion. The collision can happen by on process or a combination of several processes (Miettinen, Ralston and Fornasiero, 2010).

**Figure 2.1: Bubble-particle collision mechanisms: a) inertia, b) gravity, c) interception and d) Brownian diffusion.**

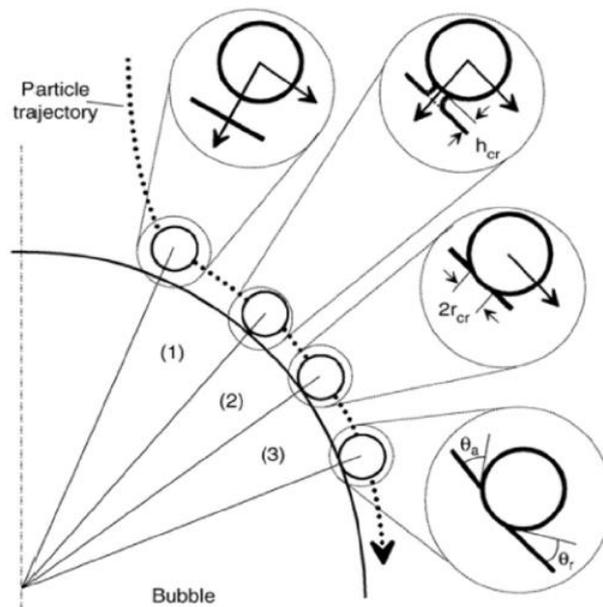


*Source: Miettinen, Ralston and Fornasiero (2010)*

If the particle is within the range of attractive surface forces with the bubble, attachment may occur. There is a thin liquid film between the liquid-solid interface (the particle) and liquid-gas interface (the bubble). This film will eventually be drained and result in a rupture of the film.

When this rupture occurs, a three-phase contact line (TPCL), a boundary between the solid particle surface, the liquid phase and the gas phase. Following, a stable wetting perimeter will be formed, and the particle will be attached to the bubble. The attachment process itself is given as the sequence of drainage of the liquid film, rupture of the liquid film and establishment of a TPCL. After collision, the particles need some time to thin the intervening liquid film, which is referred to as the induction time required. The particles may leave the bubble surface before the required induction time, that is before the intervening film reaches the critical thickness,  $h_{cr}$ , and a TPCL can form (Nguyen, Schulze and Ralston, 1997; Verrelli, Koh and Nguyen, 2011). An illustration of the establishment of a TPCL is shown in Figure 2.2.

**Figure 2.2: Schematic illustration of the formation of TPCL.**



*Source: Xing et al. (2017)*

The flotation process is linked to the wetting (hydrophilicity) and nonwetting (hydrophobicity) of particles. The better the wetting of a particle is, the more difficult it is for the particle to stick to the gas bubbles (worse adhesion). A measure for wettability of particles is by using contact angle ( $\theta_c$ ), that is the angle tangent to the liquid surface. There are three boundary conditions in bubble-solid interaction that determines if flotation will occur or not (Sillanpa and Shestakova, 2017):

1.  $\theta_C = 0^\circ\text{C}$ , completely wettable. The particles are then completely hydrophilic and flotation will not occur.
2.  $\theta_C = 90^\circ\text{C}$ , in between.
3.  $\theta_C = 180^\circ\text{C}$  completely nonwettable. The particle is completely hydrophobic and maximum adhesion is reached, meaning flotation will occur.

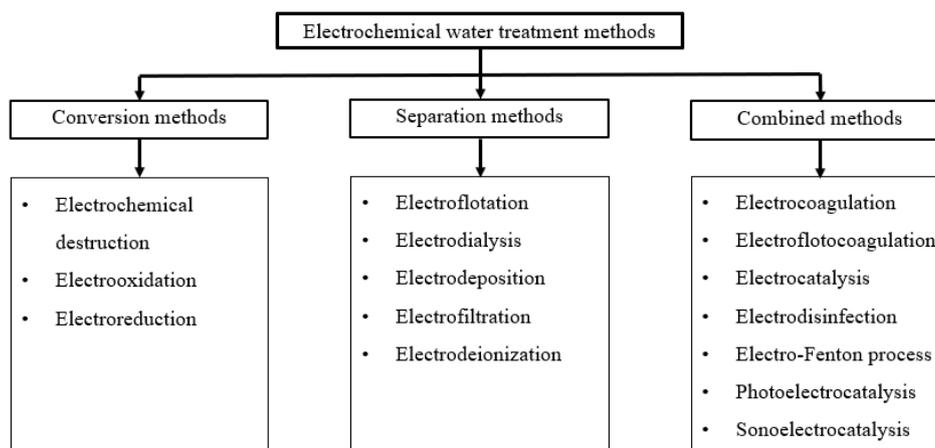
From the above, the conclusion is that flotation is more prominent for hydrophobic particles (Sillanpa and Shestakova, 2017). Most inorganic, and also some organic, particles are hydrophilic and therefore do not float. In order to make these float, one can use surfactants. A surfactant, short for surface active agents, are molecules that have both a hydrophilic and a hydrophobic part and are therefore amphiphilic (Bristol, no date).

### **2.2.2 Electrochemical treatment methods**

Electrochemical treatment are physical-chemical water treatments methods. Common for all is the use of electrochemical reactions to fulfill the process desired. An electrochemical process differs from a chemical process with the fact that the transfer of electrons happens over a significantly long path in an electrochemical process, whereas for a chemical reaction a collision of the reactant is required (Sillanpa and Shestakova, 2017). There is always one component that is reduced and one that is oxidized in an electrochemical reaction.

There exist several types of electrochemical treatment processes classified into two groups, being conversion methods and separation methods. A third group consists of combined methods, which encompasses one or more of the methods in the latter mentioned groups (Sillanpa and Shestakova, 2017). Figure 2.3 shows common treatments methods within each group.

**Figure 2.3: Classification of electrochemical treatment methods.**



*Source: Adapted from Sillanpa and Shestakova (2017)*

The process of electrolysis, which is often the basis for the abovementioned methods, requires water with sufficient conductivity in order to be energy efficient. Applying higher voltage to increase the current flow in the water will be costly. This might be one reason why electrochemical treatment methods have mainly been experimented on industrial water or wastewater (Kobyas, Can and Bayramoglu, 2003; Chen, 2004; Daneshvar, Sorkhabi and Kasiri, 2004; Metcalf *et al.*, 2008; El-Hosiny *et al.*, 2017).

### **2.2.3 Electroflotation**

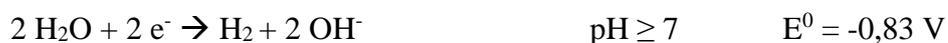
Electroflotation (EF) is a process that uses electrolysis as a particle separation method. Bubbles are generated with electrolysis with insoluble electrodes (Sillanpa and Shestakova, 2017). Particles are attached to bubbles that are generated, and float to the surface of the suspension where they are removed. It was first introduced by Elmore in 1904 for flotation of valuable minerals from ores, but it was first in the end of the 1960s that it was used in the field of treating wastewater (Sillanpa and Shestakova, 2017; Martínez-Huitle, Rodrigo and Scialdone, 2018). Since then new electrode materials and applications have been developed. One of the biggest advantages in EF is the removal of tiny particles because of the small and uniform bubbles that are generated (Comninellis and Chen, 2010; Mickova, 2015; Kyzas and Matis, 2016). However, a big disadvantage is that the electrolysis process requires a high conductivity in order to have a good current flow in the water (Mickova, 2015), which may be a limiting factor in the application of drinking water treatment.

In general, EF processes in water treatment are based on electrolysis that generate gas bubbles. In the case of electrolysis of water, the bubbles generated are hydrogen gas, H<sub>2</sub>, and oxygen gas, O<sub>2</sub>. An external power source is connected to the electrodes submerged in the solution, often called the electrolyte. When power is applied it will start a process where oxidation occurs at the anode and generates oxygen gas, and reduction occurs at the cathode where hydrogen gas is generated. The electrochemical reactions during electrolysis of water are shown below. The pH demonstrates which half reaction that will occur in acidic or alkaline solutions. E<sup>0</sup> is the theoretical standard potential for the half reaction, meaning the theoretical voltage that needs to be applied for the reaction to occur (Sillanpa and Shestakova, 2017).

- At the anode:



- At the cathode:



- The two equations summarized gives the total reaction



As seen from the formula, the EF process generated twice as much hydrogen gas than oxygen. The standard potential of the total reaction is the sum of the two half reactions at the anode and cathode, within the same pH range.

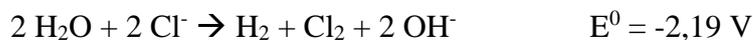
However, pure water is a poor conductor of electricity and generally an electrolyte is needed. If the suspension contains chlorine ions, for instance NaCl, electrodisinfection (ED), sometimes referred to as electrochemical oxidation (EO) may occur as a result of chlorine gas generation. The standard potential of the chlorine generation shows that it requires more voltage to generate Cl<sub>2</sub> compared to O<sub>2</sub>. However, in practice, the reaction of Cl<sub>2</sub> shows to be favorable. This is often referred to as overpotential, that is the difference between the standard cell potential and the actual voltage the reaction requires in a situation. O<sub>2</sub> has shown to have a high overpotential, resulting in the generation of Cl<sub>2</sub> in electrolysis of NaCl solutions (Robinson, no date).

From the  $\text{Cl}_2$  gas, hypochlorous acid ( $\text{HClO}$ ) and hypochlorite ions ( $\text{OCl}^-$ ) can be formed. These substances are strong oxidizing agents and can oxidize the organic pollutants in the water (Comminellis and Chen, 2010; Sillanpa and Shestakova, 2017; Martínez-Huitle, Rodrigo and Scialdone, 2018). The reactions that will occur will then become (Robinson, no date; Sillanpa and Shestakova, 2017):

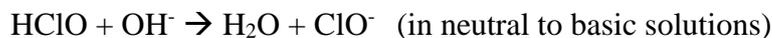
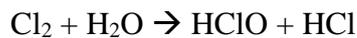
- At the anode:



- Total reaction:



The chlorine gas will quickly react with the water and form  $\text{HClO}$  and  $\text{OCl}^-$  in accordance with the following reactions (Sillanpa and Shestakova, 2017):



### 2.2.3.1 Electroflotation reactor

The EF system consists of two or more electrodes, one part where hydrogen gas is generated (cathode) and one part where oxygen gas is generated (anode). The electrodes are submerged into the water that is treated, referred to as the electrolyte in electrochemistry, and connected to an external power source.

#### 2.2.3.1.1 *Electrode materials*

For the cathode it is mostly common to use metals or alloys as the electrode material. Stainless steel is a good choice for the cathode as it is cheap and readily to use. Titanium has the advantage of being very stable and therefore work well as a cathode in corrosive waters, but it is expensive. Nickel has the advantage of low overpotential for hydrogen evolution, which can

reduce the energy consumption (Comninellis and Chen, 2010; Martínez-Huitle, Rodrigo and Scialdone, 2018).

Available anodes are harder to find than cathodes as there is a great risk of severe electrochemical corrosion when common metals and alloys are used. For the same reason, the lack of stable anodes has limited the use of EF-processes in industry. Anodes can be divided into two types; soluble and insoluble anodes, or active and inert electrodes respectively. Common soluble anodes are iron, aluminium and stainless steel and they can perform electrocoagulation (EC) and EF simultaneously (Chen, Chen and Yue, 2002), a process often referred to as just EC or electrocoagulation-electroflotation (ECEf). As we will perform only EF, we will only focus on insoluble anodes in the following.

Graphite,  $\text{PbO}_2$  and Pt are three of the most commonly used insoluble or inert electrode materials used for anodes (Hosny, 1996; Burns, Yiacoymi and Tsouris, 1997; Comninellis and Chen, 2010; Martínez-Huitle, Rodrigo and Scialdone, 2018). Although cheap and easily accessible, the durability of graphite is poor. One reason for this is due to oxidation of carbon creating  $\text{CO}_2$  gas, in addition to wearing of the electrode from the gas evolution occurring, giving graphite a service life of only 6-24 months. The  $\text{PbO}_2$  are not very stable as there is a risk of generating highly toxic  $\text{Pb}^{2+}$  which may lead to secondary pollution (Chen, Chen and Yue, 2002; Comninellis and Chen, 2010; Martínez-Huitle, Rodrigo and Scialdone, 2018). The Pt or Pt-plated anodes are much more stable in comparison, but the high costs of these has limited the use in high-scale industry (Chen, 2004).

The dimensionally stable anode (DSA<sup>®</sup>) was invented by Beer in the late 1960s and they are the most important anodes of electrochemical engineering today. Initially, Beer introduced a  $\text{TiO}_2\text{-RuO}_2$  DSA<sup>®</sup> that was good for chlorine evolution. Further development of this technology has led to DSA<sup>®</sup> with several different materials with improvements for oxygen evolution. Common for all DSA<sup>®</sup> is that they usually have a surface coating layer made by precious metal oxides (for instance  $\text{RuO}_2$  or  $\text{IrO}_2$ ), as electrocatalysts, and nonconductive metal oxides as stabilizers or dispersers (for instance  $\text{TiO}_2$ ), on a valve metal substrate (for instance Ti or Ta) (Comninellis and Chen, 2010; Martínez-Huitle, Rodrigo and Scialdone, 2018). The composition of DSA<sup>®</sup> are often written with the substrate metal first, followed by the coating metal oxide mixture, for instance  $\text{Ti/RuO}_2\text{-TiO}_2$  or  $\text{Ti/Ru}_{0,34}\text{Ti}_{0,66}\text{O}_2$ , the latter showing the

percentage of each oxide in the coating layer. The nonconductive metal oxides are often used to save costs and improve the coating property of the electrode (Chen, Chen and Yue, 2002). With the DSA<sup>®</sup> the electrochemical reaction is limited to the surface layer of the electrode (Duby, 1993), giving them a longer durability by maintaining their shape.

The original TiO<sub>2</sub>-RuO<sub>2</sub> types of electrodes work well for chlorine evolution, but their oxide layer is quickly degraded for oxygen evolution and thus decreases their service life (Hine et al. cited in Comninellis and Chen, 2010). The IrO<sub>x</sub>-based DSA<sup>®</sup> on the other hand has a service life 20 times longer than that of the equivalent RuO<sub>2</sub> (Alves et al. cited in Comninellis and Chen, 2010). Often Ta<sub>2</sub>O<sub>5</sub>, TiO<sub>2</sub> and ZrO<sub>2</sub> are used as dispersing/stabilizing agents to decrease the cost and/or improve the coating property of the IrO<sub>x</sub> (Comninellis and Vercesi, 1991; Cardarelli *et al.*, 1998; Comninellis and Chen, 2010; Martínez-Huitle, Rodrigo and Scialdone, 2018). Although the amount of valuable Ir is reduced by adding the above-mentioned, the molar percentage of Ir still needs to be high, having an optimal dose of IrO<sub>x</sub> at 80 mol%, 70 mol% and 40 mol%, for respectively IrO<sub>x</sub>-ZrO<sub>2</sub>, IrO<sub>x</sub>-Ta<sub>2</sub>O<sub>5</sub> and IrO<sub>x</sub>-TiO<sub>2</sub> (Comninellis and Vercesi, 1991). The IrO<sub>x</sub>-Ta<sub>2</sub>O<sub>5</sub> has the highest electrochemical stability of the abovementioned. Although the IrO<sub>x</sub>-Ta<sub>2</sub>O<sub>5</sub>-coated titanium electrodes (Ti/ IrO<sub>x</sub>-Ta<sub>2</sub>O<sub>5</sub>) have been successfully applied as anodes in EF, they are costly and therefore limited in use (Mráz and Krýsa, 1994; Comninellis and Chen, 2010).

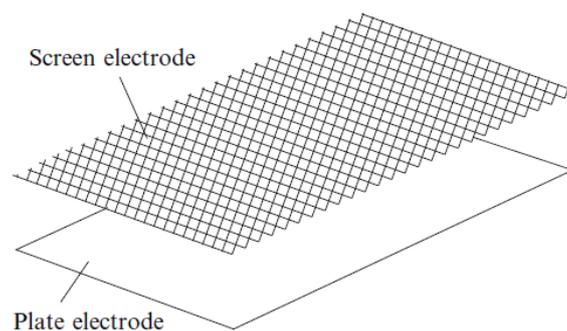
The Ti/IrO<sub>x</sub>-Sb<sub>2</sub>O<sub>5</sub>-SnO<sub>2</sub> electrode has shown to be very stable and can perform good oxygen evolution (Chen, Chen and Yue, 2002; Comninellis and Chen, 2010). Low amounts of the precious IrO<sub>x</sub> is required due to, among others, the good conductivity of Sb<sub>2</sub>O<sub>5</sub>-SnO<sub>2</sub> and a compact structure of the IrO<sub>x</sub>-Sb<sub>2</sub>O<sub>5</sub>-SnO<sub>2</sub> film (Comninellis and Chen, 2010).

#### 2.2.3.1.2 *Electrode arrangement*

There are many ways to arrange the electrodes, and the arrangement is important in order to maximize the performance of the EF. There are three arrangements commonly used; *conventional arrangements*, *vertical arrangements* and *open arrangements* (Martínez-Huitle, Rodrigo and Scialdone, 2018).

The conventional electrode set up usually consists of a screen electrode placed 10-15 cm above a plate electrode as shown in Figure 2.4 (Mostefa and Tir, 2004; Khelifa, Moulay and Naceur, 2005). With this arrangement it is only the upper screen electrode that faces the water flow. The disadvantage of this is that the bubbles generated at the lower electrode will not disperse immediately into the water, and hence lowers the availability of small bubbles needed for the flotation. There is also a greater risk of breaking the flocs that have been formed previously and affect the flotation efficiency. There is also a risk of short circuit if the plates do not have sufficient electrode spacing, especially since the upper electrode screen is flexible. On the contrary, too large spacing between the electrodes combined with a low conductivity would lead to a high energy consumption. With regards to maintenance it may also be a problem if larger deposits get stuck in the screen electrode. However, this may be less relevant if EF is used to drinking water treatment (Comninellis and Chen, 2010).

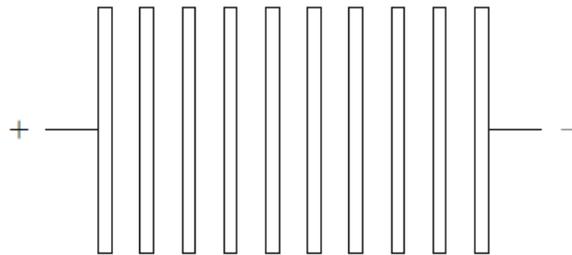
**Figure 2.4: Conventional electrode arrangement.**



*Source: Comninellis and Chen (2010)*

The electrodes can also be arranged vertically (Tsai, Hernlem and Huxsoll, 2002; Choi *et al.*, 2005), as shown in Figure 2.5, where both the anode and cathode are plate shaped, being beneficial with regards to maintenance of the electrodes. The disadvantage with this arrangement is that the bubbles that are generated often rise along the surface of the electrodes. This way quick bubble coalesce may occur and affect the flotation efficiency (Comninellis and Chen, 2010; Martínez-Huitle, Rodrigo and Scialdone, 2018).

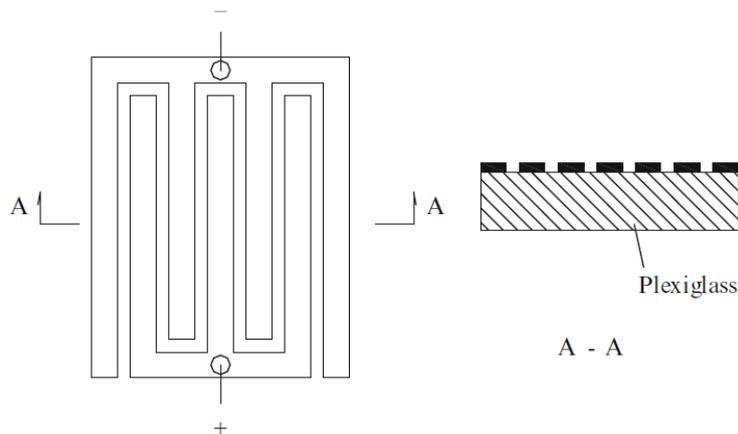
**Figure 2.5: Vertical electrodes arrangement**



*Source: Comninellis and Chen (2010)*

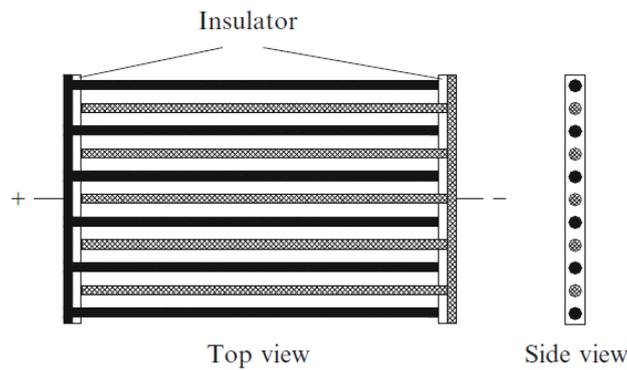
An open electrode arrangement is also possible. One way of having this arrangement is by using a forkshaped anode and cathode (Shen *et al.*, 2003), as shown in Figure 2.6. This arrangement is effective as the shape gives a quick bubble dispersion. Also, both the bubbles from the anode and the cathode can contribute in the removal of sediments. Another way of setting up the open electrode arrangement is shown in Figure 2.7. Because of the small spacing between the electrodes, this system saves a lot of energy, and the gap between the electrodes in Figure 2.6: Open electrodes arrangement Figure 2.6 and Figure 2.7 can be as small as 2 mm (Comninellis and Chen, 2010).

**Figure 2.6: Open electrodes arrangement**



*Source: Comninellis and Chen (2010)*

**Figure 2.7: Alternative open electrodes arrangement**



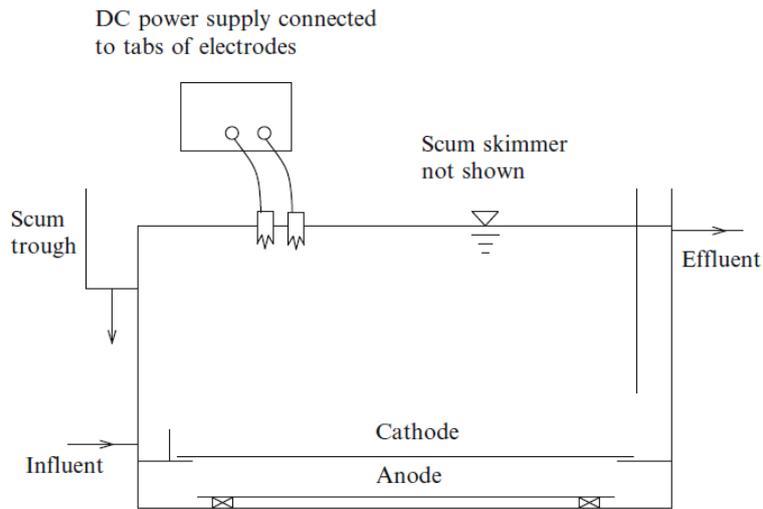
*Source: Comninellis and Chen (2010)*

### 2.2.3.1.3 Reactor design

There exist many types of systems for EF configurations. Due to the simplicity of it, a single stage EF with a horizontal flow is a good choice in general, see Figure 2.8. Another alternative to this is a single stage system with a vertical flow shown in Figure 2.9, and this system has the advantage of increased separation efficiency because of the uniform distribution of the flow (Comninellis and Chen, 2010).

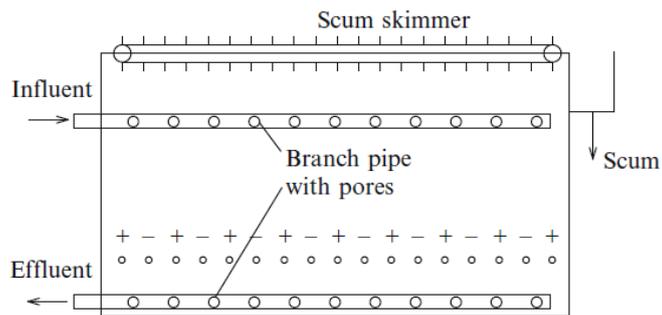
If the EF system is for large scale treatment as single-stage EF with contacting chamber and separation chamber may be a better option, see Figure 2.10. The disadvantage of this system is that some fragments may drop from the scum skimmer and down in the separation chamber, where they cannot float up again (Comninellis and Chen, 2010).

**Figure 2.8: Single-stage EF with a horizontal flow**



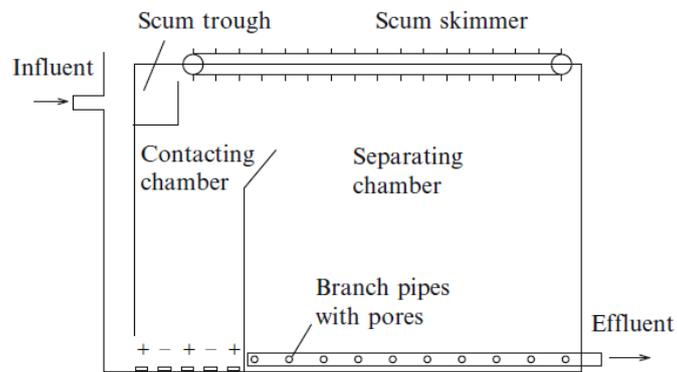
Source: *Comminellis and Chen (2010)*

**Figure 2.9: Single-stage EF with a vertical flow**



Source: *Comminellis and Chen (2010)*

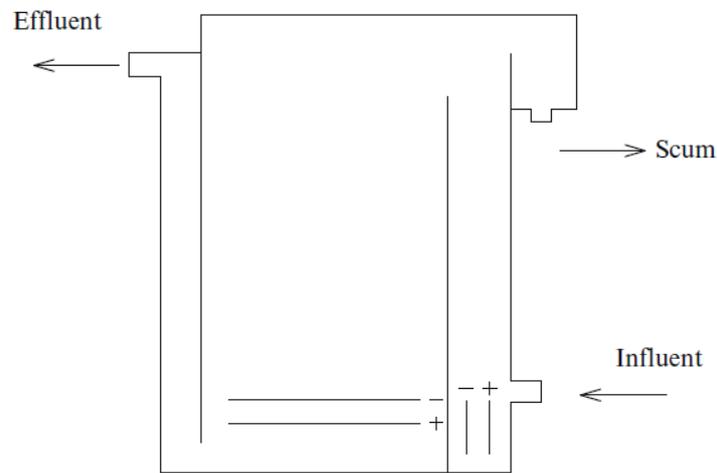
**Figure 2.10: Single-stage EF with a contacting chamber and a separation chamber**



Source: *Comminellis and Chen (2010)*

A two-stage EF may be implemented in order to increase the separation efficiency, see Figure 2.11. In this system, the first stage of EF is done with a high current, creating a rapid production of gas bubbles and creating a turbulent mixing. In this stage about 80-90% of the impurities are moved to the foam layer. The current in the second step is set to make the bubbles generated to float up under close to laminar conditions, which can remove suspended impurities with a size less than 10  $\mu\text{m}$ . In addition to this, the tiny bubbles work a filter. When the water streams downward through this layer of tiny bubbles additional purification can be reached (Comninellis and Chen, 2010).

**Figure 2.11: Two-stage electroflotation**



*Source: Comninellis and Chen (2010)*

### 2.2.3.2 Variables

Several factors affect the efficiency of the EF process. Among these are electrode potential and current density, the current distribution, the mass-transport regime, the cell design (shape of electrode, electrode spacing etc.), the electrolyte, the electrode material, particle surface charge and flow rate of the solution (Comninellis and Chen, 2010; Sillanpa and Shestakova, 2017). EF is a complex process where the variables do not have a separate impact, but rather depend on each other as well.

#### 2.2.3.2.1 *Effect of pH*

The pH of the suspension in EF affect the size of the bubbles generated, which is strongly associated with the removal efficiency (Comninellis and Chen, 2010; Mickova, 2015). However, the literature demonstrated different results of how pH affects the bubble size. Some literature claims the smallest hydrogen bubbles are formed in neutral and slightly acidic conditions (Chen, 2004; Comninellis and Chen, 2010; Jiménez *et al.*, 2010; Mickova, 2015). On the contrary, some literature claims hydrogen bubbles generated are generally larger in acid conditions than neutral to alkaline conditions, and the contrary applies for oxygen bubbles (Martínez-Huitle, Rodrigo and Scialdone, 2018).

If EF is combined with electrocoagulation, the importance of pH is enhanced as it is known from conventional coagulation that Al and Fe have an optimal pH range in order to accumulate flocs. In addition to this, the pH with electrocoagulation will change as the metal hydroxides are formed, and may be beneficial as it will neutralize both acidic and alkaline effluents (Koby, Can and Bayramoglu, 2003; Chen, 2004).

#### 2.2.3.2.2 *Effect of temperature*

It is fairly known that chemical reactions, speed up with increased temperatures. Higher temperatures give higher conductivity, which lowers the power consumption (Chen, 2004). This is reflected in electrolysis requiring less applied voltage when the temperature is high (Rhodes *et al.*, 2007). The electrolysis process will often release heat as the electric input often is higher than the required input, which will result in increased temperature (Gheraout, Benblidia and Khemici, 2015).

For EC processes on dye and algae, the removal rate have improved with increased temperature (Daneshvar, Sorkhabi and Kasiri, 2004; Gao *et al.*, 2010), explained by a higher collision rates between the pollutants and the ions. However, the removal rate of dye seem to decrease again when temperatures are above 300 K (Daneshvar, Sorkhabi and Kasiri, 2004; Gao *et al.*, 2010). This can be explained by the significant increase in movement of the ions, resulting in a difficulty for the ions to aggregate and create hydroxide flocs (Daneshvar, Sorkhabi and Kasiri, 2004).

#### 2.2.3.2.3 *Effect of conductivity*

The conductivity of a suspension reflects its ability to pass electric current. This is directly related to the concentration of ions in the suspension, and the higher the conductivity, the stronger the ability to drive the electric current in the electrolyte. The EF process requires good conductivity to function as it effects the applied cell voltage and current density and therefore is important in order to maintain a low energy consumption. An increase in conductivity, at a constant current density, reduces the cell voltage because it causes a reduction in the ohmic resistance in the solution (Chen, 2004). Since the voltage and electric current is proportional to the energy consumption, this results in decreased energy consumption (Kobyas, Can and Bayramoglu, 2003; Merzouk, Madani and Sekki, 2010). A common practice in order to increase the conductivity is to add NaCl into the suspension (Kobyas, Can and Bayramoglu, 2003; Chen, 2004).

#### 2.2.3.2.4 *Effect of inter-electrode spacing*

The inter-electrode spacing is proportional to the ohmic potential drop, also called IR-drop, which reflects the solution resistance (Chen, 2004; Mickova, 2015). Therefore, a larger inter-electrode spacing will increase the resistance and hence the energy consumption. Inter-electrode distance required to have a successful EF depends on the conductivity of the effluent that is treated. If the effluent has a high conductivity, the effects from the resistance due to spacing is weaker. However, the risk of short circuit must be evaluated when using a small inter-electrode spacing (Chen, 2004; Comninellis and Chen, 2010).

#### 2.2.3.2.5 *Effect of current density*

The current density is the electric current per unit cross section area. The current density is most important parameter in the EF process (Jiménez *et al.*, 2010; El-Hosiny *et al.*, 2017) as it affects the bubble generation directly. The bubble production increases with the increase of the current density (Jiménez *et al.*, 2010; Merzouk, Madani and Sekki, 2010; Sillanpa and Shestakova, 2017). The current density can be calculated using equation (2.1):

$$CD = \frac{I}{A_{anode}} \quad (2.1)$$

Where:

CD = Current density, A/m<sup>2</sup>

I = Electric current, A

A<sub>anode</sub> = Area of cross-section, m<sup>2</sup>

In addition, higher current densities decrease the bubble size (Chen, 2004; Sillanpa and Shestakova, 2017), which is favorable in with regards to removal rate. One explanation for this is that the repulsion from the negatively charged cathode and the hydrogen bubble will increase with higher current densities. The hydrogen bubble will have shorter nucleation time and it is then followed by an earlier detachment from the cathode. However, this patterns only applies for lower end of current densities. Higher current densities give greater bubble production that increase the collision, and may cause bubbles to coalesce. For this reason an optimum current density should be determined for the water (Jiménez *et al.*, 2010; Sillanpa and Shestakova, 2017). The energy and electrode consumption also increases with higher current densities (Kobyas, Can and Bayramoglu, 2003; Chen, 2004).

#### 2.2.3.2.6 *Electrode deactivation, passivation and polarity inversion*

Electrode deactivation is a sudden increase in the electrode potential, reaching very high values, resulting in an electrochemical failure. This deactivation may occur for several reasons. For DSA<sup>®</sup> electrodes among the common ones are (Martelli, Ornelas and Faita, 1994):

- Electrode passivation
- Coating consumption (most probable for medium to low current density).
- Coating detachment is possible if the bond between the substrate and the coating layer, especially if the coating layer is porous combined with quick gas evolution.
- Mechanical damages of the coating

Electrode passivation is a phenomena of an oxide layer formation on the electrode, which may partly or fully prevent further transfer of electron and hence stop the process of electrolysis. It is the most frequent reason for electrode deactivation associated with high current densities (Martelli, Ornelas and Faita, 1994). With regards to passivation, more studies have been

conducted within EC processes than EF processes, likely due to the high risk of passivation of Al electrodes, that is often used in EC (Comninellis and Chen, 2010).

There are alternatives to prevent passivation from happening or treat it once it has occurred. One alternative to reduce the passivation is to add Cl<sup>-</sup>, for instance by adding NaCl, into the suspension (Daneshvar, Sorkhabi and Kasiri, 2004; Comninellis and Chen, 2010). Regularly electrochemical cleaning the electrodes will also prevent the oxide film from growing. Increasing the turbulence in the reactor will also reduce the risk of passivation (Mollah *et al.*, 2004).

Another recommended solution is to reverse the polarity of the electrodes. Polarity reversal or polarity inversion, is a change in the poles of the electrodes, making the current flow the contrary direction. That way the previous cathode will act as an anode and the previous anode will be the new cathode. Polarity inversion can be done with frequency of minutes, hours or weeks, depending on the current density. The higher the current density, the more frequently the polarity reversal should be done. One disadvantage with polarity inversion is that it can be inefficient in removal of pollutants because the current efficiency drops significantly during the polarity change (Sillanpa and Shestakova, 2017).

#### 2.2.3.2.7 *Energy consumption*

The electrolysis voltage applied has to be at least the summation of the equilibrium potential difference, the anode and cathode overpotential and the ohmic potential drop of the aqueous solution (Comninellis and Chen, 2010). The energy consumption is dependent on the abovementioned factors such pH, conductivity, temperature and inter-electrode distance, that can regulate the current flow. The specific energy consumption can be calculated as with formula (2.2) (Comninellis and Chen, 2010):

$$W = \frac{IU}{1000Q_W} \quad (2.2)$$

Where:

$W$  = Specific energy consumption, kWh/m<sup>3</sup>

$U$  = Electrolysis voltage, V

$I$  = Electric current, A

$Q_W$  = Water flow rate, m<sup>3</sup>/h

In accordance with the Joule effect, electric current, with a constant resistance, may transform into thermal heat that is released to the surroundings due to the resistance when the current flows through the conductor (Cyclopedia, 2017). This power dissipation should be avoided in order to maintain an efficient power consumption.

### 2.2.3.3 Gas volume and bubble/particle ratio

The gas generation rate at standard temperature and pressure during electrolysis of water can be calculated using Faraday's law, shown in equation (2.3) and (2.4) (Comninellis and Chen, 2010).

$$Q_H = \frac{IV_0}{n_H F} \quad (2.3)$$

$$Q_O = \frac{IV_0}{n_O F} \quad (2.4)$$

Where:

$Q_{H/O}$  = Gas generation rate for H<sub>2</sub> and O<sub>2</sub> respectively, L/s

$V_0$  = molar volume of gases at normal state, 22,4 L/mol

$I$  = Electric current, A

$n_{H/O}$  = Electron transfer number for the respective reactions of H<sub>2</sub> and O<sub>2</sub>

$F$  = Faraday's constant, 96 500 C/mol

The minimum volume of gas needed to achieve flotation can be approached by using equation (2.5). As the density of air relative to water is small equation (2.5) can be simplified to equation (2.6) (Crittenden *et al.*, 2012).

$$\frac{\Phi_g}{\Phi_p} = \frac{\rho_p - \rho_w}{\rho_w - \rho_g} \quad (2.5)$$

$$\frac{\Phi_g}{\Phi_p} \cong \rho_p - 1 \quad (2.6)$$

Where:

$\Phi_g$  = Minimum volume of gas required for flotation, mL/L, ppm

$\Phi_p$  = Volume of particle, mL/L, ppm

$\rho_p$  = Density of particle, kg/m<sup>3</sup>

$\rho_w$  = Density of air, kg/m<sup>3</sup>

#### 2.2.3.4 Particle charge

All suspended particles have a charge and the charge is highly pH-dependent. The bubbles generated in EF have a charge the moment they detach from the electrode. Generally, the hydrogen bubbles are negatively charged, while the oxygen bubbles being positively charged. If the bubble and particle have the same charge, a repulsion will occur which will hinder attachment. Thus, higher EF efficiency is obtained when there is countercharge between particles and bubbles. For this reason, hydrogen bubbles have a higher metal removal efficiency than oxygen (Sillanpa and Shestakova, 2017).

#### 2.2.3.5 Advantages and disadvantages of electroflotation

There are several advantages of using EF. The EF reactor is compact and easy to operate. The bubbles generated in EF are smaller compared to DAF and other flotation technologies, creating a larger surface area that is favorable in for flotation (Comninellis and Chen, 2010). In addition, the bubble size and production can be regulated by the applied current, and the system has a

low turbulence (Kyzas and Matis, 2016). The regulation in current makes it easy to fit the bubble production to variation in flow rate and the concentration of particles in the water (Comninellis and Chen, 2010). As the system is run at low voltage (5-20 V) it is also safe in operation (Kyzas and Matis, 2016).

Should it be difficult to dissolve air in the suspension, as done in DAF, EF can be used as an alternative. The sludge created in the process is very dense, and therefore has low water losses (Sillanpa and Shestakova, 2017). If chloride ions are present, there is a possibility of having a parallel process of disinfection (Comninellis and Chen, 2010; Sillanpa and Shestakova, 2017).

However, there are some disadvantages as well. EF becomes costly to operate if the conductivity in the suspension is low, as a higher electric current must be applied to reach the required bubble production. The risk of deactivation of the anodes, particularly passivation, limits the use.

#### 2.2.3.6 Application of EF

The application of EF in drinking water treatment has been limited, possibly due to the low conductivity in the source water resulting in a high energy consumption. EF has shown good effectivity in treatment of wastewater and industrial water, among others heavy metal containing effluents, oily water and wastewater, mining wastewater and groundwater (Srinivasan and Subbaiyan, 1989; Alexandrova, Nedialkova and Nishkov, 1994; Hosny, 1996; Poon, 1997; Ibrahim *et al.*, 2001; Comninellis and Chen, 2010; Campos *et al.*, 2017; Sillanpa and Shestakova, 2017).

A study made by Ghernaout, Benblidia and Khemici (2015) looked at the efficiency of EF processes on microalgae removal using horizontally placed stainless steel electrodes. Although cyanobacteria are not considered algae anymore, there high resemblance in characteristics may indicate that treatments used for algae removal might have the same effect on cyanobacteria. The results from the study showed a removal rate of approximately a 100%, with the optimal conditions being a current density of  $170 \text{ Am}^{-2}$ , an inter-electrode distance of 1 cm, pH 7,8 and EF duration of 15 minutes (Ghernaout, Benblidia and Khemici, 2015). The study did not, however, study the risk of cell lysis and potential toxins release.

Although few studies on EF in drinking water treatment have been conducted, some have used a combination of EC and EF processes, ECEF, by using soluble electrodes such as Al and Fe for drinking water treatment (Gao *et al.*, 2010).

### **2.3 Filtration**

Filtration has been used for thousands of years to clarify water, dating back to 2000 BC in India (Crittenden *et al.*, 2012). Filtration is a separation process characterized by flow through a permeable layer, such as membrane, sieve or porous media. The suspended solids are retained by the filter when water flows through. As the filter pores are gradually filled with the retained solids, the hydraulic resistance increases, and the filter needs to be cleaned in order to avoid clogging or break through of the pollutants (TU Delft, 2007).

Within granular filtration, where sand is often used as filter media, filtration can be divided into pressure filters, vacuum filters and gravity filters, the latter being the most frequently used. Gravity filters can be divided in slow filtration, rapid filtration and high rate filtration. The essential difference between these are the filtration rate they run at, slow filtration having the lowest rate and high rate filtration having the highest (G.Pizzi, 2011). A comparison of typical design criteria for slow sand filtration and rapid filtration can be found in Table 2.1. Rapid filtration is used more frequently in water treatment (TU Delft, 2007), and in the following we will only focus on rapid filtration by porous media.

**Table 2.1: Comparison of slow sand filtration and rapid filtration design criteria\*.**

Process Characteristics	Slow Sand Filtration	Rapid Filtration
Filtration rate	0,08 - 0,25 m/h	5 - 15 m/h
Media effective size	0,15 – 0,30 mm	0,50 – 1,2 mm
Media uniformity coefficient	< 2,5	< 1,4
Bed depth	0,9 – 1,5 m	0,6 – 1,8 m
Required head	0,9 – 1,8 m	1,8 – 3,0 m
Run length	1 – 6 months	1 – 4 days
Ripening period	Several days	15 min – 2 h
Pretreatment	None required	Coagulation
Dominant filtration	Straining, biological activity	Depth filtration
Regeneration method	Scraping	Backwashing
Maximum raw water turbidity	10 NTU	Unlimited with proper pretreatment

\* Typical ranges. Some filters are designed and operated outside these ranges

*Source: Adapted from Crittenden et al. (2012)*

### 2.3.1 Rapid filtration

Rapid filtration is the most common type of filtration used for water treatment. Usually, downward flow is used, but upward flow has also been implemented in some treatment plants (Edzwald James K., 2010). For treatment of surface water, the water generally goes through flocculation process before filtration. For ground water treatment the filters usually comes after a aeration process in order to remove iron, manganese and ammonium (TU Delft, 2007).

#### 2.3.1.1 Classifications of rapid filtration

The sequence of treatment before filtration can vary depending on the characteristics of the raw water. Shortly, the process sequences can be divided into four types; conventional filtration, contact filtration, direct filtration and two-stage filtration (Crittenden *et al.*, 2012).

Conventional filtration is a combined process of mixing with coagulation, flocculation and sedimentation before the water enters the filtration step. The sedimentation step is the success of this process as it separates most of the suspended particles in the water and leaves the treated water with a turbidity of 2 to 3 NTU. For this reason, conventional treatment can be applied to raw water with high NOM, turbidity and algae level (Edzwald James K., 2010; G.Pizzi, 2011; Crittenden *et al.*, 2012).

Direct filtration consists of the same steps as conventional treatment, except that it does not have a sedimentation step, and for this reason is less costly than conventional filtration. For this reason, direct filtration is more suitable for raw waters with turbidity < 15 NTU (Edzwald James K., 2010; Crittenden *et al.*, 2012).

Contact filtration, also called in-line filtration, is the same as direct filtration, but further reduced by partly or fully removing the flocculation step. It requires high quality raw water with a turbidity < 10 NTU (Crittenden *et al.*, 2012).

Two-staged filtration are pre-engineered systems for small treatment plants. They consist of a coagulation step, followed by a roughing filter before filtration and can handle raw water with turbidity < 100 NTU (Crittenden *et al.*, 2012).

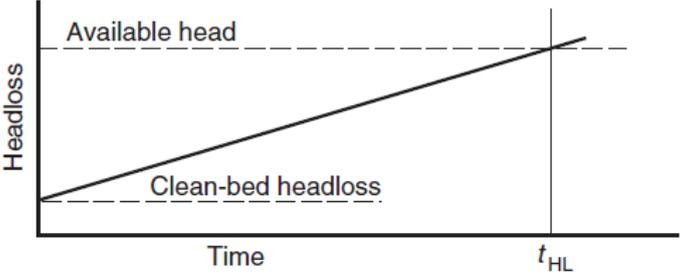
#### 2.3.1.2 Filtration stage

The filtration efficiency for particle capture is reflected in the head loss and the effluent turbidity. Both of these will vary during one filtration stage, called a filter run. The end of a filter run can be triggered by many factors, such as the filter head loss reaching the time of available head  $t_{HL}$ , or the turbidity reaching a point where it rapidly increases, called turbidity breakthrough. The available head in gravity driven filters are typically 1,8-3 m. In an optimal filter design, the filter will reach terminal head loss and filter breakthrough at the same time (Crittenden *et al.*, 2012).

After one of, or both, events have ended the filter run, the filter needs to be cleaned by removing the filtered material, a process called backwashing. When the filter is operated again after the backwash, the turbidity of the effluent will rise rapidly and decrease again, known as ripening,

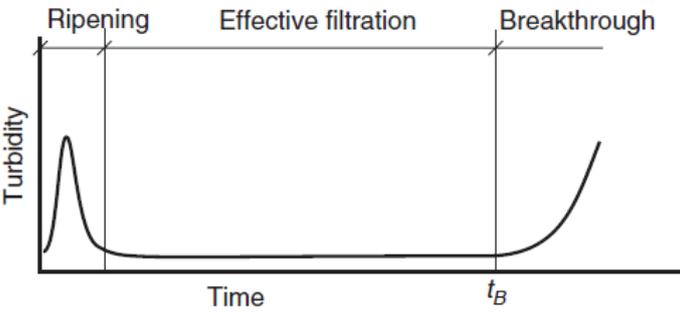
or maturation. The reason for this is that captured particles in the filter will create a better filter efficiency than uncoated grains. The effluent from the ripening phase will be filtered to waste or recycled to the head of the plant until the ripening phase is over and the turbidity is stabilized. A typical filter run is shown in Figure 2.12 and Figure 2.13 (Crittenden *et al.*, 2012).

**Figure 2.12: Head loss versus time during filtration.**



Source: Crittenden *et al.* (2012)

**Figure 2.13: Effluent turbidity versus time during filtration.**



Source: Crittenden *et al.* (2012)

Some filters do not reach terminal head loss or breakthrough in a long time, but are generally still backwashed to maintain a convenient schedule for plant operators (Crittenden *et al.*, 2012).

2.3.1.3 Clean bed head loss

As previously mentioned, the head loss through a filter will increase during filtration. The clean bed head loss depends among others on the flow regime in the filter, that is the Reynolds number (Re) of the flow, which is often between 0,5 and 5 in rapid filtration. There has been developed formulas that can calculate the clean bed head loss. The first formula that calculated the head

loss through granular filter media was set by Henry Darcy, equation (2.7), for creeping flow, that is an Re of about less than 1 (Crittenden *et al.*, 2012).

$$v = k_p \frac{h_L}{L} \quad (2.7)$$

Where:

$v$  = Superficial velocity (filtration rate), m/s

$k_p$  = Hydraulic permeability, m/s

$h_L$  = Head loss across media bed, m

$L$  = Depth of granular media, m

Darcys does not take account for the filter media. Kozenys equation, equation (2.8), takes into account the filter media for head loss in a granular filter for laminar flow. Kozenys equation is based on Poiseuille's law of laminar flow through cylindrical tubes. It is further developed by equating the bed void volume to the total internal channel volume, and the media surface area to internal channel surface area. The Kozeny coefficient is an empirical coefficient (Crittenden *et al.*, 2012).

$$\frac{h_L}{L} = \frac{\kappa_k \mu S^2 v}{\rho_w g \varepsilon^3} \quad (2.8)$$

Where:

$\kappa_k$  = Kozeny coefficient, uniteless

$\mu$  = Dynamic viscosity of fluid, kg/m s

$g$  = Acceleration due to gravity, 9,81 m/s<sup>2</sup>

$\rho_w$  = Density of water, kg/m<sup>3</sup>

$\varepsilon$  = Porosity of filter bed

$S$  = Specific surface area, m<sup>-1</sup>

The head loss for Re larger than 1 was later shown to be larger than shown in equation (2.8) This resulted in equation (2.9), proposed by Forchheimer in 1901, that was more accurate for larger media and higher velocities (Crittenden *et al.*, 2012).

$$\frac{h_L}{L} = \kappa_1 v + \kappa_2 v^2 \quad (2.9)$$

Where:

$\kappa_1$  = Permeability coefficient for liner term, s/m

$\kappa_2$  = Permeability coefficient for liner term, s<sup>2</sup>/m<sup>2</sup>

Ergun developed equation (2.10) in 1952 with the flow conditions of Forchheimer regime, known as the Ergun equation. The Ergun equation was based on experimental data from 640 experiment with Re ranging from 1 to 2000 (Crittenden *et al.*, 2012).

$$\frac{h_L}{L} = \kappa_V \frac{(1 - \varepsilon)^2}{\varepsilon^3} \frac{\mu L v}{\rho_w g d^2} + \kappa_I \frac{1 - \varepsilon}{\varepsilon^3} \frac{L v^2}{g d} \quad (2.10)$$

Where:

$\kappa_V$  = Head loss coefficient due to viscous forces, unitless

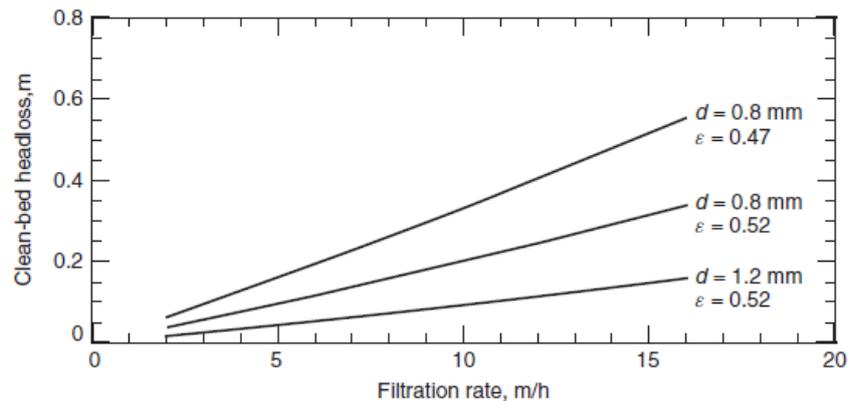
$\kappa_I$  = Head loss coefficient due to inertial forces, unitless

d = Media grain diameter, m

$\rho_w$  = Fluid density, kg/m<sup>3</sup>

The clean bed head loss is sensitive to filtration rate, porosity and media diameter, as shown in Figure 2.14. The head loss also depends on temperature, increasing with lower temperatures.

**Figure 2.14: Effect of filtration rate, media size and bed porosity on clean bed head loss.**



Source: Crittenden *et al.* (2012)

### 2.3.2 Filter media

The filter media used for filtration must be prepared specifically for filtration use. Commonly sand, anthracite coal, granular activated carbon (GAC) and garnet sand are used as filter media, either alone or in combination. The desired qualities for the filter media are (Noel *et al.*, 1995; TU Delft, 2007):

- Course enough so large flocs can be retained
- Fine enough in order to prevent breakthrough of suspended particles
- Deep enough to maintain a long operation of the filter
- Well graded in order to improve backwashing and cleaning of the media
- Hard and durable
- Insoluble in water and not react with substances in the water

One must consider the relation between head loss, which is smaller for larger media, and filtration efficiency, which is larger for larger media when choosing filter media. Some recommend a rule of thumb that the ratio between filter depth and effective size of filter media ( $L/d$ ) is between 1000-2000. This should however only be used as a general guidance, as two filters with the same  $L/d$  ratio will not necessarily perform equally (Crittenden *et al.*, 2012).

### 2.3.2.1 Grain size and distribution

There are some important characteristics of the filter media that should be considered when choosing. One of these are the size and size distribution. The filter media size is expressed in the effective size, ES or  $d_{10}$ , that is the 10-percentile diameter, meaning 90% of the material has a diameter larger than this. The size distribution, or uniformity, of the material can be expressed by calculating the uniformity coefficient, U, which is the ratio of the 60-percentile,  $d_{60}$ , and  $d_{10}$ . A uniformity coefficient value of 1 means that the material is uniform and higher values means less uniform material. Both  $d_{10}$  and  $d_{60}$  is found by sieve analysis of the filter media. In addition to these, the  $d_{90}$  is also important as it is used to calculate the backwash rate, as the minimum backwash rate should fluidize the  $d_{90}$ . In water treatment, conventional sand medium usually has an effective size of 0,45-0,55 and a uniformity coefficient of 1,6-1,75, while a uniformity coefficient of less than 1,4 is recommended for rapid filter media (Camp, no date; G.Pizzi, 2011; Crittenden *et al.*, 2012).

$$ES = d_{10} \quad , \quad U = \frac{d_{60}}{d_{10}} \quad (2.11)$$

### 2.3.2.2 Grain shape

The grain shape is an important parameter as it affects the sieve analysis, how the filter grains pack in the bed and the hydraulics through the filter bed. However, it is a difficult parameter to measure. Usually, the grain shape is given by either the sphericity ( $\psi$ ) or shape factor ( $\xi$ ), shown in. The sphericity expresses how close to a sphere a particle is. It is given by a ratio of the surface area of an equivalent-volume sphere and the actual surface area of the grain, meaning a sphericity of 1 is a perfect sphere. The equations for sphericity and shape factor are shown in (2.12) and (2.13) (Crittenden *et al.*, 2012).

$$\psi = \frac{\text{surface area of equivalent – volume sphere}}{\text{actual surface area of grain}} \quad (2.12)$$

$$\xi = \frac{\psi}{6} \quad (2.13)$$

Where:

$\psi$  = Sphericity, dimensionless

$\xi$  = shape factor, dimensionless

### 2.3.2.3 Grain density and hardness

The grain density, or specific weight, is also an important characteristic as it influences the fluidization and settling velocity during and after backwash. Denser materials of equal size require a higher backwash velocity (Crittenden *et al.*, 2012).

The grain hardness is important as it affects the durability of the filter material, and is expressed by Mohs scale of hardness (talc=1, diamond=10). A low hardness will result in deformation or breaking of the grains during backwashing. It is not applicable for some material, such as sand, garnet and ilmenite, but must be specified for anthracite and GAC. A minimum value of 2,7 on Mohs scale is often set for anthracite (G.Pizzi, 2011; Crittenden *et al.*, 2012).

### 2.3.2.4 Specific surface area and filter porosity

Lastly, the specific surface area and porosity are important as they affect the beds ability to retain particles and the head loss through the filter. Filter bed porosity usually ranges from 40-60%. The porosity and specific surface area can be calculated with equations (2.14) and (2.15), respectively (Crittenden *et al.*, 2012).

$$\varepsilon = \frac{V_V}{V_T} = \frac{V_V - V_M}{V_T} \quad (2.14)$$

Where:

$\varepsilon$  = Filter bed porosity, dimensionless

$V_V$  = Void volume in media, m<sup>3</sup>

$V_T$  = Total volume of media med, m<sup>3</sup>

$V_M$  = Volume of media, m<sup>3</sup>

$$S = \frac{(\textit{number of grains})(\textit{surface area of each grain})}{\textit{bulk volume of filter bed}} \quad (2.15)$$

Where:

$S$  = Specific surface area, m<sup>-1</sup>

### 2.3.2.5 Arrangement of filter media

In an ideal filter, the porosity should be higher at the top and gradually decrease toward the bottom (Camp, no date). The reason for this is that the particles will be able to penetrate deeper in the filter and that way there will be larger available area to retain the particles. As a result, the increase in filter resistance will be spread across the filter and longer filter runs are possible (TU Delft, 2007).

For single media filters, the porosity will be contrary to the ideal filter, that is that the porosity is higher at the bottom of the filter rather than the top. This happens as a result of backwashing, leaving the largest grains to settle down first. To solve this problem one can use two or more filter medias. Often crushed anthracite coal is placed above a sand layer, creating a filter referred to as a dual-filter media. The anthracite grains are coarser and have a lower density than the sand, creating a larger porosity of the at the top of the filter. Placing a very dense layer below the sand, like garnet or ilmenite, allows the addition of a very fine grained third layer. During backwashing some mixing will occur, leaving the filter with no distinct interface between the layers. That way a gradual decrease in porosity downwards to the bottom of the filter will occur,

and the filter bed will approach the ideal (Camp, no date; TU Delft, 2007; G.Pizzi, 2011; Crittenden *et al.*, 2012).

Use of granular activated carbon (GAC) instead of anthracite is also possible. GAC is a good adsorbent as it is highly porous and has a large surface area. GAC is commonly used to remove taste and odor in water. One disadvantage of GAC is that it has to be removed and regenerated after its effectiveness has ceased (G.Pizzi, 2011).

Often a layer of gravel, usually 150-450 mm thick depending on the underdrain system, is placed below the filter media as support to prevent the media from entering the underdrain system. Today there exists filters that are designed to be able to support the filter media, and therefore do not require a layer of gravel (G.Pizzi, 2011).

At the bottom of the filter is the underdrain system and they serve two services. One is collecting the filtered water uniformly across the filter, to maintain the filtration rate across the filter. In addition, they distribute the backwash water evenly without disturbing the filter media unruly (G.Pizzi, 2011).

### **2.3.3 Filtration backwash**

Backwashing of filters, or filter cleaning, is critical in order to maintain efficient filtration, and poor backwashing is the cause of most operating problems in filtration processes. While the filtration is running, the voids between the media grains will be filled with filtered flocs. In addition to this, the flocs will cover the media grains, making them sticky. Because of this, the filter must be agitated violently, in order to dislodge the sticky coating (G.Pizzi, 2011), but without using too much water and energy in the process.

#### **2.3.3.1 Factors determining the frequency of backwash**

The frequency of backwash needed can vary from treatment plants. Head loss, turbidity of the effluent filter and the unit filter run volume (UFRV), that is the volume of filtered water during one filter run divided by the cross-section area of the filter, must be considered in the determination of the backwash frequency required. According to G.Pizzi (2011) a filter should usually be backwashed when one or more of the below points, in order of importance, occur:

- Turbidity breakthrough is reached, meaning that limit for effluent turbidity is reached a point where it will start to rapidly increase. An increase in cell count can also be used in this point if applicable.
- Terminal head loss is reached, meaning that the head loss has rose to a level where water is not produced at the desired rate anymore and air binding may occur.
- UFRV rising towards unreasonable limits. Usually the interest is to keep the UFRV between 5 000 and 10 000. Higher values may lead to floc breakthrough.

### 2.3.3.2 Mechanism

Treated water is always used for backwashing to avoid further contaminating of the filter, and around 1-5 % of produced water is used for backwashing. The filter media will expand, and the flocs washed out of the filter will end up in the water-wash trough. Backwash water should always be discharged in a water receptor, such as rivers or lakes, but are sometimes recycled to head of the plant. The process of backwashing is in short this sequence (G.Pizzi, 2011):

1. Drainage of the water in the filter to a height of about 150 mm above the filter surface.
2. If the plant operates with surface washers, they are turned on and allowed to operate for about 1-2 minutes. This way the filtered material on the surface will break up. Air scouring can be used as an alternative here.
3. The backwash valve is partly opened and allows the bed to expand. This way the top layer, that contains most of the filtered material, will be exposed to violent scrubbing, detaching the particles form the filter grains.
4. The backwash valve is fully opened and expand the filter to between 20-30 %. How much expansion that is needed depends on how much is required to suspend the coarsest grains in the filter. For multimedia filter, the bed must be expanded so that surface washers can wash the interface between the layers as this is where most filtered material has penetrated.
5. The surface washers are turned off a little before the backwash flow is stopped. Filter is left to restratify into layers.

The expanded bed is usually washed for 5-15 minutes, depending on what is required. The time of backwashing should not be too long as this will increase the time for the filter to ripen. As a result the filter will produce water of high turbidity for a longer time, before the filter stabilizes. It is especially important for filters that cannot filter to waste to pay attention to this. An indicator of when to stop washing can be approached by measuring the turbidity of the water that passed the wash-water troughs (G.Pizzi, 2011; Crittenden *et al.*, 2012).

After the backwash is completed, the filter needs to ripen. In this time the water filtered is filtered to waste as it does not meet the requirement of turbidity level. It is also recommended to let the filters rest if possible, as this has been shown to reduce the ripening time (G.Pizzi, 2011).

### 2.3.3.3 Backwash rate and filter bed expansion

The backwash rate, or fluid velocity, during backwash needs to be adequate to fluidize the bed to the required expansion. If it is too high, the filter bed will expand too much and filter media may be lost in the wash-waters. The required backwash rate to fluidize a particle  $d$  can be calculated with equation (2.16) (Crittenden *et al.*, 2012).

$$v_b = \frac{\mu Re}{\rho_w d} \quad (2.16)$$

Where:

$v_b$  = backwash velocity, m/s

$\mu$  = dynamic viscosity of fluid, kg/m s

Re = Reynolds number for flow around a sphere, dimensionless

$\rho_w$  = water density, kg/m<sup>3</sup>

$d$  = media grain diameter, m

There has been shown that Ergun's equation applies for fixed and expanded bed. Equation (2.10) can then be combined with the equation for head loss through a fluidized bed. By using Reynolds number and rearrangement of the equation, the backwash calculation factor,  $\beta$ , can

be introduced as shown in (2.17) and Reynolds number can be calculated with equation (2.18) (Crittenden *et al.*, 2012).

$$\beta = \frac{g\rho_w(\rho_p - \rho_w)d^3\varepsilon^3}{\mu^2} \quad (2.17)$$

$$Re = \frac{-\kappa_V(1 - \varepsilon) + \sqrt{\kappa_V^2(1 - \varepsilon)^2 + 4\kappa_I\beta}}{2\kappa_I} \quad (2.18)$$

Where:

$\beta$  = backwash calculation factor, dimensionless

$g$  = acceleration due to gravity, 9,81 m/s<sup>2</sup>

$\rho_p$  = particle density, kg/m<sup>3</sup>

$\varepsilon$  = porosity, dimensionless

$\kappa_V$  = head loss coefficient due to viscous forces, unitless

$\kappa_I$  = head loss coefficient due to inertial forces, unitless

The filter bed expansion related to the porosity of the bed can be expressed by equation (2.19) (Crittenden *et al.*, 2012).

$$\frac{L_E}{L_F} = \frac{1 - \varepsilon_F}{1 - \varepsilon_E} \quad (2.19)$$

Where:

$L_E$  = depth of expanded bed, m

$L_F$  = depth of bed at rest (fixed bed), m

$\varepsilon_F$  = porosity of expanded bed, dimensionless

$\varepsilon_E$  = porosity of bed at rest (fixed bed), dimensionless

### **2.3.4 Process challenges with filtration**

According to G.Pizzi (2011) the most common operation problems in filtration are related to:

1. Chemical treatment
2. Control of filter flow rate
3. Backwashing the filter

#### 2.3.4.1 Chemical treatment

Proper coagulation/flocculation is important to have successful filtration. The required coagulant dose can change with the raw water characteristics such as temperature and turbidity. For this reason, the dosage changes during filtration are often necessary, and instruments continuously measuring turbidity, head loss and flow rate are important. If short filter runs are caused by turbidity breakthrough, more coagulant or better mixing might help. If the short filter runs are caused by rapid buildup of head loss, less coagulant may be required (G.Pizzi, 2011).

#### 2.3.4.2 Control of filter flow rate

Rapid fluctuations in the flow rate can force previously deposited particles through the filter media. The more deposited material there is in the filter initially, the more problems the rate fluctuations cause. The reason for these may be caused by an increase in total plant flow, malfunctioning flow-of -rate controller, a flow increase when the filter is taken out of service for backwashing, or an operator error (G.Pizzi, 2011).

If the flow rate needs to be increased to meet demands, the increase should be made gradually. Filter aids, for instance polymers, reduces the risk of flocs breaking when entering the filter and may reduce the problems related to the flow increase. With regards to flow rate after backwashing, an abrupt surge though the filters may occur when the filters remaining in operation take over the load from the filter that is backwashed. To avoid this problem, a clean filter should be kept in reserve, although this may not be possible for treatment plants with few filters. Filters that only operate part of the day should be backwashed before they are placed into service again to avoid that filtered material break through because of the surge that occurs (G.Pizzi, 2011).

### 2.3.4.3 Problems related to backwashing

Ineffective backwashing can cause a series of problems and keeping good standard operating procedures and operator training is important to maintain high quality water.

#### *2.3.4.3.1 Mudball formation*

The filter grains are covered with sticky floc material during filtration. If this material is not removed during backwashing, the grains will clump together and form mudballs. When the size of mudballs become larger, they may sink into the filter bed during backwashing and clog the areas they settle, creating areas in the filter that become inactive. This can cause higher filtration rates, that are not favorable, in the active areas of the filter and unequal distribution of backwash water. To avoid the problem, periodic check for mudballs should be done and adequate backwash flow rate and surface agitation is required. For multimedia filters, filter agitation is important as the mudballs may form deep within the filter bed (G.Pizzi, 2011).

#### *2.3.4.3.2 Shrinkage of filter*

The filter may be exposed to shrinkage or compaction if the backwashing is not efficient. Dirty filter media grains have filtered material separating them. When the head loss increases, the bed will compress and shrink. This will create cracks in the filter and the filter media may separate from the filter walls. The water will then pass through the cracks, being exposed to little or no filtration, resulting in bad quality of the effluent water (G.Pizzi, 2011).

#### *2.3.4.3.3 Gravel displacement*

The supporting gravel bed can be displaced into the overlaying filter media when the backwashing valve is opened to quickly or if a part of the underdrain system is clogged. When the gravel is displaced, it may create a sand boil, with little or no filter media over the gravel at the boil. The water passing through during filtration will receive little to no filtration. Also, the filter media may be washed into the undertrain system. Some displacement of the gravel will always occur, but the filter should be checked in case of serious displacement. If the displacement is too severe, the filter media must be removed and the gravel must be regraded or replaced. Severe gravel displacement can be avoided by not using too high backwash rates and placing a layer of coarse garnet above the gravel (G.Pizzi, 2011).

#### 2.3.4.4 Media loss

Some media loss always occurs during backwashing, especially if surface washers are used in addition. However, if there are considerable quantities being lost the procedures should be examined. Having lower filter expansion during backwashing may help. Since the filter bed is usually completely fluidized at 20 % expansion, further expansion may not be needed. If surface washers are used, turning them off 1-2 minutes before the main backwashing is stopped the loss of filter media can be reduced. If these implementations does not suffice, the wash-water troughs must be raised in order to prevent loss of media (G.Pizzi, 2011).

#### 2.3.4.5 Air binding

Air binding is a process where air is trapped in the filter. This occurs when the filter is operated at a pressure that is lower than the atmospheric, called negative head, and often occurs in filters with less than 1,5 m of water over the unexpanded bed. The air dissolved in the water will then form bubbles within the filter bed. Air binding creates resistance to the flow and results in short filter runs. In addition, during backwashing the trapped bubbles will agitate the filter further, and may cause loss of filter media in the wash-water troughs (G.Pizzi, 2011).

### **2.3.5 Plastic grains used as filter media**

The polyvinyl chloride (PVC) used as filtration media in this study have to the authors' knowledge never been used as a filter media. One motivation of using PVC, or other plastic components, as filter media could be that it is a lightweight and reusable material. In Norway the water treatment plant at Skullerud uses a three-layered filter, two layers of plastic granules with different density above one layer of sand (Schöntag and Sens, 2015).

Schöntag and Sens (2015) made a study using polystyrene spheres as granular filter media. The filtration seems to work similarly to sand. Backwashing rates required were lower, but the duration was longer and therefore not necessarily considered economically beneficial.

*(This page is left blank intentionally)*

### **3 Methodology**

The experiments were conducted at Laboratório de Potabilização das Águas (LAPOA), localized at Department of Sanitary and Environmental Engineering at Universidade Federal de Santa Catarina (UFSC) in Florianópolis, Brazil.

#### **3.1 Raw water collection**

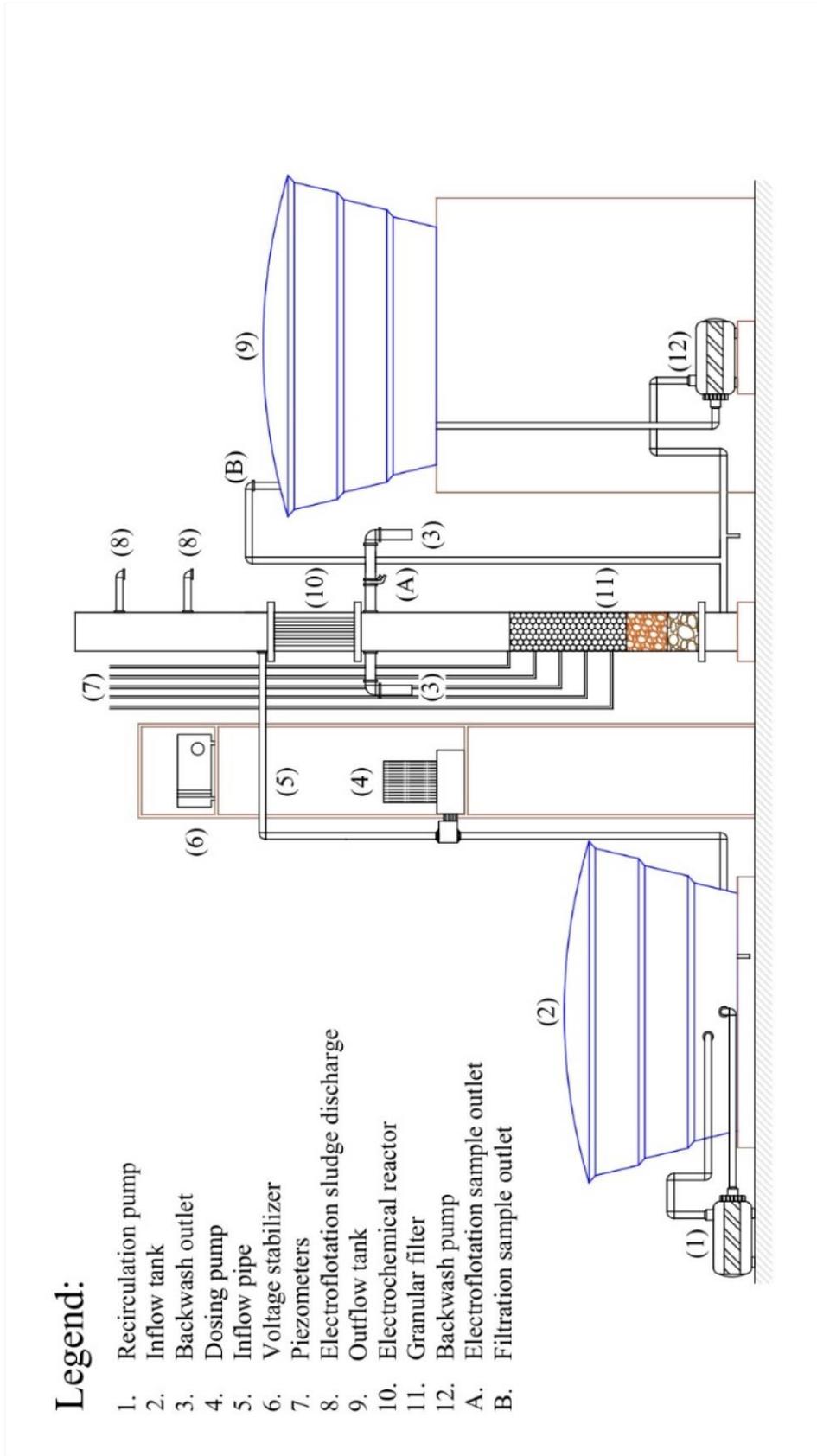
The water used in this study was collected from the tank of pumped raw water from the treatment plant of Lake Peri in Florianopolis, Brazil. The water was collected in barrels of 25 L. Each barrel was washed with the raw water before it was filled and driven to the pilot location at LAPOA, UFSC. For each experiment, a quantity of around 200 L of water was collected and each experiment was conducted on the day of collecting the water, apart from one experiment that was conducted the following day because of flood related challenges.

#### **3.2 Pilot system**

The pilot was projected, developed and constructed in the LAPOA/UFSC. It was prebuilt and had been used for previous experiments (Campos *et al.*, 2017, 2018). For this experiment, the upper part of the cylinder with the EF reactor was dismantled in order to add the PVC spheres in the filter before it was mounted again.

The pilot system consisted of a 500 L tank to store the raw water and a main cylinder with a descending filter and an electroflotation reactor above the filter. The EF reactor was connected to a voltage stabilizer (INSTRUTEMP-ITFA 5020). Three pumps were connected to the system, two ½ HP pumps (Schneider-BC-98), one used to recirculate the water in the inflow tank and one used for filter backwash, and one dosage pump (Grabe-DDM 130-07-PP/TF-1). The dosage pump feeds the EF-reactor and goes through the flotation process before the water passes the electrodes and goes through the filter. The treated water goes to an outflow tank. The water in this tank is used for filter backwashing. A schematic of the pilot can be seen in Figure 3.1.

**Figure 3.1: Schematic of pilot**

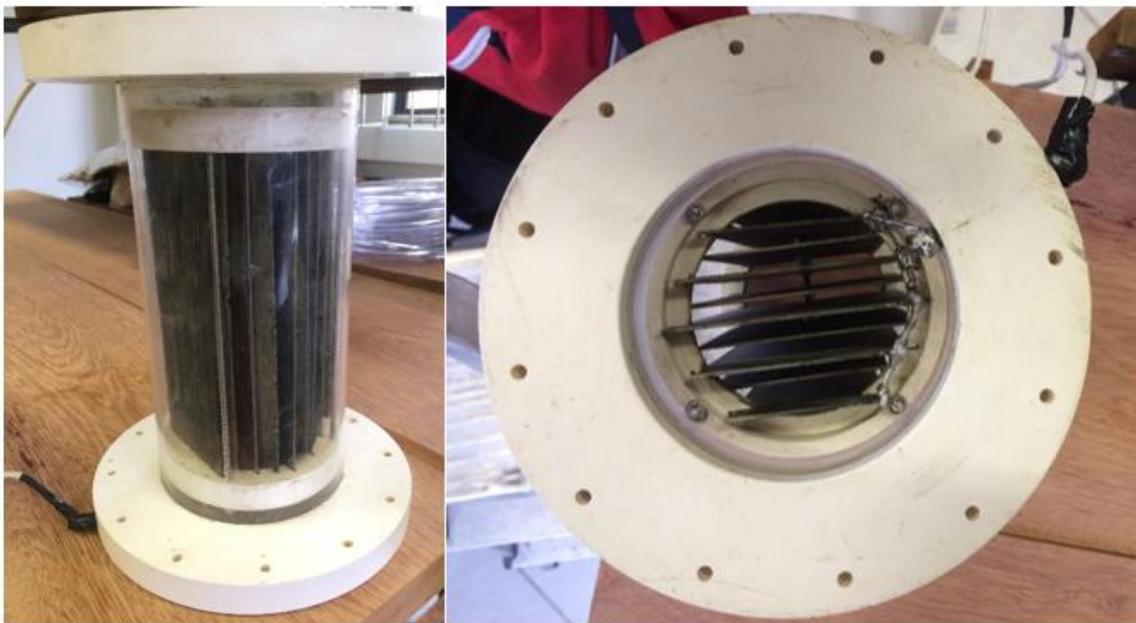


*Source: By author*

### 3.2.1 Electrochemical reactor

The electro flotation reactor consisted of 10 electrodes, 5 DSA<sup>®</sup>, composed of Ti/Ru<sub>0,34</sub>Ti<sub>0,66</sub>O<sub>2</sub>, a titanium base covered with a mixed material layer consisting of RuO<sub>2</sub> and TiO<sub>2</sub>, and 5 titanium cathodes as seen in Figure 3.2. The electrodes were set up vertically, alternately DSA<sup>®</sup> and cathode, and with an electrode distance of approximately 0,8 cm, and a total effective area of 785 cm<sup>2</sup>. The electrochemical reactor has been used previously (Campos *et al.*, 2017, 2018) and some corrosion is observed on the DSA<sup>®</sup>.

**Figure 3.2** Electrode set up seen from the side (left) and above (right).



*Source: By author*

The electrodes are connected to a voltage stabilizer (INSTRUTEMP-ITFA 5020), used to adjust the current density in the experiments.

### 3.2.2 Filtration

The filter media used in the filtration cylinder consisted of polyvinyl chloride (PVC) spheres (airsoft pellets often used in airsoft guns), and two layers of coarser gravel support at the bottom as shown in Figure 3.3. The filter height of the PVC spheres was 34 cm, 12 cm for the gravel support below (support layer 1) the spheres and 9 cm for the coarsest gravel support (support layer 2) at the bottom of the filter. The internal cylinder cross section area was 102 cm<sup>2</sup>.

**Figure 3.3 Total filter column (left) and two layers of gravel support (right)**



*Source: By author*

Each PVS sphere, with a sphericity of 1, had a diameter of 6 mm and weighed 0,12 g, meaning they have a low density of only 1,061 g/cm<sup>3</sup>, and had a filter porosity of 38%. A study by (Dalsasso, 2005) consisted three spheres with approximately same properties as the PVC spheres used in this study. For the specific surface area of the PVS spheres used in this study, an average value of those given in Dalsasso (2005) was applied, resulting in a specific surface area of approximately 1007 m<sup>2</sup>/m<sup>3</sup>.

Five piezometers were installed in the filter from previous experiments (Campos *et al.*, 2017, 2018). These piezometers will from here on be referred to as Piezo 1, 2, 3, 4 and 5, where Piezo 1 is the above the filter bed and Piezo 5 is the piezo placed at the lowest depth. The distance between the filter surface and each piezometers is shown in Table 3.1. Piezo 4 did not function after attempts of cleaning it and was therefore not used in the experiments.

**Table 3.1: Depth of piezometers**

<b>Distance below filter surface</b>	<b>Piezo 1</b>	<b>Piezo 2</b>	<b>Piezo 3</b>	<b>Piezo 4</b>	<b>Piezo 5</b>
cm	N/A*	0,5	10,5	N/A*	30,5

\* Not applicable

All the piezometers are within the PVC filter media, as can be seen from the right side photo in Figure 3.3, showing the deepest piezometer, Piezo 5. Piezo 5 is placed around 5 cm above the support layer 1.

### **3.3 Experimental procedure**

The integrated process of EF and rapid filtration was studied in using an electrochemical reactor placed above a rapid filter column for the separation of cyanobacteria from raw water collected from Lake Peri.

A total of 6 main experiments were conducted. As some challenges were encountered, two additional experiments were done, one assessing the effects of retention time and sample outlet and the other assessing the effects of polarity inversion. Experiment that assessed retention time and sample outlet was done before any of the 6 main experiments were conducted, see section 3.3.2.1.

#### **3.3.1 Experiments**

In the study by Campos *et al.* (2018) it was found that the optimal current density was 70,1 A/m<sup>2</sup> with an inflow rate of 33% of the pumps maximum discharge, resulting in a flow rate of around 12,1 ml/s, with regards to removal of cyanobacteria. This study was conducted by using the same pilot system and water from Lake Peri. For this reason, the optimal conditions that resulted from the study was used as a base for this thesis.

In order to evaluate the performance of the EF reactor a total of 6 experiments were conducted with a fixed inflow rate 12,1 ml/s and a varied current density. Table 3.2 gives an overview of the experiments conducted and their respective variables. The experiments are written in

chronological order, Experiment 1 being the first one conducted and Experiment 6 being the last. Experiment 2 was the only experiment conducted the day after collection of water, this due to flood related complications on the day of collection.

**Table 3.2: Overview of experiments conducted**

<b>Experiment</b>	<b>Inflow rate* (ml/s)</b>	<b>Duration (hours)</b>	<b>Salt concentration (mg/l)</b>	<b>Current density (A/m<sup>2</sup>)</b>	<b>Polarity</b>
1	12,1 ml/s	6	58,7	70,1	Normal**
2	12,1 ml/s	6	43,7	31,8	Normal**
3	12,1 ml/s	6	115,9	114,6	Inverted***
4	12,1 ml/s	6	46,7	114,6	Inverted***
5	12,1 ml/s	6	103,3	89,2	Normal**
6	12,1 ml/s	6	40,5	51	Normal**

\* Not the necessarily actual inflow rate. See section 4.2.4

\*\* DSA® used as anodes, titanium electrodes used as cathodes

\*\*\* DSA® used as cathodes, titanium electrodes used as anodes

As seen from Table 3.2 Experiment 3 and 4 were conducted with polarity inversion. This was chosen in order to avoid further corrosion of the DSA® as the current density was high and would probably fasten the speed of corrosion. Initially, Experiment 3 was set to be used, but as the results came out quite different from the two previous experiments, the experiment was conducted again using a lower salt concentration, resulting in Experiment 4.

### 3.3.1.1 Addition of salt

As the water from Lake Peri has a conductivity that was too low for the voltage stabilizer used in this pilot system. This meant that passing current through the water while maintaining certain amperes was not possible for the given voltage stabilizer. For that reason, NaCl was added to the raw water in the tank to increase the conductivity.

Required amount of NaCl was tested by adding a certain amount in the tank and see if the current density reach the desired level. The final concentration was calculated and is presented in Table 3.2.

#### 3.3.1.2 Sample collection and measurements

For each experiment in Table 3.2 one sample of raw water before addition of salt and one after addition of salt was collected and measured for turbidity, colour, pH, conductivity and temperature immediately after collection. Cyanobacteria cell count was done only for raw water after addition of salt. The analysis was only based on the raw water with addition of salt, characteristics raw water without addition of salt can be found in Appendix A.

In addition, in the experiments of Table 3.2, 2 samples of 250 ml where collected, one after EF and one after filtration, for each hour during the experiment. Turbidity, colour, pH, conductivity and temperature were measured immediately after collection. Cyanobacteria cell count was also conducted for each sample collection.

Only one sample after EF was collected at the end of the experiments in Table 3.3. The samples were immediately measured for turbidity, colour, pH, conductivity and temperature. Cyanobacteria cell count was also conducted.

#### 3.3.1.3 Water column height, head losses and effluent rate

The change in water column height ( $\Delta H$ ) was measured every hour, by measuring the height of the water column and subtract by the initial height of water column when the flow starts.

For each hour during the experiments from Table 3.2, the pressure loss in the piezometers was measured. The measure was done as difference in water level relative to Piezo 1, that is the current water level at each time step. The results are given in meter water column (mWC).

The effluent rate was also measured each hour during the experiments. The measure was done by collecting water at the outlet for 1 minute.

#### 3.3.1.4 Sludge removal and filter backwash

After each experiment, as much as possible of the sludge formed during the electroflotation was removed through one of the outlets above the EF-reactor. In order to achieve this, a sufficient head loss was required, and this did not occur for all experiments. When the maximum possible amount of sludge was drained out of the outlet, the water level in the cylinder was decreased with the remaining sludge to the level of the backwash outlets.

The filter was expanded 50% during backwash, requiring a backwash velocity of approximately 51,2 m/h. Only the PVC spheres were possible to backwash, as the denser gravel required higher backwash velocity, causing loss of PVC sphere filter media. The water used for backwash was the water raw water that had been treated by the integrated process of flotation and filtration.

To evaluate the backwash efficiency samples were collected before the backwash, at time 0 and each following minute for a backwash duration of 10 minutes. Each sample was then measured for turbidity. Before the backwashing of the filter with the sample collection was started, the filter was expanded 50% for 1 minute to remove the sludge settled from the EF, in order to have measures of backwash turbidity that represented the captured particles in the filter.

The filtered water did not have a good quality. In addition, the backwash procedure was not considered sufficient as particles were observed in the filter after the procedure was finalized, see section 4.2.1.1 and 4.2.5. For this reason, tap water was added to tank 2 and the filter was backwashed again for each experiment. This backwash was not regulated and was done by observation.

#### 3.3.2 Additional experiments and measurements

As some of the results after the termination of experiments in Table 3.2 shown lack of consistency, two additional experiments/measurements were done in order to locate where the experiments failed. The first one evaluated the effects of retention time and sample outlet and the second evaluated the effect of polarity inversion.

### 3.3.2.1 Retention time and sample outtake

After the pilot was finalized, a test run of the pilot was done (result not presented in this study as the pilot had leakages at this time) showed an increase in turbidity after EF. One hypothesis was that this might have been due to the placement of the sample outtake. Another hypothesis was that the water did not have sufficient retention time in the EF as the water simultaneously passes the filtration process.

To test these hypotheses, two pre-experiments were conducted, one without salt and one with salt. The salt was not quantified as it was conducted for comparison only. The experiment was 1 hour long for each water with and without addition of salt, and was done with a fixed amount of water in the cylinder (no inflow or outflow of water) resulting in a water height of 44,5 cm above the EF reactor. The voltage was kept at maximal capacity at 29-30 V, meaning the current density was not constant during the experiment.

Water samples were collected for each 30 min from two outlets above the EF reactor, located 2,5 cm and 32,5 cm above the EF reactor, referred to as outlet 1 and outlet 2, respectively. These are number 5 (inflow pipe dismantled) and the lowest outlet number 8 in Figure 3.1. The water was tested for turbidity, colour, pH, conductivity and temperature.

### 3.3.2.2 Polarity inversion

As the results from Experiment 4 were similar to Experiment 3, 2 smaller experiments were conducted with the remaining raw water after Experiment 4. This was done with the objective to study the effects of polarity inversion without any changes in raw water characteristics. The experiments can be seen in Table 3.3.

**Table 3.3: Overview of experiments for polarity comparison**

<b>Experiment</b>	<b>Inflow rate (ml/s)*</b>	<b>Duration (min.)</b>	<b>Salt concentration**** (mg/l)</b>	<b>Current density (A/m<sup>2</sup>)</b>	<b>Polarity</b>
I	12,1	60	46,7	89,2*****	Normal*
II	12,1	25	46,7	89,2	Inverted***

\* Not the necessarily actual inflow rate. See section 4.2.4

\*\* DSA® used as anodes, titanium used as cathodes

\*\*\* DSA® used as cathodes, titanium electrodes used as anodes

\*\*\*\* Same as Experiment 4

\*\*\*\*\* Average current density as it decreased during the experiment

For Experiment I two samples were collected, one after 30 minutes and one after 60 minutes. Measurements taken were turbidity, colour and FTC. Cyanobacteria was only counted after 60 minutes. The duration of Experiment II was shorter than Experiment I as the remaining water was not sufficient for a 60 minutes experiment. Therefore, only one sample was taken after Experiment II and measure for turbidity, colour, FTC and cyanobacteria cell count.

Experiment I also experienced more resistance and the current density decreased. An average value was set and became the set current density for Experiment II that was conducted afterwards.

### 3.4 Analysis

Turbidity, colour, pH, conductivity and temperature were measured for each sample immediately after collection. Cyanobacteria cell count for each sample was done within a week for each sample. The samples that were not counted for cyanobacteria cells the day of the respective experiment were stored in a refrigerator in the meantime.

#### 3.4.1 Parameters

Turbidity, colour, pH, conductivity and temperature were measured for raw water before and after addition for all experiment in Table 3.2. The same measurements were done for 1 hour time steps after EF and filtration throughout the experiment for the same experiments in Table

3.2. The analyses followed the AWWA, APHA and the Water Environment Federation's *Standard Methods for the Examination of Water and Wastewater* (AWWA, 2012).

**Table 3.4: Overview of analysis conducted**

Parameter	Method	Equipment	Unit
Turbidity	2130 (AWWA, 2012)	Turbidimeter Hach model 2100p	NTU
Colour (apparent)	2120 C (AWWA, 2012)	Hach DR 2800 Spectrophotometer	HU (Hazen units)
pH	4500 H <sup>+</sup> (AWWA, 2012)	Hach Multi Meter HQ40 d	N/A
Conductivity	2510 (AWWA, 2012)	AZ Instruments RS232 Conductivity/TDS/Salinity/Temperature Model 8306	$\mu\text{S cm}^{-1}$
Temperature	2550 (AWWA, 2012)	Mercury Thermometer and HACH Conductivity Meter	$^{\circ}\text{C}$
Free and total chlorine (FTC)*	4500 Cl – G (AWWA, 2012)	Chlorine (Free and total) Color Disk Test Kit, Hach model CN-66	mg/L Cl <sub>2</sub>

\* Not measured for Experiment 1

Free and total chlorine (FTC) were measured for raw water with and without salt, after 1 hour of EF and after 6 hours of EF. FTC measurements were not available for Experiment 1.

### 3.4.2 Cyanobacteria cell count

After each sample collection from the experiment, water from the sample was poured into a test tube on 10 ml, followed by adding 3 drops of Lugol using a pasteur pipette. Cyanobacteria cell counts were done within 5 days after each experiment. During the time between the experiment and cell count, the samples were stored in a refrigerator. The cyanobacteria cell count was done microscopically.

Each counting cell sample was prepared and left to rest for a minimum 10 minutes before the cell count was started. The steps for the process of cell counts is given below:

1. Prepare and clean the counting cell (Sedgewick rafter cell, 1 ml) and cover slip (Knittel Glass)
2. Place the diagonally over coverslip over the counting cell
3. Use a pasteur pipette to fill the counting cell until the cover slip covers it.
4. Place the sample under the microscope. Count 10 cells of 1 mm<sup>2</sup> each diagonally across the counting cell

### 3.4.3 Removal rate

The turbidity, colour and cyanobacteria removal rates after EF and the overall integrated process were calculated using the following formula (3.1).

$$R = 100 \frac{(C_0 - C_t)}{C_0} \quad (3.1)$$

Where:

R = Removal rate, %

C<sub>0</sub> = Concentration in raw water

C<sub>t</sub> = Concentration in treated water after hour t

As the turbidity and colour was increased after EF for the majority of the experiments, the removal rate from equation (3.1) did not represent the filters performance on turbidity and colour. For that reason, results from turbidity and colour was also expressed as removal rate after filtration relative to EF. The removal rates from filtration relative to the EF was calculated by using formula (3.2).

$$R_{Rel} = 100 \frac{(C_t^{EF} - C_t^F)}{C_t^{EF}} \quad (3.2)$$

Where:

$R_{Rel}$  = Removal rate after filtration relative to EF, %

$C_t^{EF}$  = Concentration after EF after hour t

$C_t^F$  = Concentration after filtration after hour t

*(This page is left blank intentionally)*

## **4 Results and discussion**

In this part of the thesis the results of the experiments will be presented and discussed. The performance of electroflotation will be discussed firstly and will be followed by the results from the integrated process, where the overall performance and performance of the filtration will be evaluated.

### **4.1 Electroflotation performance**

In this section the results from the samples after EF will be presented and discussed. Corrosion on the DSA<sup>®</sup>s was found to largely impact the results, in particular the turbidity, and making it difficult to conclude a pattern of performance in relation to the current density applied. As mentioned in the methodology section, the experiments with polarity inversion showed rather different results than the other experiments, and this was believed to be caused by the corrosion on the electrodes. This will be explained in small parts throughout the presentation of the results from experiments in Table 3.2 and be further explained in a section where results from the experiments in Table 3.3 will be presented.

#### **4.1.1 Parameters after electroflotation**

The results from the parameters in Table 3.4 after EF will be demonstrated and discussed in this section.

##### **4.1.1.1 Turbidity**

The turbidity levels and removal rates are shown in Figure 4.1 and Figure 4.2. As seen from the figures, the turbidity increased for all experiments with normal polarity and had only small increases and decreases for Experiment 3 and 4 that were conducted with inverted polarity.

During the experiments with normal polarity sedimentation from the sludge that accumulated at the surface was observed and is identified as the main reason for the turbidity increase. There are five possible explanations to the sedimentation that occurred:

1. Coalesce of bubbles on electrodes due to vertical electrode arrangement

2. Coalesce of bubbles due to corrosion on DSA<sup>®</sup>, because of the unsmooth electrode surface
3. Non-homogenous dispersion of bubbles, due to lower bubble generation at DSA<sup>®</sup>s because of corrosion, creating turbulence in some areas
4. Turbulence caused by inflow rate
5. Retention time and sample outlet

These five points will be further explained in the following.

When electrodes are arranged vertically it may cause bubbles to rise along the surface of the electrode and possibly coalesce (Comminellis and Chen, 2010; Martínez-Huitile, Rodrigo and Scialdone, 2018). When bubbles coalesce, they become larger and therefore rise with a higher velocity to the water surface. The collision with the sludge on the surface can lead to sedimentation and this was also observed in the experiments with normal polarity. Another explanation to the larger bubbles is based on the corrosion on the DSA<sup>®</sup>s. The DSA<sup>®</sup>s had some corrosion already in the first experiment, and the corrosion was more severe after the last one. The unsmooth surface of the DSA<sup>®</sup> from corrosion may lead to more bubble coalesce and enhance the sedimentation from the sludge.

**Figure 4.1: Turbidity level after EF**

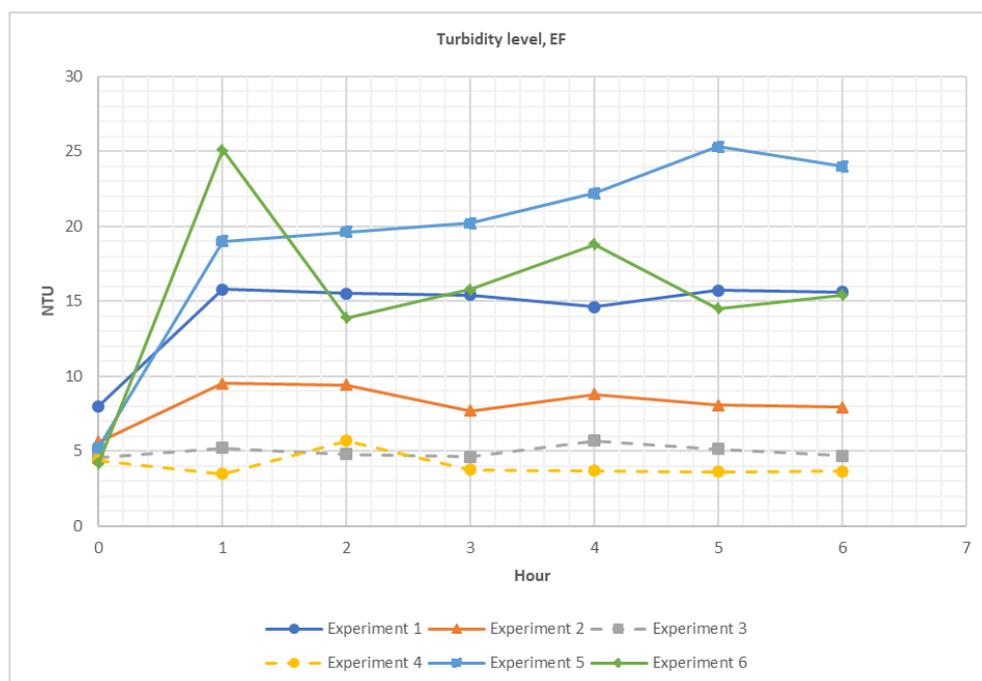
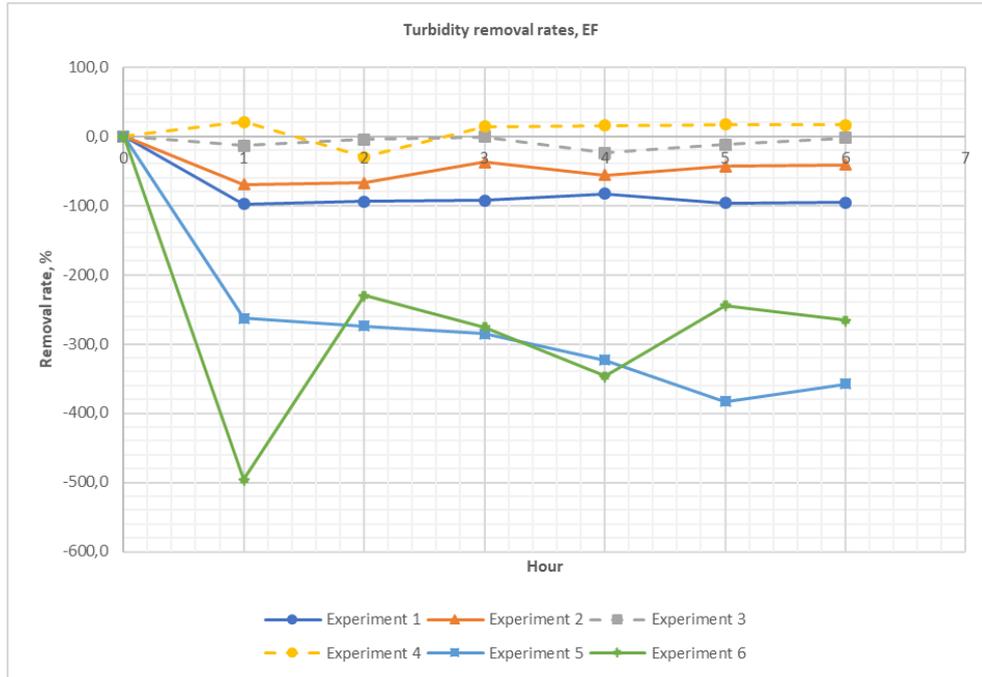


**Figure 4.2: Turbidity removal rates after EF**



The effects of current density on the turbidity removal are not clearly seen from Figure 4.2. Experiment 1 and 2 were both within a removal rate of -35% to -100%, whereas Experiment 5 and 6 were within the range of -200% and -400%. As Experiment 5 and 6 were the last ones conducted, they were done with electrodes that had experienced severe corrosion, see Figure 4.3. Since they seem to partly have similar removal rates and in another range of Experiment 1 and 2, it is probable that the corrosion impacted the results largely. The large increase in turbidity after 1 hour in experiment 6 was likely due to sediments stuck in the sample outlet from a backwashing in the previous experiment. This was further confirmed as a turbidity measure for Experiment 6 after 1 hour and 20 minutes showed a turbidity of 10,3 NTU (not shown in the figures).

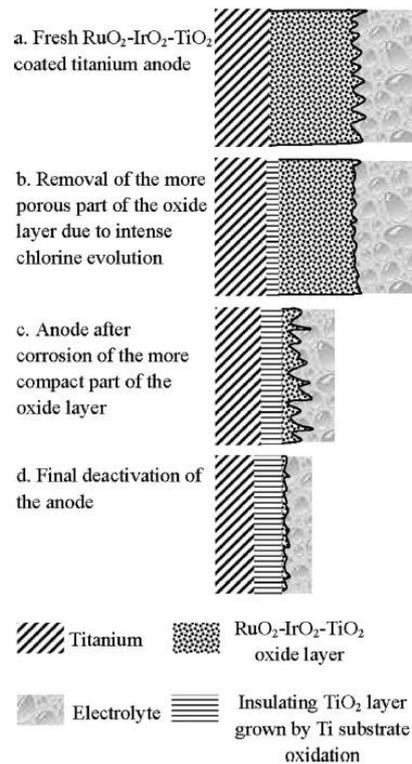
**Figure 4.3: Corrosion on the anodes after Experiment 6**



*Source: By author*

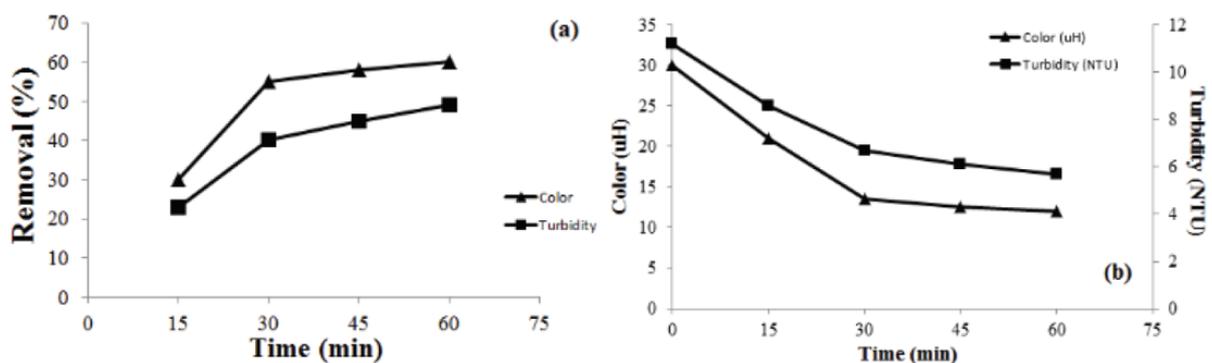
As the anodes used in the experiment were DSA<sup>®</sup>, the corrosion probably had a large impact on the electrolysis reactions and efficiency as the coating with the reactive metal was partly destroyed. As the substrate metal in the DSA<sup>®</sup> used was titanium, this can be very severe. The reason for this is that as the RuO<sub>2</sub>-TiO<sub>2</sub> layer corrodes, the titanium substrate underneath will oxidize and create an insulating layer of TiO<sub>2</sub> that will partly inhibit the current until the electrode reaches total deactivation. A schematic of this process can be seen in Figure 4.4. In addition, a previous study made by Campos *et al.* (2018) with water from Lake Peri and usage of the same pilot, only with different filter media (sand), showed a reduction in turbidity, as seen in Figure 4.5. Although other differences in the studies may impact the results, such as characteristics of water at the time of experiments, it is believed that due to the DSA<sup>®</sup> having been less corroded at the time of that study, the results enhance the theory of corrosion being the reason for the turbidity increase.

**Figure 4.4: Proposed schematic on the deactivation mechanism of Ti/RuO<sub>2</sub>-IrO<sub>2</sub>-TiO<sub>2</sub>**



Source: Hoseinieh, Ashrafizadeh and Maddahi (2010)

**Figure 4.5: Turbidity and colour removal from a previous study (a) Removal rates (b) Turbidity and colour level**



Source: Campos et al. (2018)

This partly destruction of the reactive layer will most likely inhibit a large bubble production at the DSA<sup>®</sup>. During the all experiments, regardless of polarity, this was also visually observed as the DSA<sup>®</sup> released less bubbles than the titanium electrodes, most likely due to the explained corrosion. Because of this, the bubble dispersion will not be homogenous on the cross-section

og the pilot cylinder, and will therefore possibly disturb the sludge. This light turbulence may lead to sedimentation, as mentioned in point 3.

In Experiments 3 and 4 very small changes in turbidity were measured in comparison to the other experiments. In addition, they produced very little sludge compared to the other experiments, see Figure 4.6.  $\text{Cl}_2$  and  $\text{O}_2$  was produced at the titanium electrode for Experiment 3 and 4, and  $\text{H}_2$  at the DSA<sup>®</sup>. Due to corrosion and inhibition of the DSA<sup>®</sup> to generate bubbles at the same rate as the titanium electrodes, the predominant gases that were produced during normal and inverted polarity were possibly different. In the experiments with normal polarity predominantly  $\text{H}_2$  was produced, whereas for the experiments with polarity inversion the gases generated was predominantly  $\text{Cl}_2$  and/or  $\text{O}_2$ , the ratio of  $\text{Cl}_2$  and  $\text{O}_2$  produced not being known. In conclusion, the little change in turbidity and little sludge generated may be explained by the flotation capacity being lower for Experiment 3 and 4 as  $\text{Cl}_2$  quickly reacts with the water and produces  $\text{HClO}$  and  $\text{ClO}^-$ , and therefore possibly does not contribute as much to flotation as  $\text{H}_2$ . That resulted in very little sludge and therefore a lower risk of sedimentation from the sludge, resulting in a turbidity level similar to the raw water turbidity. The effects of polarity inversion will be discussed further in section 4.1.4.

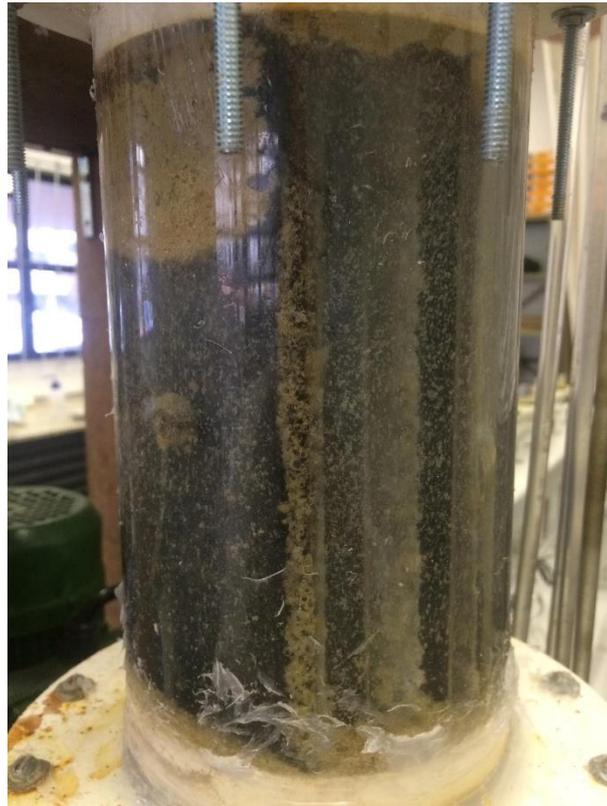
**Figure 4.6: Sludge accumulation in Experiment 4 (left) and 6 (right)**



*Source: By author*

The inflow could also influence as it may create a turbulence that disturbs the sludge or destroys bubble-particle aggregates that have formed. At last, the retention time and sample outlet could have an effect. The retention time is difficult to control in this system as it is highly dependent on the filter head loss and effluent rate. For that reason, the retention time may not have been sufficient to reduce the turbidity. It was also observed that flocs were stuck in the different spaces near and around the electrodes, see Figure 4.7. When water passes through the EF reactor and gets collected in the electroflotation sample outlet below the EF reactor, some of these flocs may follow. For this reason, the sample outtake may have an effect. Retention time and sample outlet will be further discussed in section 4.1.3.

**Figure 4.7: Floccs trapped in the electrochemical reactor. From Experiment 5**



*Source: By author*

#### 4.1.1.2 Colour

The colour also increased for all experiments with normal polarity. As measure of colour was done by apparent colour, the turbidity of the water will affect the measuring equipment. This is demonstrated as the experiments that had the highest increase in turbidity also had the highest increase in colour measurement. For this reason, the true colour might have been the same or even have been reduced in the treatment. To confirm this a proper filtration of the samples (also the raw water sample) before measuring colour would be required.

Experiments with polarity inversion removed some colour. Experiment 3 removed only in one time step, with a rate of 1,9%, while Experiment 4 removed throughout the whole experiment, with the highest removal rate at 26,7%.

As previously explained, Experiment 3 and 4 generated more chlorine gas than the other experiments. This chlorine production reacts quickly with the water and become HClO and

$\text{ClO}^-$  as explained in section 2.2.3.  $\text{HClO}$  and  $\text{ClO}^-$  are oxidizing agents are able to remove colour, which may be an explanation to the removal of colour in Experiment 4. Still, Experiment 3, being only different in salt concentration, had an increase in colour, possibly showing that the oxidation did not work as well. The difference in turbidity levels was very similar for Experiment 3 and 4, meaning that the difference in colour probably is not due to higher turbidity in one of them.

**Figure 4.8: Colour level after EF**

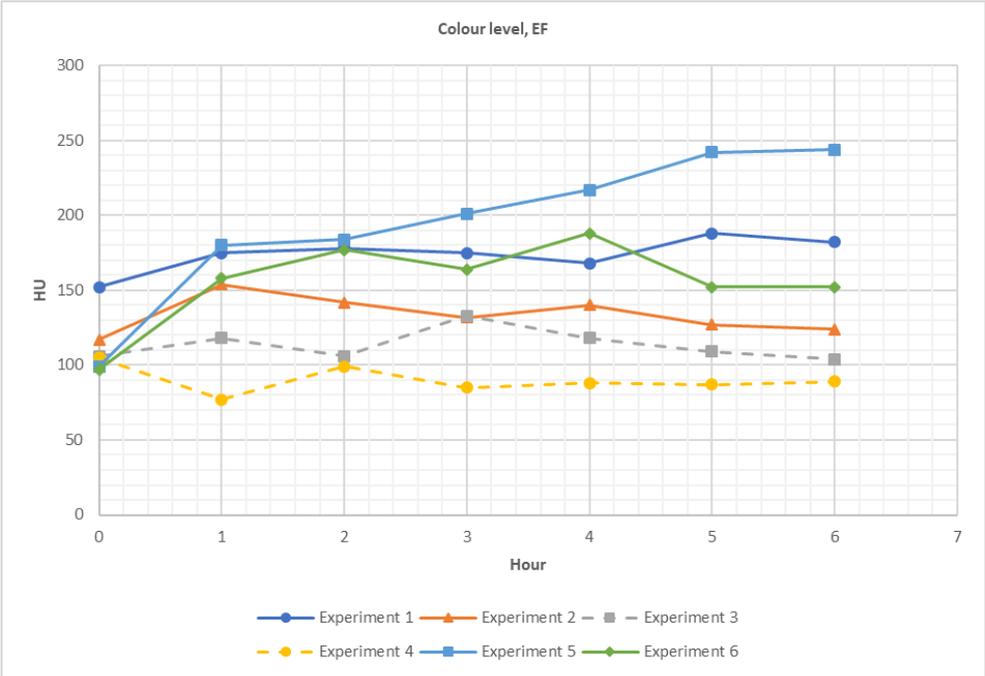
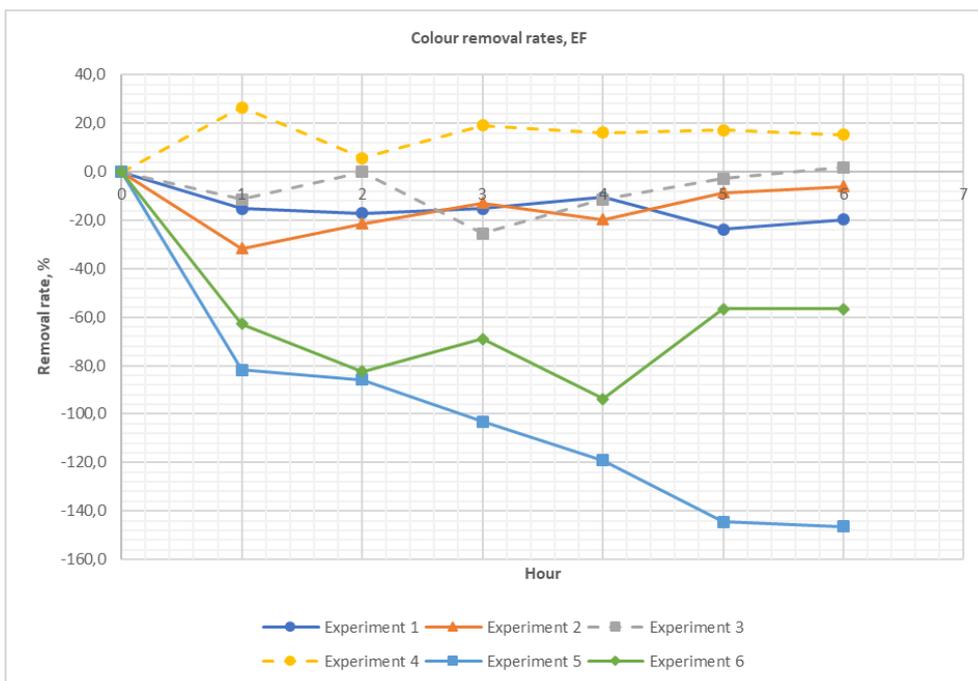


**Figure 4.9: Colour removal rates after EF**



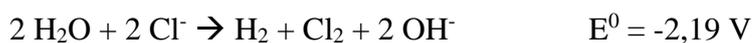
Electroflotation has been shown to be effective in dye removal in wastewater (El-Hosiny *et al.*, 2017).

#### 4.1.1.3 pH, conductivity, temperature and free/total chlorine

The results of pH, conductivity and temperature can be seen from Figure 4.10 and Figure 4.11.

Firstly, the pH increased for all experiments. In electrolysis of pure water this should not happen as shown in the total reaction in 2.2.3. However, since the solution contained NaCl, the total reaction will produce  $\text{OH}^-$ , as seen in the reactions below.

- Total reaction:



Another important notion is that with polarity inversion, that is Experiment 3 and 4, the pH did not increase as much as in the other experiments. This can possibly be explained with the corrosion that was present as explained in 4.1.1.1. As the initial pH of the water was basic for all experiments, the reaction at the cathode generating  $\text{H}_2$  would follow reactions for basic

conditions, the half reactions shown below, creating  $\text{OH}^-$ . As previously explained, the DSA<sup>®</sup> released less bubbles than the titanium electrodes. From this it may be concluded that when the polarity inversion was done, the reaction at the cathode for  $\text{H}_2$  generation did not occur at the same rate as in experiments with normal polarity, leaving the solution with less  $\text{OH}^-$  production and hence a lower increase in pH.

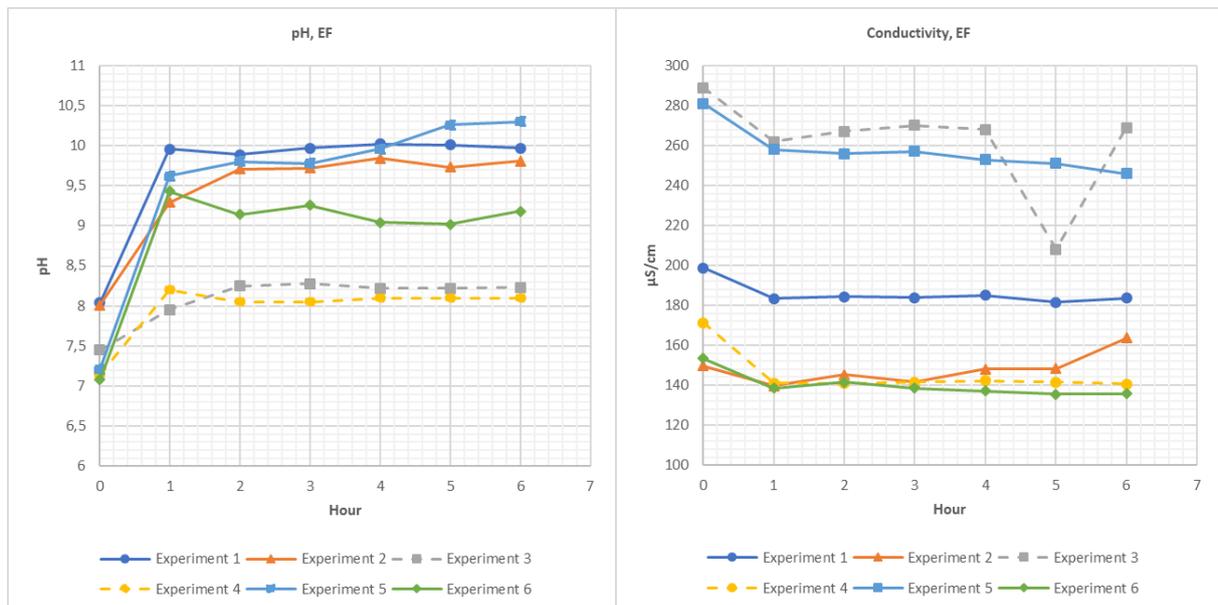
- At the anode:  

$$2 \text{Cl}^- \rightarrow \text{Cl}_2 + 2\text{e}^-$$
- At the cathode:  

$$2 \text{H}_2\text{O} + 2 \text{e}^- \rightarrow \text{H}_2 + 2 \text{OH}^- \quad \text{pH} \geq 7$$

The Brazilian Ministry of Health's guidelines N° 2.914 (Art.39, § 1º) recommends a pH of the water between 6 and 9,5 in the distribution system, and the results are within this

**Figure 4.10: pH (left) and conductivity (right) after EF**



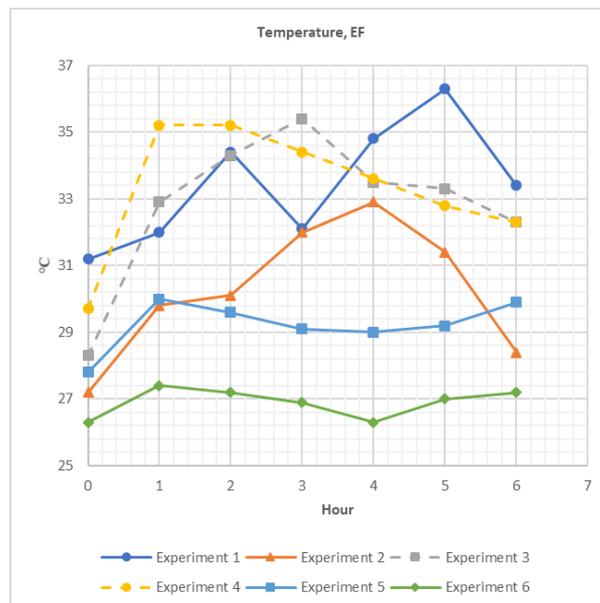
The conductivity of the solution decreased slightly for all experiments, possibly due to the use of the ions in the solutions to form molecular bonds, such as  $\text{Cl}_2$ . The number of electrons released per time is dependent in the current density applied, meaning more electrochemical reactions will occur per time. This might explain why the lower current densities have a smaller

decline in conductivity the first hour, than the higher current densities. This can be seen from Figure 4.10 by comparing the decline the first hour for Experiment 2, 4 and 6.

For Experiment 2 a gradual increase in conductivity occurred again after the third hour. This might have been due to residual metal ions that were corroded away. However, this may not be a valid explanation as it would have occurred in the other experiments as well. Lastly, the drop in conductivity that appears in the fifth hour of Experiment 3 is most likely due to error in the measurements. This is confirmed in Appendix A, where the conductivity after filtration for the same time step is shown to be similar to the other values after EF.

During electrolysis the temperature will rise due to energy dissipation in the solution. From Figure 4.11 this is not a consistent trend. This can have many explanations. The time between sample collection and measure of temperature can cool down the sample. In addition, the pump used to recirculate the water in the tank also heated up the water. The hose in the inflow tank feeding the pilot would sometimes get sucked into the pipes for water circulation, and for that reason the pump that kept the solution in suspension had to be turned off from time to time. This can partly explain the jumping values of some of the experiments.

**Figure 4.11: Temperature after EF**

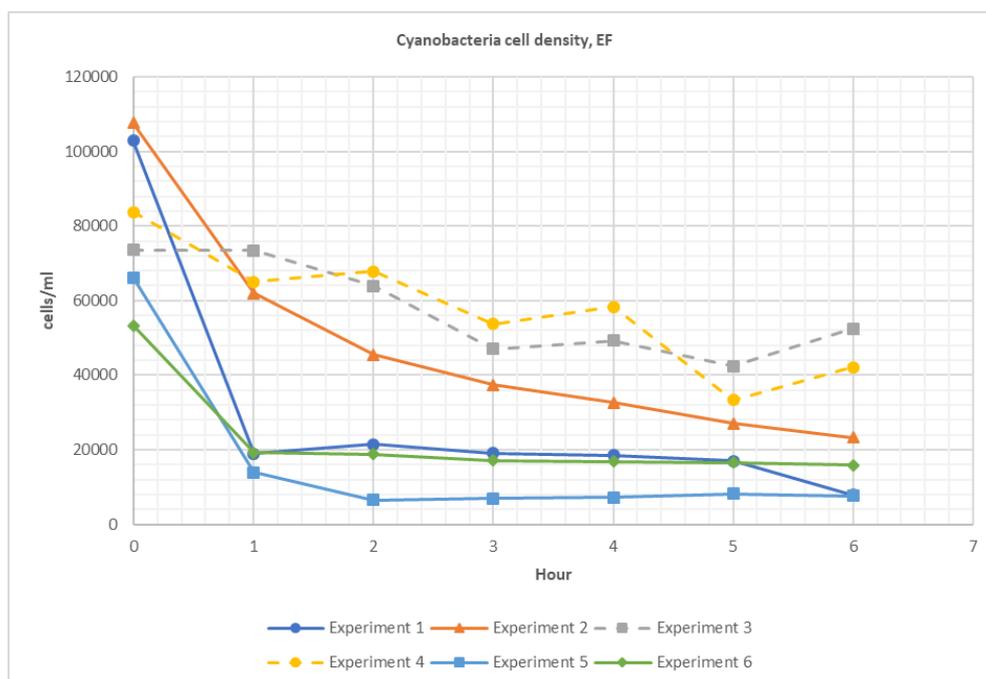


The measurements for FTC were very low for all experiments. As the equipment used to measure is not a very accurate method, the conclusion was to draw that for all experiments without polarity inversion the FTC level was between 0-0,2 mg/L. On the contrary, for experiments with polarity inversion, that is Experiment 3 and 4, the FTC level was very high. The level went above the maximum limit of detection of the equipment used at 3,5 mg/L with quite a clear deeper pink colour, representing high levels of FTC. This means both experiments had a level  $> 3,5$  mg/L, and possibly  $\gg 3,5$  mg/L. This will be discussed more in section 3.3.2.2.

#### 4.1.2 Removal of cyanobacteria

The results from cyanobacteria removal after electroflotation is shown in Figure 4.12 and Figure 4.13. As seen from the graphs, all experiments removed cyanobacteria during the pilot run, with a maximum removal rate of 92,3% after 6 hours in Experiment 1 and a minimum removal of 0,3% after 1 hour in Experiment 3.

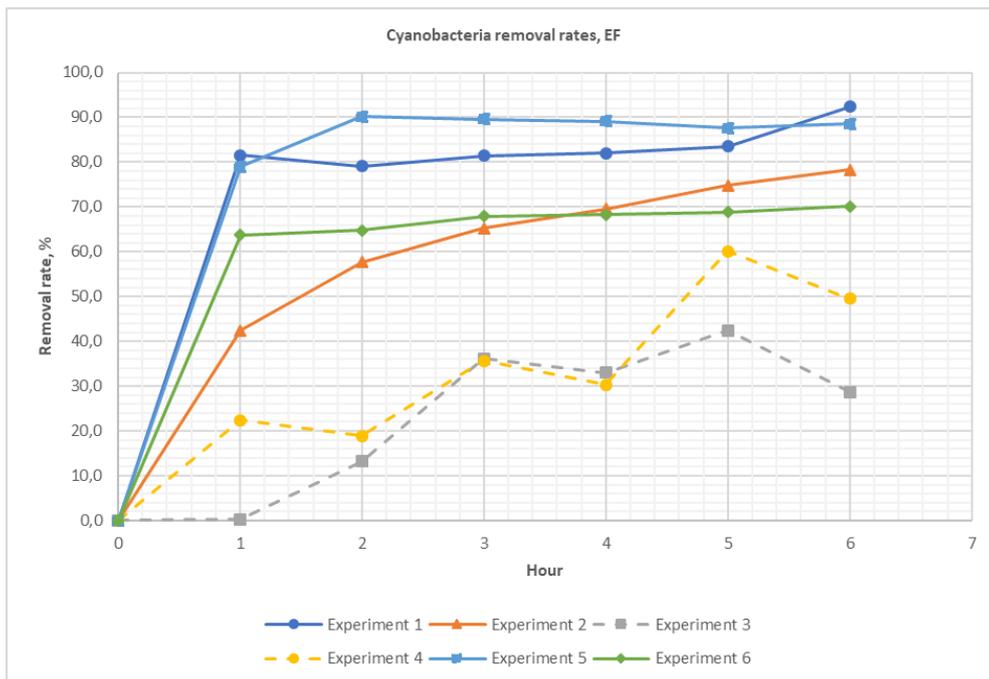
**Figure 4.12: Cyanobacteria cell density after EF**



According to Annex XI and XII of the Brazilian Ministry of Health's guidelines N° 2.914, a monthly monitoring is required when the cell density is  $\leq 10\ 000$  cells/ml and weekly monitoring is required when the cell density exceeds 10 000 cells/ml. If the cell density is  $\geq 20\ 000$  cells/mL, weekly monitoring of cyanotoxins, after the water has passed through the

water treatment plant, becomes mandatory (MS, 2012). Experiments 5 had cell densities < 10 000 cells/ml after the second hour and throughout the experiment, the lowest value being 6500 cells/ml. Experiment 1 reached below 10 000 cells/ml only after the sixth hour, with a level of 7900 cells/ml. None of the remaining experiments reached below 20 000 cells/ml after EF except Experiment 6 that had < 20 000 cells/ml after the first hour and throughout the experiment, the lowest cell density being 15 900 cells/ml.

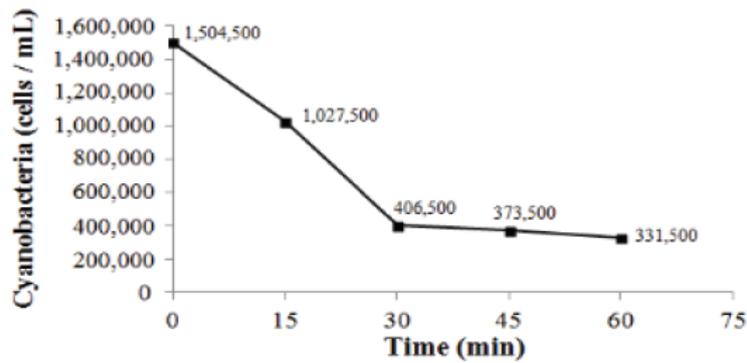
**Figure 4.13: Cyanobacteria removal rates after EF**



Experiments 1, 5 and 6 had a very stable removal rate after the first hour, with little variations after. Experiment 2 did not stabilize completely during the experiment and kept a steady increase in removal rate from start to end. Experiment 3 and 4 stand out with a low removal rate, the maximum occurring at the fifth hour for both, with a removal rate of 42,4% and 60,1%, respectively. In addition, the removal had a pattern with fluctuations. Experiments 4 generally had a higher removal rate than Experiment 3, with the exception of a slightly lower level in time step 3 and 4. This might be due to the lower level of NaCl added to the solution. As O<sub>2</sub> also may be produced at the anode in a NaCl solution, a lower amount of Cl<sup>-</sup> ions in the solution may have a lower Cl<sub>2</sub> to O<sub>2</sub>. O<sub>2</sub> is believed to contribute more to flotation than Cl<sub>2</sub>.

The study of Campos *et al.* (2018), using the same pilot system with different filter material, had cyanobacteria removal rate of 73% and 78% after 30 and 60 minutes of electrolysis respectively.

**Figure 4.14: Cyanobacteria removal in previous study**



*Source: Campos et al. (2018)*

Experiment 2 had higher removal rate than Experiment 6 after about 3 and a half hour. Experiment 5 was higher than Experiment 1 except being slightly lower at the first and sixth hour. The average removal rate for all the experiments are given in Table 4.1. An important notion, is that the average removal rate for Experiment 2, 3 and 4 is not representative the same way as the other experiments, as they did not have a stable removal rate most of the time.

**Table 4.1: Average removal rate of experiments**

	<b>Exp.1</b>	<b>Exp.2</b>	<b>Exp.3</b>	<b>Exp.4</b>	<b>Exp.5</b>	<b>Exp.6</b>
Removal rate, %	83,3	64,7	25,6	36,2	87,3	67,3

Experiment 5 had the highest average removal rate of 87,3%, and the average removal rate decreases with the CD, with the exception of Experiments 3 and 4 that had the highest CD, but were conducted with inverted polarity. The higher removal with higher CD can be explained by the bubble production being directly dependent on the CD, giving a higher bubble production with a higher current density (Sillanpa and Shestakova, 2017).

Since the turbidity increased for all experiments, as mentioned in 4.1.1.1, much of the cyanobacteria was trapped in flocs, and this was observed during the cyanobacteria cell counting. For this reason, although the number of cyanobacteria was consistently reduced, a reduction in turbidity is also crucial in order to reduce the amount of cyanobacteria. This is especially important to emphasize with regards to the results in Table 4.1, as Experiment 5 came out with the highest removal rate, but was also shown in Figure 4.2 to have the highest increase in turbidity as well.

At last, although cyanobacteria were removed at high rates in some cases, the generation of chlorine gas should be assessed. With polarity inversion large amounts of FTC was produced as mentioned in sections 4.1.1.3 and 4.1.4.1. The experiments with normal polarity would be expected to produce the same amount, given the same salt concentration and CD, had it not been for the corrosion of the DSA<sup>®</sup>s. Chlorine may damage the cyanobacteria cells, resulting in toxin release that may end up in the treated water. If salt is added to the water as in this study to increase the conductivity, monitoring of cyanotoxins should be done in addition to control of the produced FTC.

#### **4.1.3 Effect of retention time and sample outtake**

The experiment to study the effects of retention time and sample outlet, as described in 3.3.2.1, will be presented in this section. Only the results from turbidity and colour analysis will be presented. The results can be found in Appendix A, in addition to results from pH, conductivity and temperature.

The results can be seen in Figure 4.15 and Figure 4.16, with and without the addition of NaCl respectively. As seen from the figures, the retention time had some effect on the results, as all measurements started decreasing after 30 minutes. This may indicate that the problem with the increase of turbidity is partly because of non-sufficient retention time.

**Figure 4.15: Turbidity and colour level without flux through filter without salt**

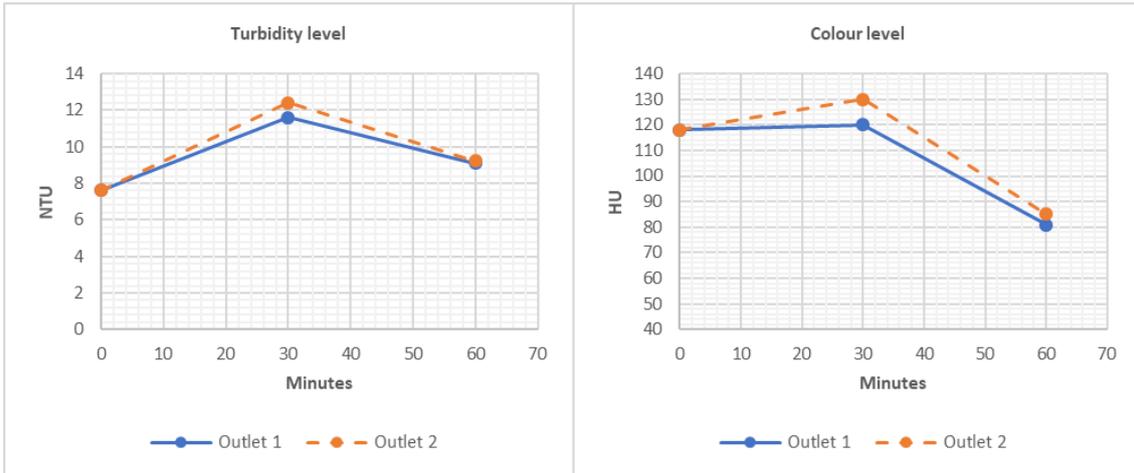
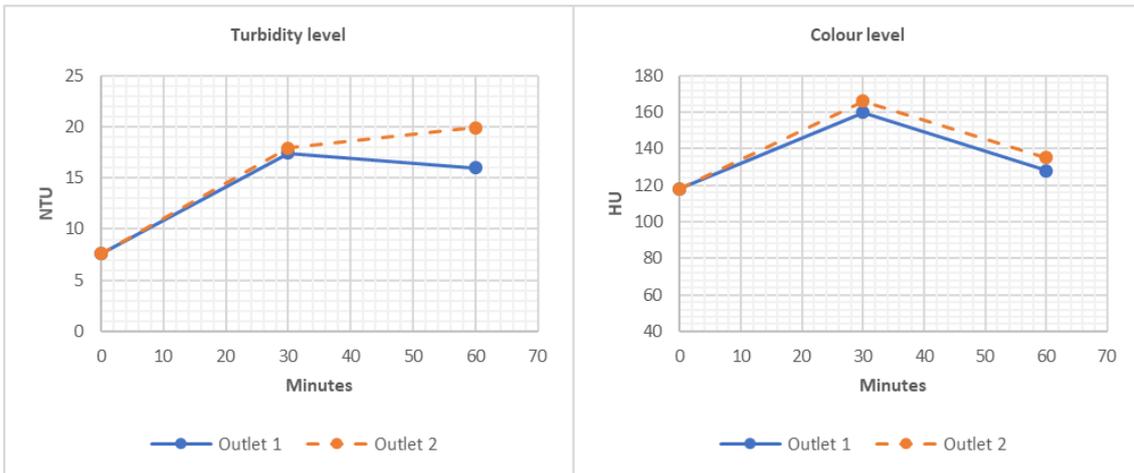


**Figure 4.16: Turbidity and colour level without flux through filter with NaCl**



The increase of turbidity from section 4.1.1.1 may have partly been due to the sample outlet of these experiments being below the EF reactor and not above as in these experiments. It was not possible to compare these outlets with the regular outlet below the EF reactor as there was no flux in these experiments, meaning the water below the reactor was untreated. Attempts of discharging the water below the EF reactor to waste in order to take a sample from the outlet below the EF reactor would not be reasonable as it would result in further mixture of the untreated water below the EF reactor and the treated water above.

#### **4.1.4 Effect of polarity inversion**

Experiments 3 and 4 in Table 3.2 were conducted with polarity inversion. As seen from Figure 4.1 and Figure 4.8, this resulted in little differences between the raw water turbidity and apparent colour compared to treated water. In addition, the cyanobacteria removal was less compared to all other experiments without polarity inversion.

In the following, the results from the experiments in Table 3.3 (see section 3.3.2.2) will be presented in order to understand the effects of polarity inversion. The general conclusions were that polarity inversion produced large amounts of FTC, had little sludge accumulation and low removal of cyanobacteria. In addition to this, with normal polarity the resistance was higher as the maximum possible current density was lower than in the case of inverted polarity for the same water.

##### **4.1.4.1 Free and total chlorine**

The free and total chlorine equipment was not available for Experiment 1. For the available experiments with normal electrode set-up, see 4.1.1.3, where chlorine measures were conducted, the levels had low values and were considered to be 0-0,2 mg/L as they were difficult to read.

As earlier mentioned, for Experiment 3, the levels of free and total chlorine were so high that they passed the maximum readable value of the equipment used for reading, at 3,5 mg/L. These high levels of free and total chlorine can be health threatening. Annex VII of Brazilian Ministry of Health's guidelines N° 2.914 having set a maximal allowed concentration of 5 mg/L of free chlorine for potable water (MS, 2012). The generated concentration with polarity inversion might have been higher than this. The treated water in outflow tank also had a very distinct chlorine odour. As Experiment 3 had a high salt concentration, the experiment was repeated with less salt, and resulted in Experiment 4 as described in the methodology section 3.3.2.2. Experiment 4 had the same high free and total chlorine levels and produced the same chlorine odour in the treated water.

With normal polarity, Experiment I in Table 3.3 produced little amounts of FTC, whereas Experiment II (with polarity inversion) created the same deep pink colour as Experiment 3 and

4, demonstrating high levels of FTC. The difference between Experiment I and II can be seen in Figure 4.17. The second tube is the blank for the respective experiments and is used to show the contrast.

**Figure 4.17: Comparison of total chlorine from Experiment I (left) and Experiment II (right)**



*Source: By author*

The generation of high amounts of chlorine was by this proved to be caused by the polarity inversion. As the  $\text{RuO}_2\text{-TiO}_2$  type of  $\text{DSA}^{\text{®}}$  used for this study are known to be good at chlorine generation (Comninellis and Chen, 2010), there is no implications regarding the material used that would indicate a lower chlorine production when the  $\text{DSA}^{\text{®}}$  were used to produce chlorine, as it was with normal polarity.

However, as mentioned several times earlier, the  $\text{DSA}^{\text{®}}$  had undergone corrosion, meaning they did not function as a proper  $\text{RuO}_2\text{-TiO}_2$  type of  $\text{DSA}^{\text{®}}$ . In section 4.1.1.3 the difference in change of pH for experiments with and without polarity inversion is explained by the electrochemical reaction on the  $\text{DSA}^{\text{®}}$  happening at a lower rate than the reaction that occurs at the titanium electrode. This was as mentioned also visually observed as less bubbles were released at the  $\text{DSA}^{\text{®}}$  in comparison to the titanium electrode, independent of polarity inversion. This is the probable explanation for the chlorine production as well. As with normal polarity, chlorine is generated at the  $\text{DSA}^{\text{®}}$ , and will therefore with the same conditions, primarily at the same current density, produce less chlorine per time than when chlorine is generated at the titanium electrode as it was during polarity inversion.

#### 4.1.4.2 Separation capacity

As previously mentioned, the experiments with polarity inversion also failed to produce a proper sludge. Sedimentation from this sludge was identified as one of the reasons for the high increase in turbidity from the experiments with normal polarity.

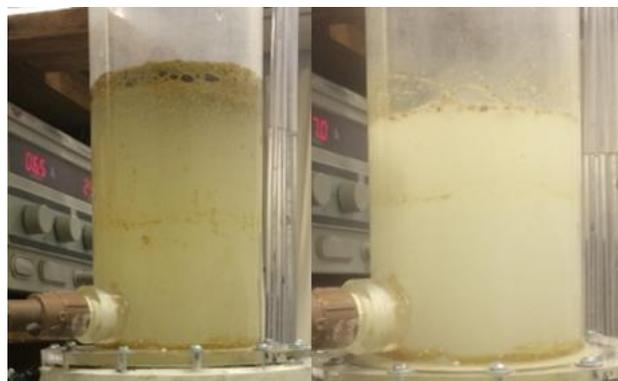
The same phenomena was observed when Experiment I and II was conducted. A comparison of sludge from the two experiments is shown in Figure 4.18 and Figure 4.19. Lack of water reduced the duration of Experiment II compared to Experiment I. The figures are still valid to use as observations, as Experiment I was observed to have already developed a thick sludge after 30 min. even though not shown here.

**Figure 4.18: Comparison of sludge after Experiment I after 60 min. (left) and Experiment II after 25 min. (right)**



*Source: By author*

**Figure 4.19: Comparison of sludge after Experiment I after 60 min. (left) and Experiment II after 25 min. (right)**



*Source: By author*

The total reaction with electrolysis of water containing NaCl shows that the ratio of Cl<sub>2</sub> and H<sub>2</sub> generated is one-to-one. However, as explained in section 2.2.3, Cl<sub>2</sub> quickly reacts with the water and produce HClO and ClO<sup>-</sup>. This might have reduced the flotation capacity as the Cl<sub>2</sub> gas was transformed before it captured particles from the water and floated to the surface. One notion is that O<sub>2</sub> also can be produced at the anode, but as the FTC levels were high and there was no way of measuring how much oxygen that might have been produced, only Cl<sub>2</sub> will be taken into account.

The difference in turbidity level and colour level is shown in Figure 4.20. Cyanobacteria cell density and removal rate is shown in Figure 4.21.

**Figure 4.20: Turbidity level (left) and colour level (right)**

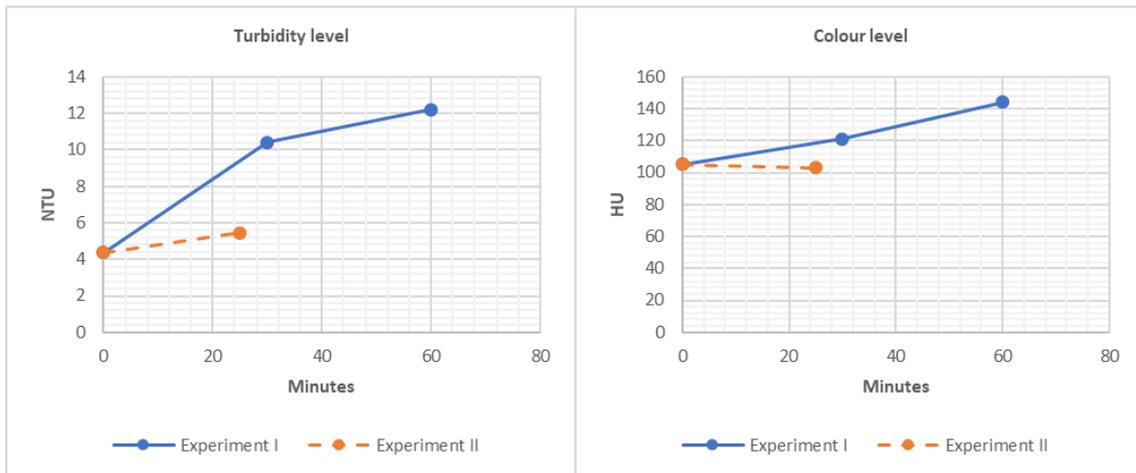
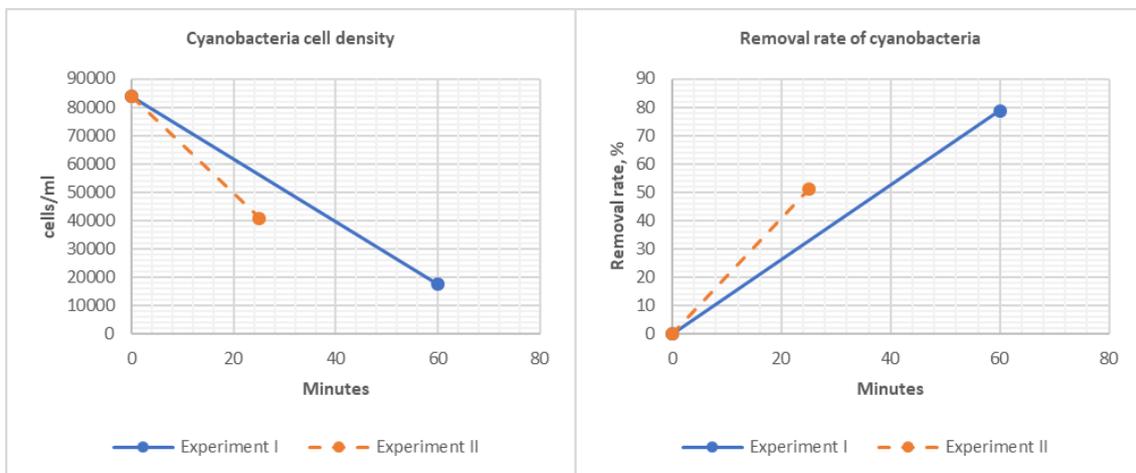


**Figure 4.21: Cyanobacteria cell density (left) and removal rate (right)**



As shown in Figure 4.20, the high increase in turbidity and colour are previously found in the experiments without polarity inversion, see Figure 4.1 and Figure 4.8. For cyanobacteria, only one sample was taken for Experiment I. With the assumption that the removal rate is linear, Experiment II would have a higher removal rate as seen from Figure 4.21. However, the removal rate is not linear, and although not proven from the results in Experiment I and II, the removal rate was most likely higher for Experiment I considering the previous results of cyanobacteria removal rates in Figure 4.13.

#### **4.1.5 Cost of operation**

The voltage and current did have some small changes during the experiments, and the voltage was regulated in order to maintain desired CD.

Assuming a constant inflow rate (as was not the case, see section 4.2.4) and using an average value of the voltage, the cost of operation can be calculated in accordance with equation (2.2). As the NaCl concentration in each experiment was different, the resistance of the water will be significantly different for each experiment. This will cause high differences in the voltage that needs to be applied as the voltage is given as  $V=RI$ , R being the resistance and I being the current. For that reason, it was decided that the formula for cost of operation is invalid to use in this study.

## **4.2 Integrated process**

The results from the integrated process of EF and filtration will be presented in the following. In general, the PVC spheres did not seem to capture large amounts of particles based on the small head loss in the piezometers. In addition, the second support layer was observed to accumulate a small layer of sand in the intersection with the PVC layer after several backwashes. This resulted in particles being trapped in this intersection, which were difficult to remove during backwash.

In the time between the conduction of Experiment 1 and 2, the pump used for backwashing started leaking. The reparation caused air to get trapped in the filter during Experiment 2. Experiment 5 it was observed that the filter bed was compressed around 3 cm after 3 hours, causing some changes in the head loss and effluent rate.

### 4.2.1 Parameters after filtration

In this section the results from the turbidity and colour removal will be discussed. The pH, conductivity and temperature can be found in Appendix A. As the turbidity and colour increased in most cases, the filter's capacity to remove turbidity and colour should be seen in comparison to the turbidity and colour after EF.

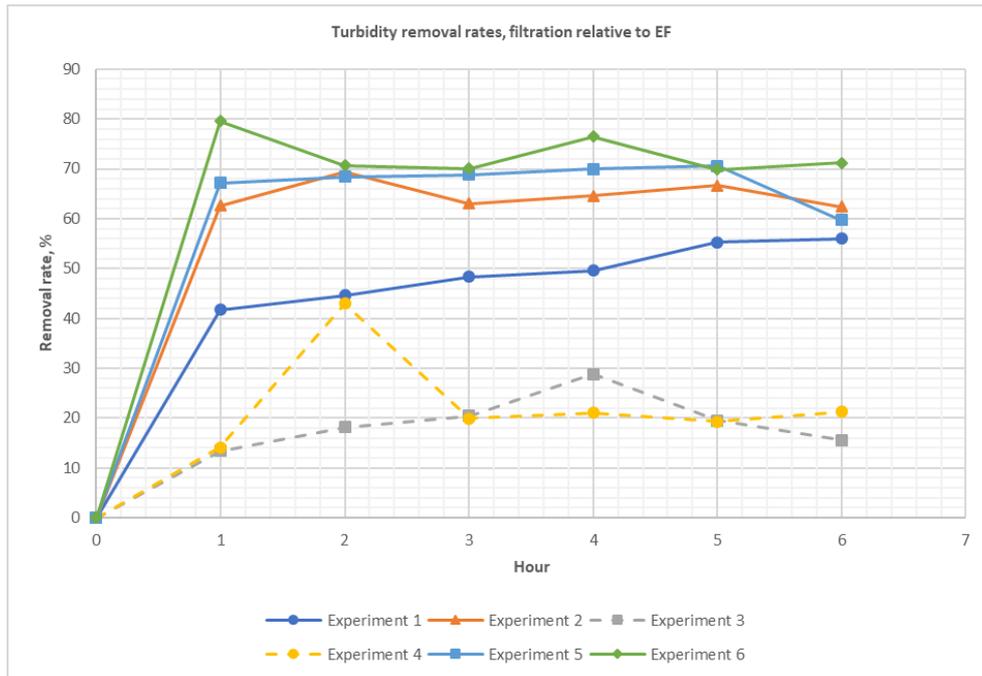
For this reason, the results from turbidity and colour removal will be given in two forms, one being the removal rate relative to the raw water characteristics (representing the performance of the integrated system) and the other being the removal rate relative to the measure after EF in the same time step (representing the filter's capacity to retain particles), see section 3.4.3. These two will be referred to as *overall turbidity and colour level* or *overall removal rate*, and *filtration removal rate relative to EF*, respectively.

The removal rates after filtration relative to EF does not necessarily represent the accurate filter performance as the assumption is that the turbidity or colour level after EF is constant within each time step.

#### 4.2.1.1 Turbidity

The turbidity removal after filtration relative to the turbidity after EF given in Figure 4.22. The flocs after EF were visually larger than in the raw water for the experiments with normal polarity, possibly giving EF the ability to work as a method of coagulation in this study. Experiment 3 and 4 had a poorer sludge accumulation and the flocs formed in these experiments after EF were visually smaller. Their respective maximal removal rates after filtration relative to EF of 28,8% 43% may indicate that the filter was capable of trapping small particles to a certain extent as well.

**Figure 4.22: Turbidity removal rate from filtration relative to EF**



From the figure, Experiment 2, 5 and 6 have the highest relative removal rates relative to EF, with maximal removal rates of 66,7%, 70,6% and 79,6%, respectively. Experiment 6 comes out with the highest average removal rate of 73%, followed by Experiment 5 removal rate at 67,5%. As mentioned in 4.1.1.1., the measure of turbidity after EF after 1 hour in Experiment 6 was likely due to trapped particles in the EF sample outlet. This indicates that the average removal rate from Experiment 6 should have been slightly lower. For that reason, the removal rate relative to EF for Experiment 6 after 1 hour of 79,6% is considered an invalid value as the highest removal rate, and instead the removal rate after hour 4, of 76,4%, will be considered the highest. Experiment 1 has a lower removal rate, probably due to the filter being cleaner as it was the first experiment that was conducted.

The overall turbidity level and turbidity removal rate is given in Figure 4.23 and Figure 4.24. As seen from the figures, the high increase in turbidity after EF resulted in poor overall turbidity removal in the integrated system in almost all experiments. Only three experiments had an overall turbidity reduction throughout the whole experiment, namely Experiment 2, 3 and 4, the two latter being conducted with polarity inversion.

Figure 4.23: Overall turbidity level after integrated process

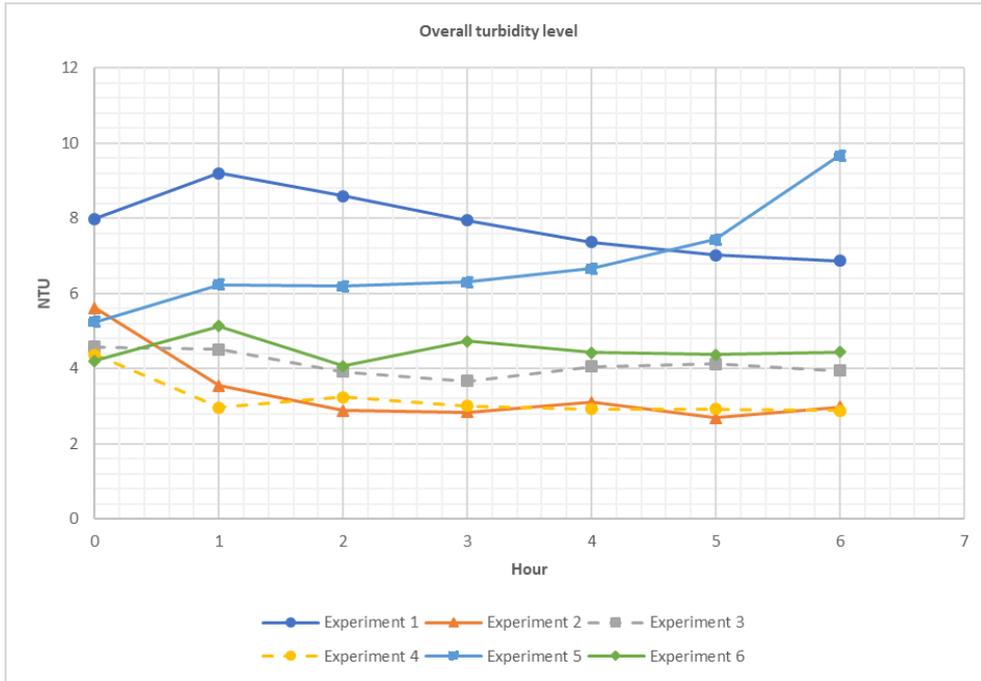
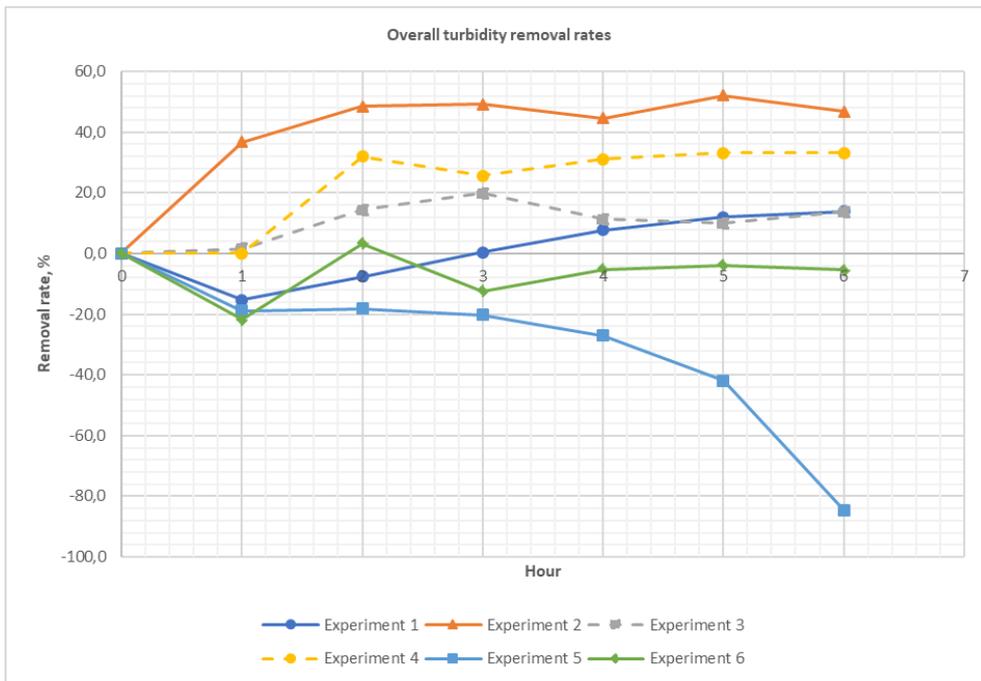


Figure 4.24: Overall turbidity removal rates after integrated process



Experiment 2 had air trapped in the filter during filtration, and had a low effluent rate, see section 4.2.4. This may possibly explain that particles were removed from the first hour, with no ripening time. The maximum overall removal rate was also found in this experiment and

was 52% after the fifth hour. Experiment 5 had a high increase in turbidity of 84,5% in hour 6 due to the large increase in turbidity from EF. As previously mentioned, after the third hour, the filter bed in Experiment 5 fell about 3 cm, making the filter more compact. The slightly steeper decline after 3 hours in Figure 4.24 suggests that it resulted from this compression. However, the increase in turbidity is not as expected as a more compact filter should create a higher removal rate.

As Experiments 3 and 4 had little change in turbidity after EF, the overall removal rate was similar to the removal rate relative to EF for these two experiments. The maximum overall removal rate was 19,9% and 34,1%, respectively for Experiment 3 and 4. A photo of the filter bed after an experiment can be seen in Figure 4.25.

Experiment 1 was the experiment with the most approximate graph to a common filtration graph, with a turbidity increase at the start of filter run, being the ripening phase, before the turbidity decreases again to a maximum removal rate of 13,9% after 6 hours.

**Figure 4.25: Retained particles in filter after Experiment 4**

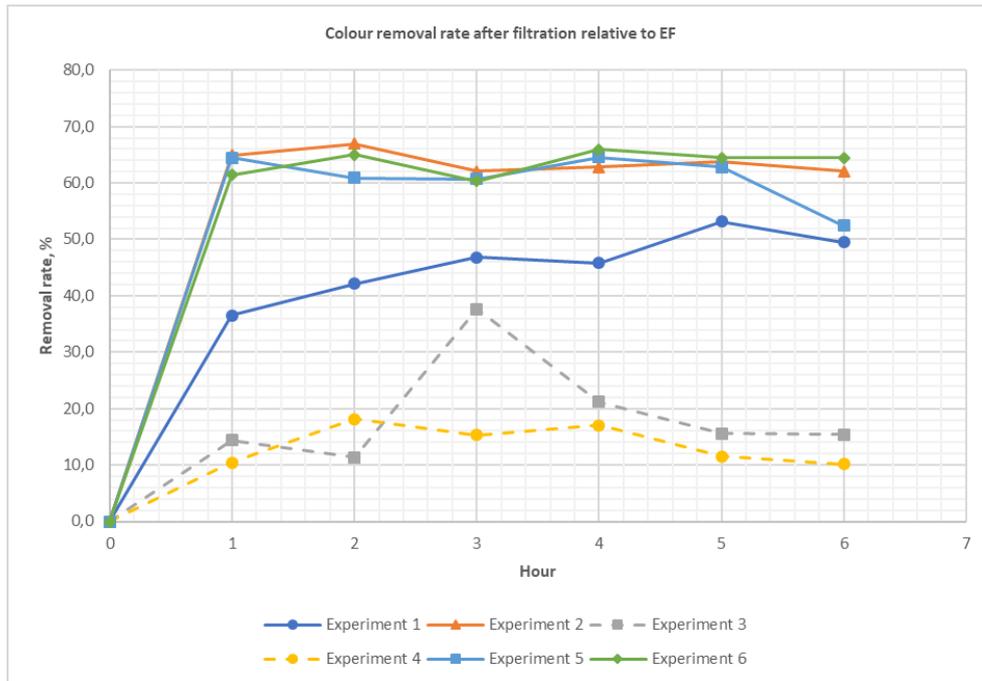


*Source: By author*

#### 4.2.1.2 Colour

The colour removal rate after filtration relative to EF is shown in Figure 4.26. The highest removal rate after filtration relative to EF was 66,9% in Experiment 2. However, Experiments 2, 5 and 6 had similar removal rates, as can be seen from the figure.

**Figure 4.26: Colour removal rate after filtration relative to EF**



The overall colour level and removal rates are shown in Figure 4.27 and Figure 4.28. Although the apparent colour in almost all cases increased after EF, the results from the overall colour removal might show that that EF partly removed true colour. The reasoning behind this is that rapid filters are not expected to significantly remove colour if coagulant is not added. For this reason, if the overall colour level decreases below the colour of the raw water in the integrated process, this might indicate that EF partly removed true colour.

**Figure 4.27: Overall colour level after integrated process**

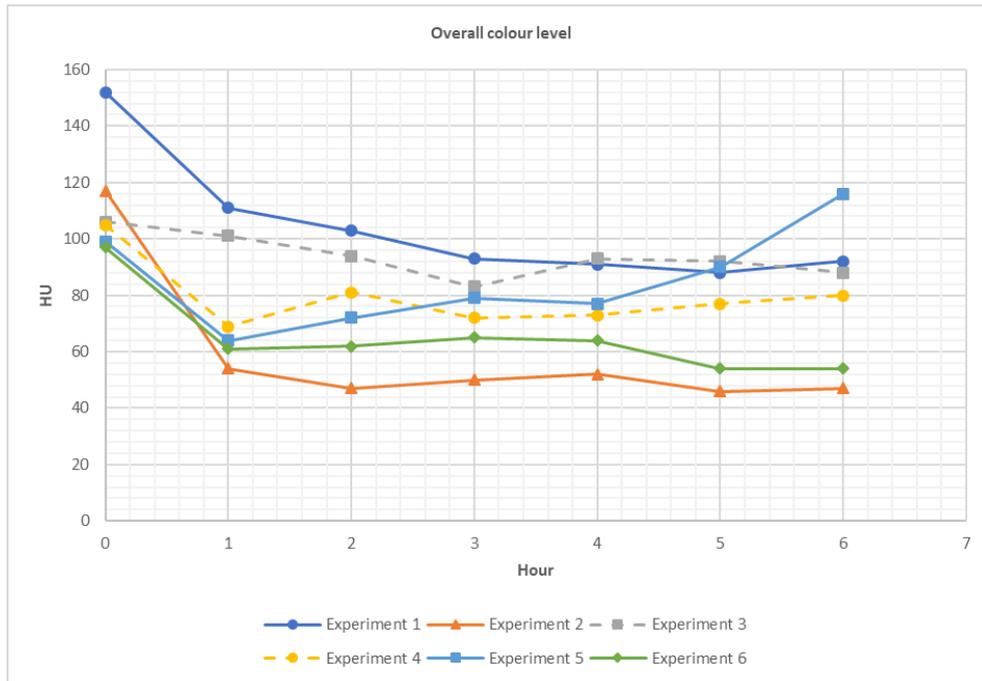
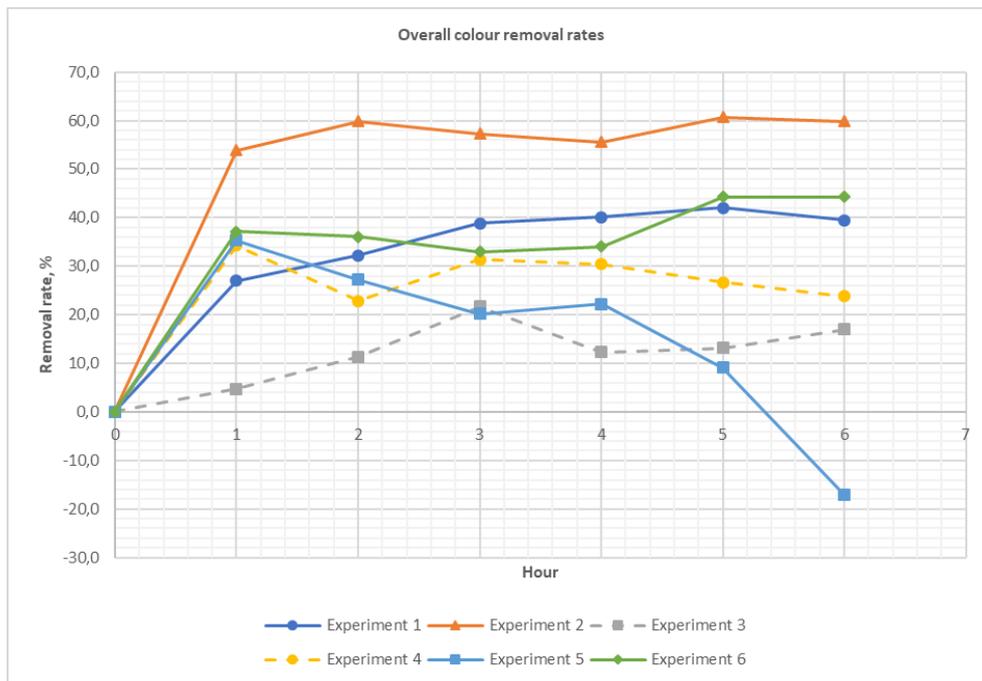


**Figure 4.28: Overall colour removal rate after integrated process**



The highest overall removal rate was clearly found in Experiment 2, with a maximum removal rate of 60,7% in the fifth hour. Experiments 1 and 6 showed somewhat of a similar pattern with removal rates ranging from 27% to 44,3%. The overall removal rate in Experiment 5 generally

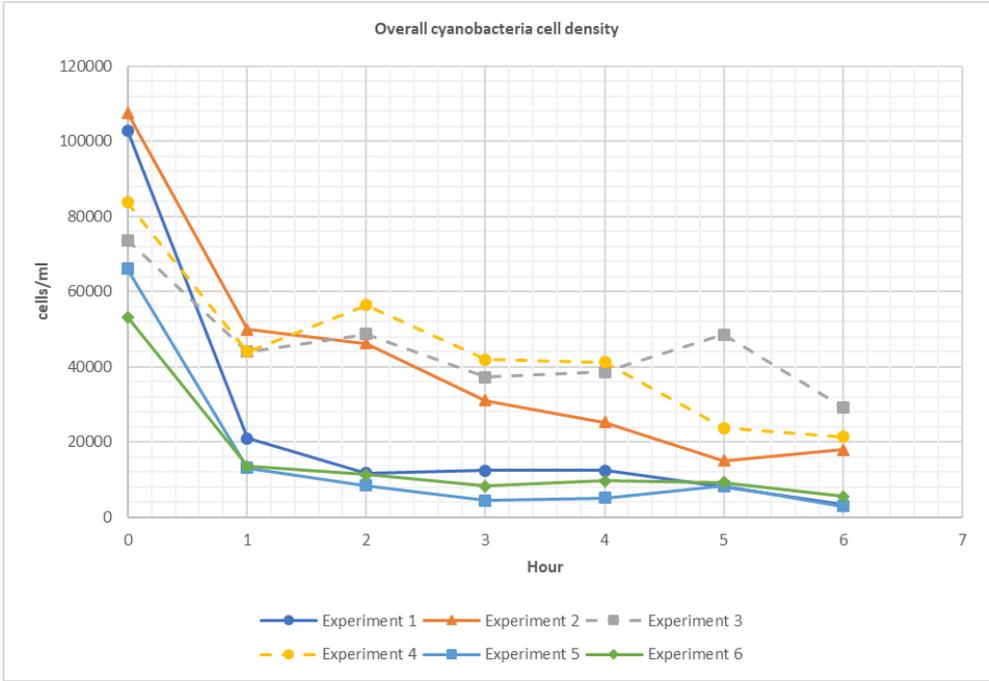
decreased again after the first hour. This might have been to the turbidity breakthrough as shown in Figure 4.23.

As Experiment 3 and 4 did not have large changes in turbidity after EF, the decrease in colour may not have been fully related to the turbidity being reduced after filtration. Another explanation may be that the chlorine generated in EF for these experiments had more time to react with the dissolved particles in the water as the water passed through the filter. Chlorine can remove NOM and therefore reduce the colour.

### 4.2.2 Removal of cyanobacteria

The overall cyanobacteria cell densities and removal rates are shown in Figure 4.29 and Figure 4.30. The maximal removal rate was found in Experiment 1 with a removal rate of 96,7%. after 6 hours. The average removal rate, see Figure 4.31, was however similar for Experiment 1 and 5, with respectively 88,8% and 89,3%.

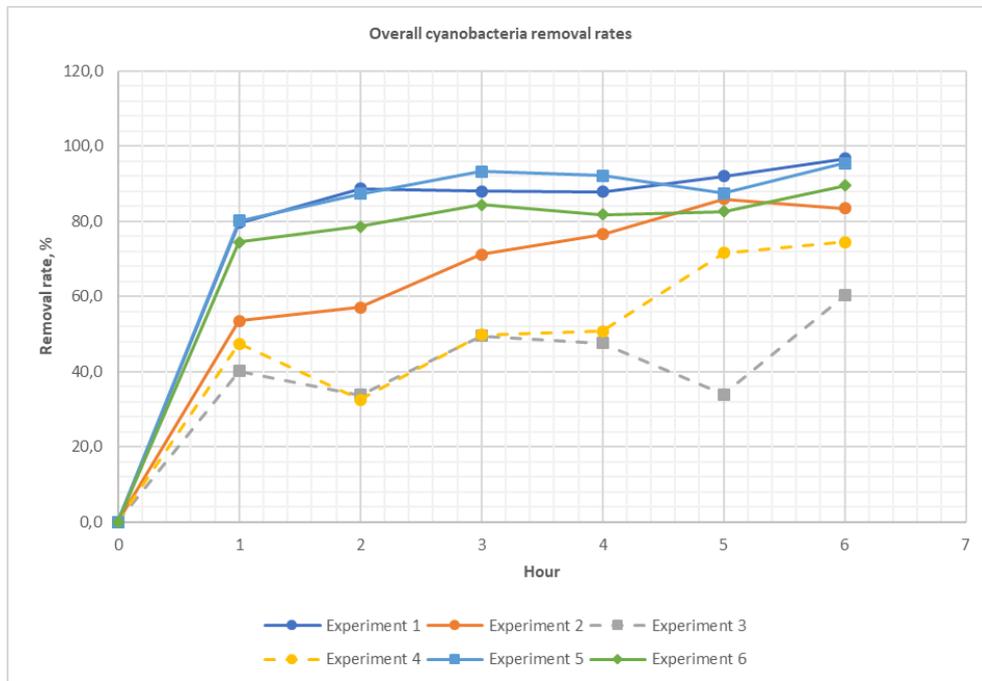
**Figure 4.29: Overall cyanobacteria cell density after integrated process**



After filtration Experiment 1, 5 and 6 reached a cell density < 10 000 cells/ml, set by the Brazilian Ministry of health as the limit for monthly monitoring. Experiment 2 reached below

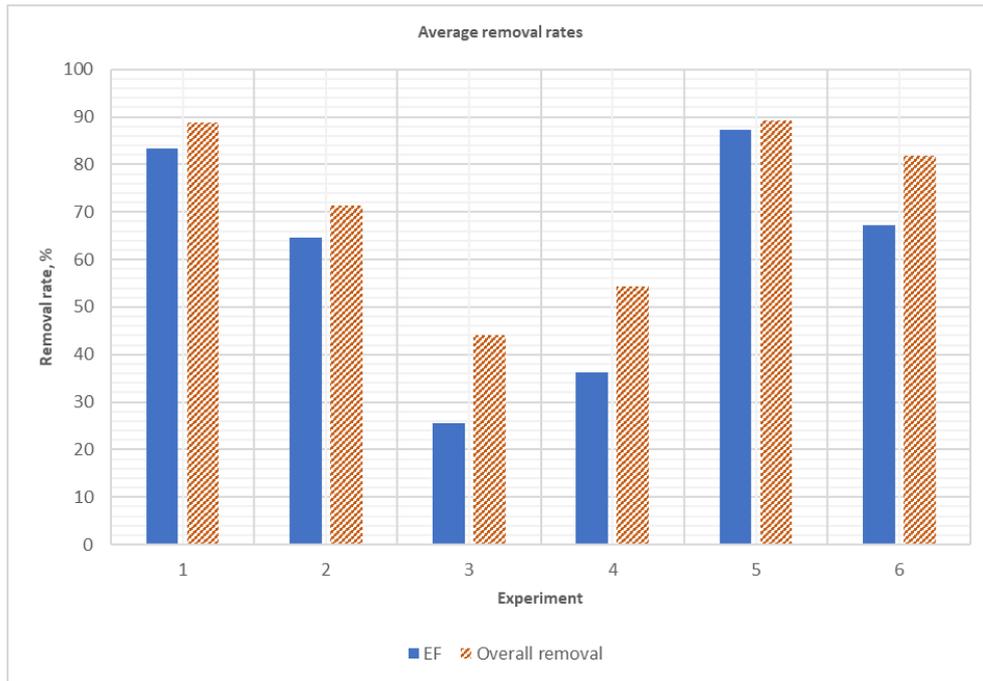
20 000 cells/ml after the last two hours, which is below the limit of mandatory weekly cyanotoxin monitoring.

**Figure 4.30: Overall cyanobacteria removal rates after integrated process**



A comparison of the average removal rates for each experiment after EF and filtration is given in Figure 4.31. As seen from the figure, filtration did not add a large additional removal for Experiment 1,2 and, and particularly, 5. The reduction was probably mostly due to reduction in flocs, that is turbidity, where much cyanobacteria can be trapped. This was also observed during the cell counting. Experiments 3 and 4 had the largest difference between cyanobacteria removal rate after EF and filtration.

**Figure 4.31: Average cyanobacteria removal rates after EF and integrated process**

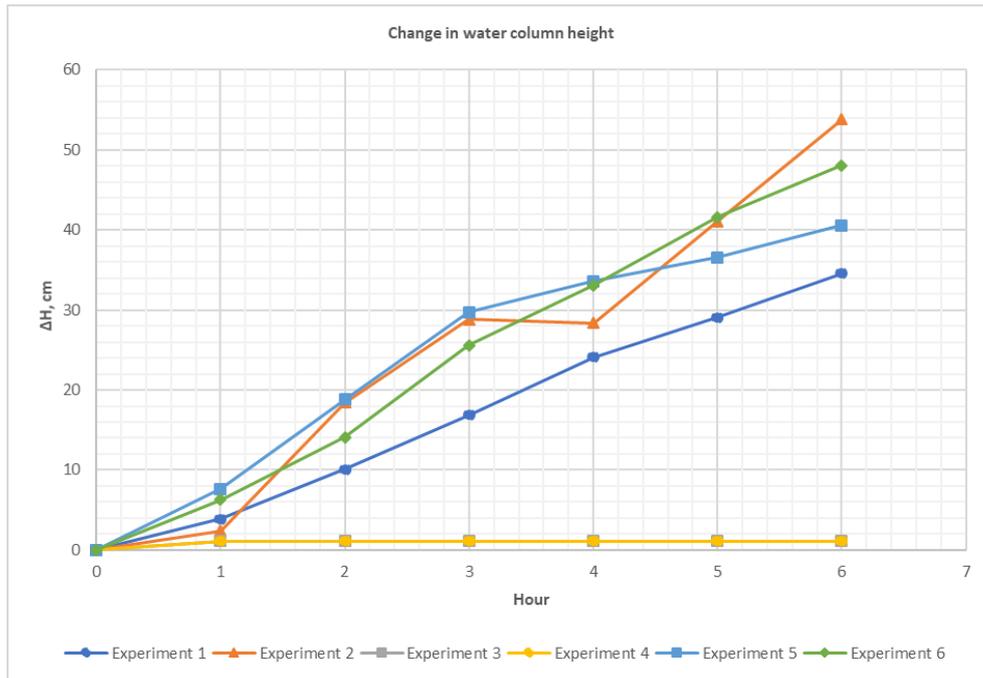


#### 4.2.3 Water column height and head losses

The change in water column height is presented in Figure 4.32. The principal notion is Experiments 3 and 4, having a constant water column height throughout the experiments. As seen from Figure 4.22, the filter in these two experiments retained little of the particles from the water. The process of EF for these two experiments, as mentioned, did not create large flocs or accumulate a thick sludge layer. However, retained particles should result in some change in water column height, given that the inflow rate is constant. For that reason, it may be assumed that there might have been an increase in height for Experiment 3 and 4, but that it was too small to measure.

The water level in Experiment 1 was lower than Experiment 2, 5 and 6. This might be due to accumulation of retained particles over time, as Experiment 1 was conducted before the other experiments.

Figure 4.32: Change in water column height



The head losses in the piezometers are shown in Figure 4.33. Since there were no piezometers placed further down than Piezo 5 the head loss in the gravel could not be measured. As observed from the figure the maximal head loss in a piezometer was found in Piezo 5 in Experiment 6, with a maximal head loss of 0,027 mWC.

No accumulation of particles from previous experiments seemed to affect the next experiment, except between Experiment 5 and 6. Experiment 6 had a very large head loss in comparison.

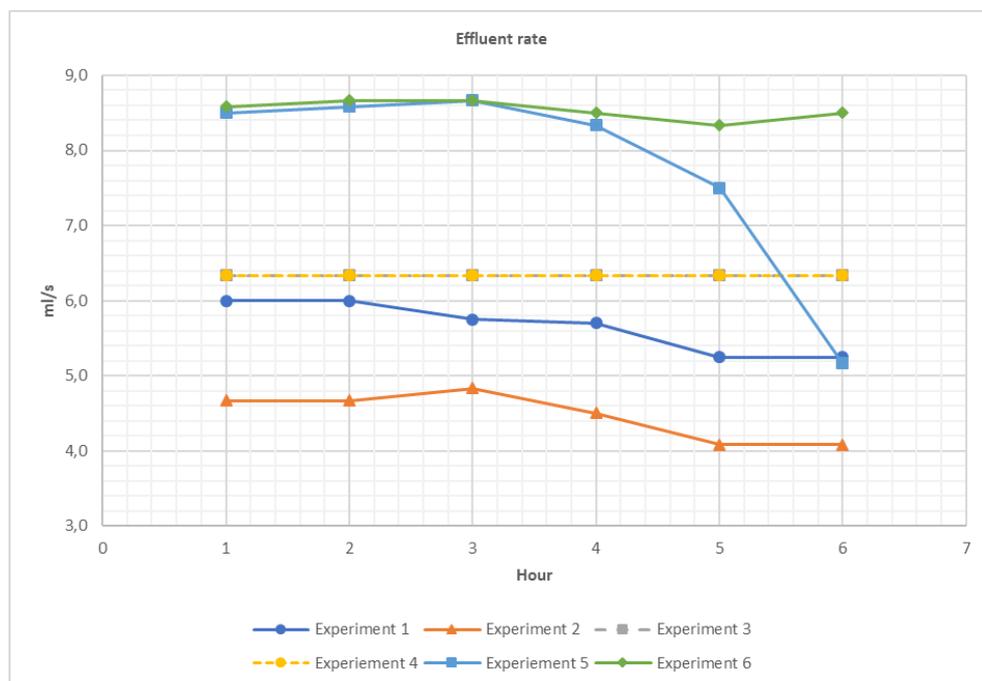
**Figure 4.33: Head loss in piezometers**



#### 4.2.4 Effluent rate

The effluent rate of the filter is given in Figure 4.34. As observed from the graphs, Experiments 3 and 4 had a constant effluent rate. Combined with the results from the water column height in Figure 4.34, showing that it did not increase after the first hour, this would mean the inflow rate to the pilot should be the same as the effluent rate. This is a crucial fact, as the set inflow rate was 12,1 ml/s, whereas both of these experiments demonstrate that the real inflow rate was 6,3 ml/s as it was constant and without any increase in water column.

**Figure 4.34: Effluent rate of experiments**



An important defect of the pump may explain the large differences in flow rates. The pump regulator setting the flow would rotate during pumping, and therefore change the flow rate. The effects of this was attempted to be minimized by often observing the regulator and rotate it back to the desired flow rate. For Experiment 3 and 4 this problem was not as severe. These two experiments also had constant head loss.

However, as all experiments with normal polarity had relatively constant effluent rates, with the exception of Experiment 5, and an approximate constant increase in water column height would mean that the inflow rate probably was somewhat constant as well. In addition, there is

room for error in the measurements as only one effluent rate sample was measured for each time step.

#### 4.2.5 Filter backwash

The turbidity level during backwash can be seen in Figure 4.35. Because of the way the pilot was set up, with an EF reactor above the filter, a conventional filter backwash was not possible. As explained in the methodology section 3.3.1.4, the sludge accumulated during the electroflotation would partly enter the filter. A lot of the sludge settled down to the filter and/or was in suspension in the water above the filter when the water level was lowered. For this reason, the turbidity for the backwashing does not represent accurately the amount of pollutants that was trapped in the filter.

During backwash it was observed that a layer of finer sand and possibly particles accumulated in the intersection between the PVC spheres and the second support layer Figure 4.36. This was probably due to poor separation with shakers, resulting in some finer grains in the support layer. The problem during the experiments was that this layer could not be backwashed, as the backwash velocity required to do so would wash out the PVC filter media.

Figure 4.35: Turbidity backwash

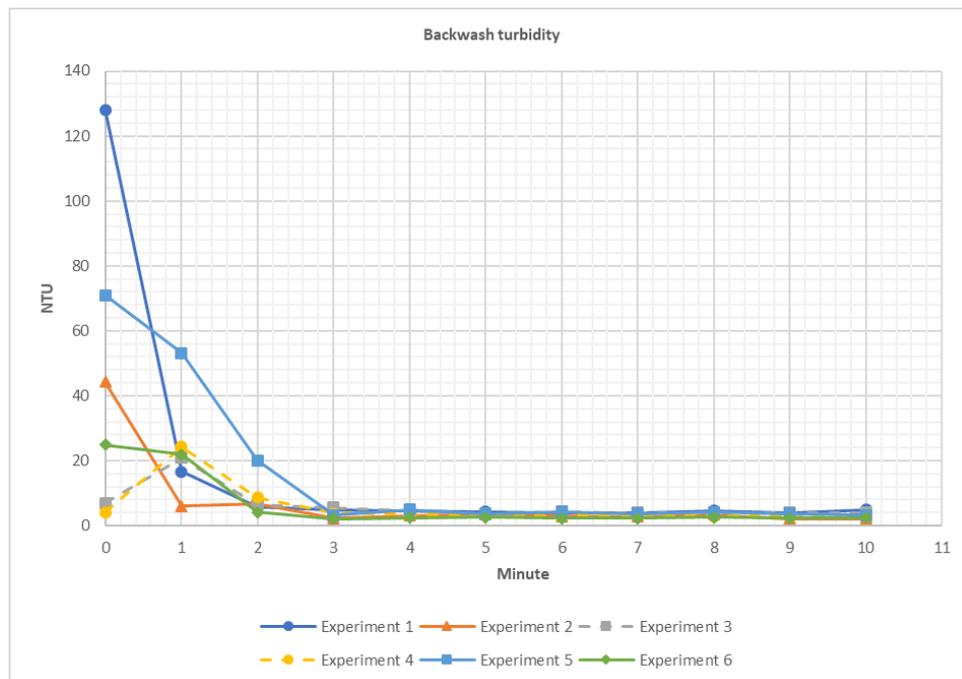


**Figure 4.36: Accumulated sand and particles in the intersection between PVC spheres and gravel after Experiment 6**



*Source: By author*

In sand filters, a backwash rate of 30 to 60 m/h is common (Crittenden *et al.*, 2012). Often the bed expansion is around 20-30%. In this study, the rate was around 51,2 m/h to achieve an expansion of 50%. This means that a very low backwash rate is required for PVC spheres, which can be economically beneficial.

However, the problem with the material being so light was that the PVC spheres easily got washed out. In the case where air in the filter was released in backwashing (air was trapped in the filter at Experiment 2), several spheres could attach to one gas bubble and float to the backwash outlet. The duration would have to be longer to maintain a clean filter, see Figure 4.37. However, this might not have helped much as it seemed some of the flocs retained in the filter has the same density as the spheres, and therefore did not get washed out.

**Figure 4.37: Start of filter backwash (left) and end of filter backwash (right).  
From Experiment 5**



*Source: By author*

The turbidity level at the end of backwash was lower than the turbidity after filtration for many of the experiments. This can be explained with the additional backwash done as explained in section 3.3.1.4, which left some tap water in tank 2 and therefore gave a lower turbidity level during backwash.

### **4.3 Challenges with conducting the experiments**

There were several challenges that occurred with regards to the pilot and the equipment attached to it. The main problem was the corrosion of the DSA<sup>®</sup> that impacted the results largely, and reduced the possibility of conducting more experiments. Other problems that occurred with the pilot, were leakages in the bolted areas of the cylinders. This was repaired before all the presented experiments. The pump used for backwashing also leaked between Experiment 1 and 2. The reparation caused air to enter the pipe that feed the filter during backwash, causing air to enter the filter. The voltage stabilizer also stopped working during one experiment because of the high current applied.

Very importantly, the pump used for inflow was impossible to keep at a constant rate. The flow rate most likely had a large impact on the results, and the lack of consistency in the feed reduces the credibility of the results.

The logistics of the experiments were in general difficult as 200 L of water needed to be transferred around 17 km for each experiment, and used the same day.

## 5 Conclusion

As there were severe corrosion damages on the DSA<sup>®</sup>s, increasing for each experiment conducted, there was observed that the DSA<sup>®</sup>s released less gas than the titanium electrodes, regardless of the polarity. This possibly inhibited the flotation process as the current density applied did not correspond to the rate of gas that theoretically should be produced at the DSA<sup>®</sup>s. In addition, the generation of larger bubbles was observed to collide with the accumulated sludge, causing sedimentation. The large bubbles generated are believed to be caused by coalescing of bubbles, due to the unsmooth surface of the electrodes and the vertical arrangement of the electrodes.

When the polarity was inverted, the removal rates had different patterns than during normal polarity. It was observed that there was little sludge accumulation and fewer changes in turbidity. In addition, a large amount of free and total chlorine was generated at the titanium anode, exceeding the maximal value that could be measured at 3,5 mg/L. The free and total chlorine was believed to remove some of the true colour. The risk of toxin release from cyanobacteria is also present because of the high chlorine concentration.

The turbidity increased for all experiments after EF, but less in the experiments with polarity inversion, where it was as times reduced as well. This is explained by the corrosion causing sedimentation and having a generally reduced potential to generate bubbles. The increase of turbidity was as high as 382,8% at maximum, with a current density of 89,2 A/m<sup>2</sup>. The highest reduction of turbidity was at the removal rate of 20,8% and happened with polarity inversion at the current density of 114,6 A/m<sup>2</sup>. Short retention time was also identified as a possible factor for the failed removal of turbidity after EF. The filter had a maximum removal rate of 76,4% relative to the value after EF, at the current density of 51 A/m<sup>2</sup>, while the highest overall removal rate in the integrated process was 52% at the current density of 31,8 A/m<sup>2</sup>.

The colour also increased for all experiments, except one with polarity inversion. As the colour was measured as apparent colour, the turbidity increase probably affected the measurement. The apparent colour was significantly reduced after filtration, while rapid filtration without coagulation are not expected to remove colour. This demonstrates that the true colour might have been reduced in the EF, but did not show on the measurements as the turbidity increased

simultaneously and disturbed the measurements. The highest removal rate of colour after EF was 26,7 % with polarity inversion at the current density 114,6 A/m<sup>2</sup>. After filtration relative to EF the highest removal was 66,9% and the highest overall removal rate was 60,7%, both at the current density of 31,8 A/m<sup>2</sup>.

The results from the process of EF proved to work for cyanobacteria removal, with a maximal removal rate of 92,3% at the current density 89,2 A/m<sup>2</sup>. Average removal rates were higher at the higher current densities, given that the polarity was not inverted. Removal rates for experiments with polarity inversion was less, with a maximal removal rate of 60,1% at the current density 114,6 A/m<sup>2</sup>. The integrated process, with a filtration step after EF, enhanced the removal of cyanobacteria slightly, the maximal overall removal rate being 96,7% at a current density of 70,1 A/m<sup>2</sup>.

Although cyanobacteria had a high removal rate at high current densities without polarity inversion, the increase in turbidity will cause much of the cyanobacteria to be trapped in the particles. This might also result in short filter runs, either from turbidity breakthrough or early reach to available head. At last, the PVCs spheres low density makes backwashing challenging. Cyanobacteria attached to the retained particles in the filter that does not get backwashed may start cell lysis and thereby release toxins and/or taste and odour compounds.

For this reason, the integrated process of electroflotation and rapid filtration using PVC spheres is not recommended as a method of removing cyanobacteria. As the corrosion was believed to have a large impact, further studies should be done assessing the effects of this. In addition, the retention time in the electroflotation reactor should also be studied further as a filter would create large variations in the time of electrolysis per volume of water. At last, adding NaCl to the water can produce dangerous large amounts of chlorine, followed by the risk of cyanotoxin release, and studies with a stronger voltage stabilizer should be used to avoid additions of salt.

## 6 References

- Alexandrova, L., Nedialkova, T. and Nishkov, I. (1994) 'Electroflotation of metal ions in waste water', *International Journal of Mineral Processing*. doi: 10.1016/0301-7516(94)90034-5.
- Almuhtaram, H. *et al.* (2018) 'Cyanotoxins and Cyanobacteria Cell Accumulations in Drinking Water Treatment Plants with a Low Risk of Bloom Formation at the Source'. doi: 10.3390/toxins10110430.
- Van Apeldoorn, M. E. *et al.* (2007) 'Toxins of cyanobacteria', *Molecular Nutrition and Food Research*, 51(1), pp. 7–60. doi: 10.1002/mnfr.200600185.
- AWWA (2012) *Standard Methods for the Examination of Water and Wastewater*. 22nd edn. Edited by E. W. Rice *et al.* Washington DC: American Public Health Association, American Water Works Association, Water Environment Federation.
- Ballot, A. *et al.* (2003) 'Cyanobacterial toxins in Lake Baringo, Kenya', *Limnologica*, 33(1), pp. 2–9. doi: 10.1016/S0075-9511(03)80003-8.
- Banker, R. *et al.* (1997) 'Identification of cylindrospermopsin in Aphanizomenon ovalisporum (cyanophyceae) isolated from Lake Kinneret, Israel', *Journal of Phycology*, 33(4), pp. 613–616. doi: 10.1111/j.0022-3646.1997.00613.x.
- Blue-green algae - organism* (2017). Available at: <https://www.britannica.com/science/blue-green-algae> (Accessed: 26 December 2018).
- Bourke, A. T. C. *et al.* (1983) 'An outbreak of hepato-enteritis (the Palm Island mystery disease) possibly caused by algal intoxication', *Toxicon*. doi: 10.1016/0041-0101(83)90151-4.
- Brand, L. E. *et al.* (2010) 'Cyanobacterial blooms and the occurrence of the neurotoxin, beta-N-methylamino-L-alanine (BMAA), in South Florida aquatic food webs', *Harmful Algae*. doi: 10.1016/j.hal.2010.05.002.
- Bristol, U. of (no date) *What Are Surfactants*, *Univeristy of Bristol*. Available at: <http://www.bristol.ac.uk/chemistry/research/eastoe/what-are-surfactants/> (Accessed: 18 October 2018).
- Burns, S. E., Yiacoymi, S. and Tsouris, C. (1997) 'Microbubble generation for environmental and industrial separations', *Separation and Purification Technology*, 11(3), pp. 221–232. doi: 10.1016/S1383-5866(97)00024-5.
- Camp, C. (no date) *Part 1 - Introduction to Water Filtration*, *Department of Civil Engineering, University of Memphis*. Available at: <http://www.ce.memphis.edu/1101/notes/filtration/filtration-1.html> (Accessed: 23 November

2018).

Campos, T. *et al.* (2017) ‘Combination of electroflotation process and down-flow granular filtration to treat wastewater contaminated with oil’, *Environmental Technology*. Taylor & Francis, 0(0), pp. 1–8. doi: 10.1080/09593330.2017.1310306.

Campos, T. *et al.* (2018) ‘Removal of cyanobacteria from supply waters by electroflotation using DSA® electrodes’, 138, pp. 134–140. doi: 10.5004/dwt.2019.23285.

Cardarelli, F. *et al.* (1998) ‘Preparation of oxygen evolving electrodes with long service life under extreme conditions’, *Journal of Applied Electrochemistry*. doi: 10.1023/A:1003251329958.

Carrasco, D. *et al.* (2007) ‘Anatoxin-a occurrence and potential cyanobacterial anatoxin-a producers in Spanish reservoirs’, *Journal of Phycology*, 43(6), pp. 1120–1125. doi: 10.1111/j.1529-8817.2007.00402.x.

Chen, G. (2004) ‘Electrochemical technologies in wastewater treatment’, 38(October 2003), pp. 11–41. doi: 10.1016/j.seppur.2003.10.006.

Chen, X., Chen, G. and Yue, P. L. (2002) ‘Novel electrode system for electroflotation of wastewater’, *Environmental Science and Technology*, 36(4), pp. 778–783. doi: 10.1021/es011003u.

Chiswell, R. K. *et al.* (1999) ‘Stability of cylindrospermopsin, the toxin from the cyanobacterium, *cylindrospermopsis raciborskii*: Effect of pH, temperature, and sunlight on decomposition’, *Environmental Toxicology*, 14(1), pp. 155–161. doi: 10.1002/(SICI)1522-7278(199902)14:1<155::AID-TOX20>3.0.CO;2-Z.

Choi, Y. G. *et al.* (2005) ‘Improvement of the thickening and dewatering characteristics of activated sludge by electroflotation (EF)’, *Water Science and Technology*. IWA Publishing, 52(10–11), pp. 219–226. doi: 10.2166/wst.2005.0697.

Chorus, I. and Bartram, J. (2000) ‘Toxic cyanobacteria in water. A guide to their public health consequences, monitoring, and management’, *Limnology and Oceanography*. doi: 10.4319/lo.2000.45.5.1212.

Comninellis, C. and Chen, G. (2010) *Electrochemistry for the environment*, *Electrochemistry for the Environment*. doi: 10.1007/978-0-387-68318-8.

Comninellis, C. H. and Vercesi, G. P. (1991) *Characterization of DSA/ oxygen evolving electrodes: choice of a coating*, *JOURNAL OF APPLIED ELECTROCHEMISTRY*. Available at: <https://link.springer.com/content/pdf/10.1007%2FBF01020219.pdf> (Accessed: 29 December 2018).

Cox, P. A. *et al.* (2005) ‘Diverse taxa of cyanobacteria produce  $\beta$ -N-methylamino-L-alanine, a neurotoxic amino acid’, *Proceedings of the National Academy of Sciences*. doi: 10.1073/pnas.0501526102.

Crittenden, J. C. *et al.* (2012) *MWH’s Water Treatment: Principles and Design*. Third Edit. John Wiley & Sons, Inc., Hoboken, New Jersey. doi: 10.1002/9781118131473.

Cyclopedia, M. (2017) *The Joule Heating Effect, Comsol*. Available at: <https://www.comsol.com/multiphysics/the-joule-heating-effect> (Accessed: 27 February 2019).

Dalsasso, R. L. (2005) *Estudo de diferentes materiasias para floculacao em meio granular precedendo a Filtracao rapida descendente no tratamento de agua para abastecimento*. Universidade Federal de Santa Catarina.

Daneshvar, N., Sorkhabi, H. A. and Kasiri, M. B. (2004) ‘Decolorization of dye solution containing Acid Red 14 by electrocoagulation with a comparative investigation of different electrode connections’, 112, pp. 55–62. doi: 10.1016/j.jhazmat.2004.03.021.

Dixon, M. B. *et al.* (2011) ‘Removal of cyanobacterial metabolites by nanofiltration from two treated waters’, *Journal of Hazardous Materials*. doi: 10.1016/j.jhazmat.2011.01.111.

Duby, P. (1993) ‘The history of progress in dimensionally stable anodes’, *JOM*, 45 (3), pp. 41–43. doi: 10.1007/BF03222350.

Edzwald James K. (2010) *Water Quality & Treatment: A Handbook on Drinking Water*. Sixth Edit, *American Water Works Association*. Sixth Edit. Edited by James K. Edzwald. McGraw-hill.

El-Hosiny, F. *et al.* (2017) ‘A Designed Electro-flotation Cell for Dye Removal from Wastewater’, *Journal of Applied Research on Industrial Engineering*, 4(2), pp. 133–147. doi: 10.22105/jarie.2017.100801.1021.

EPA (2014) ‘Cyanobacteria and Cyanotoxins : Information for Drinking Water Systems’, pp. 1–11. Available at: [https://www.epa.gov/sites/production/files/2014-08/documents/cyanobacteria\\_factsheet.pdf](https://www.epa.gov/sites/production/files/2014-08/documents/cyanobacteria_factsheet.pdf).

Esterhuizen, M. and Downing, T. G. (2008) ‘ $\beta$ -N-methylamino-l-alanine (BMAA) in novel South African cyanobacterial isolates’, *Ecotoxicology and Environmental Safety*. doi: 10.1016/j.ecoenv.2008.04.010.

Fastner, J. *et al.* (2003) ‘Cylindrospermopsin occurrence in two German lakes and preliminary assessment of toxicity and toxin production of *Cylindrospermopsis raciborskii* (Cyanobacteria) isolates’, *Toxicon*, 42(3), pp. 313–321. doi: 10.1016/S0041-0101(03)00150-8.

Fristachi, A. *et al.* (2008) ‘Cyanobacterial Harmful Algal Blooms: Chapter 3: Occurrence of

Cyanobacterial Harmful Algal Blooms Workgroup Report', *Cyanobacterial Harmful Algal Blooms*, pp. 44–103. doi: 10.1007/978-0-387-75865-7.

G.Pizzi, N. (2011) *Water Treatment - Principles and practices of water supply operations series*. Fourth edi. American Water Works Association. Available at: <http://www.metrovancouver.org/services/water/quality-facilities/facilities-processes/treatment-process/Pages/default.aspx>.

Gao, S. *et al.* (2010) 'Electro-coagulation-flotation process for algae removal', *Journal of Hazardous Materials*. Elsevier B.V., 177(1–3), pp. 336–343. doi: 10.1016/j.jhazmat.2009.12.037.

Gheraout, D., Benblidia, C. and Khemici, F. (2015) 'Microalgae removal from Ghrib Dam (Ain Defla, Algeria) water by electroflotation using stainless steel electrodes', *Desalination and Water Treatment*. Taylor & Francis, 54(12), pp. 3328–3337. doi: 10.1080/19443994.2014.907749.

Graham, J. L. *et al.* (2008) 'Cyanobacteria in Lakes and Reservoirs: Toxin and Taste-and-Odor Sampling Guidelines', in *U.S. Geological Survey TWRI Book 9*, pp. 1–65.

Grützmacher, G. *et al.* (2002) 'Removal of microcystins by slow sand filtration', *Environmental Toxicology*. doi: 10.1002/tox.10062.

Gugger, M. *et al.* (2005) 'First report in a river in France of the benthic cyanobacterium *Phormidium favosum* producing anatoxin-a associated with dog neurotoxicosis', *Toxicon*, 45(7), pp. 919–928. doi: 10.1016/j.toxicon.2005.02.031.

Hillborn, E. . *et al.* (2007) 'Serologic evaluation of human microcystin exposure', *Environmental Toxicology*, 22 (5), pp. 459–463. doi: 10.1002/tox.20281.

Hoseinieh, S. M., Ashrafizadeh, F. and Maddahi, M. H. (2010) 'A Comparative Investigation of the Corrosion Behavior of RuO<sub>2</sub>-IrO<sub>2</sub>-TiO<sub>2</sub> Coated Titanium Anodes in Chloride Solutions', *Journal of The Electrochemical Society*, 157(4), p. E50. doi: 10.1149/1.3294569.

Hosny, A. Y. (1996) 'Separating oil from oil-water emulsions by electroflotation technique', *Separations Technology*. doi: 10.1016/0956-9618(95)00136-0.

Huang, W. J., Cheng, B. L. and Cheng, Y. L. (2007) 'Adsorption of microcystin-LR by three types of activated carbon', *Journal of Hazardous Materials*. doi: 10.1016/j.jhazmat.2006.06.122.

Humbert, J. F. (2009) 'Toxins of cyanobacteria.', in Gupta, R. C. (ed.) *Handbook of Toxicology of Chemical Warfare Agents*. Academic Press. doi: <https://doi.org/10.1016/B978-0-12-374484-5.X0001-6>.

- Humpage, A. R. and Falconer, I. R. (2003) 'Oral toxicity of the cyanobacterial toxin cylindrospermopsin in male Swiss albino mice: Determination of no observed adverse effect level for deriving a drinking water guideline value', *Environmental Toxicology*. doi: 10.1002/tox.10104.
- Ibrahim, M. Y. *et al.* (2001) 'UTILIZATION OF ELECTROFLOTATION IN REMEDIATION OF OILY WASTEWATER', *Separation Science and Technology*, 36(16), pp. 3749–3762. doi: 10.1081/SS-100108360.
- Jiménez, C. *et al.* (2010) 'Study of the production of hydrogen bubbles at low current densities for electroflotation processes', *Journal of Chemical Technology and Biotechnology*, 85(10), pp. 1368–1373. doi: 10.1002/jctb.2442.
- Jochimsen, E. M. *et al.* (1998) 'Liver Failure and Death after Exposure to Microcystins at a Hemodialysis Center in Brazil', *New England Journal of Medicine*, 338(13), pp. 873–878. doi: 10.1056/NEJM199803263381304.
- Johnson, H. E. *et al.* (2008) 'Cyanobacteria (*Nostoc commune*) used as a dietary item in the Peruvian highlands produce the neurotoxic amino acid BMAA', *Journal of Ethnopharmacology*. doi: 10.1016/j.jep.2008.04.008.
- Khelifa, A., Moulay, S. and Naceur, A. W. (2005) 'Treatment of metal finishing effluents by the electroflotation technique', *Desalination*. doi: 10.1016/j.desal.2005.01.011.
- Kobya, M., Can, O. T. and Bayramoglu, M. (2003) 'Treatment of textile wastewaters by electrocoagulation using iron and aluminum electrodes', 100, pp. 163–178. doi: 10.1016/S0304-3894(03)00102-X.
- Kyzas, G. Z. and Matis, K. A. (2016) 'Electroflotation process: A review', *Journal of Molecular Liquids*, 220, pp. 657–664. doi: 10.1016/j.molliq.2016.04.128.
- Lecrivain, G. *et al.* (2015) 'Attachment of solid elongated particles on the surface of a stationary gas bubble', *International Journal of Multiphase Flow*. Elsevier Ltd, 71, pp. 83–93. doi: 10.1016/j.ijmultiphaseflow.2015.01.002.
- Li, A. *et al.* (2010) 'Detection of the neurotoxin BMAA within cyanobacteria isolated from freshwater in China', *Toxicon*. doi: 10.1016/j.toxicon.2009.09.023.
- Li, R. *et al.* (2001) 'Isolation and identification of the cyanotoxin cylindrospermopsin and deoxy-cylindrospermopsin from a Thailand strain of *Cylindrospermopsis raciborskii*', *Toxicon: Official journal of the International Society on Toxinology*, 39 (7), pp. 973–980. Available at: <https://www.sciencedirect.com/science/article/pii/S0041010100002361> (Accessed: 26 December 2018).

- Martelli, G. N., Ornelas, R. and Faita, G. (1994) ‘Deactivation mechanisms of oxygen evolving anodes at high current densities’, *Electrochimica Acta*. Pergamon, 39(11–12), pp. 1551–1558. doi: 10.1016/0013-4686(94)85134-4.
- Martínez-Huitle, C. A., Rodrigo, M. A. and Scialdone, O. (2018) ‘Electrochemical Water and Wastewater Treatment’, *Electrochemical Water and Wastewater Treatment*. Elsevier Inc., p. 570. doi: 10.1016/B978-0-12-813160-2.09986-7.
- Merel, S. *et al.* (2013) ‘State of knowledge and concerns on cyanobacterial blooms and cyanotoxins’, *Environment International*. Elsevier Ltd, 59, pp. 303–327. doi: 10.1016/j.envint.2013.06.013.
- Merzouk, B., Madani, K. and Sekki, A. (2010) ‘Using electrocoagulation – electro flotation technology to treat synthetic solution and textile wastewater , two case studies ☆’, *DES*. Elsevier B.V., 250(2), pp. 573–577. doi: 10.1016/j.desal.2009.09.026.
- Metcalf, J. S. *et al.* (2008) ‘Co-occurrence of  $\beta$ -N-methylamino-L-alanine, a neurotoxic amino acid with other cyanobacterial toxins in British waterbodies, 1990-2004’, *Environmental Microbiology*. doi: 10.1111/j.1462-2920.2007.01492.x.
- Mickova, I. (2015) ‘Advanced Electrochemical Technologies in Wastewater Treatment. Part II: Electro-Flocculation and ElectroFlotation’, *American Scientific Research Journal for Engineering, Technology, and Sciences (ASRJETS)*, 14(2), pp. 273–294. Available at: [http://asrjetsjournal.org/index.php/American\\_Scientific\\_Journal/article/view/1017/613](http://asrjetsjournal.org/index.php/American_Scientific_Journal/article/view/1017/613).
- Miettinen, T., Ralston, J. and Fornasiero, D. (2010) ‘The limits of fine particle flotation’, *Minerals Engineering*. Elsevier Ltd, 23(5), pp. 420–437. doi: 10.1016/j.mineng.2009.12.006.
- Molica, R. *et al.* (2005) ‘Occurrence of saxitoxins and an anatoxin-a (s)-like anticholinesterase in a Brazilian drinking water supply’, *Harmful Algae*, 4 (4), pp. 743–753. doi: 10.1016/J.HAL.2004.11.001.
- Mollah, M. Y. A. *et al.* (2004) ‘Fundamentals, present and future perspectives of electrocoagulation’, *Journal of Hazardous Materials*, 114(1–3), pp. 199–210. doi: 10.1016/j.jhazmat.2004.08.009.
- Mostefa, N. M. and Tir, M. (2004) ‘Coupling flocculation with electroflotation for waste oil/water emulsion treatment. Optimization of the operating conditions’, *Desalination*. Elsevier, 161(2), pp. 115–121. doi: 10.1016/S0011-9164(04)90047-1.
- Mráz, R. and Krýsa, J. (1994) ‘Long service life IrO<sub>2</sub>/Ta<sub>2</sub>O<sub>5</sub> electrodes for electroflotation’, *Journal of Applied Electrochemistry*. doi: 10.1007/BF00249891.
- MS (2012) *PORTARIA Nº 2.914, Ministério da Saúde Gabinete do Ministro*. Available at:

[http://bvsmms.saude.gov.br/bvs/saudelegis/gm/2011/prt2914\\_12\\_12\\_2011.html](http://bvsmms.saude.gov.br/bvs/saudelegis/gm/2011/prt2914_12_12_2011.html) (Accessed: 25 January 2019).

Namikoshi, M. *et al.* (2003) 'Simultaneous production of homoanatoxin-a, anatoxin-a, and a new non-toxic 4-hydroxyhomoanatoxin-a by the cyanobacterium *Raphidiopsis mediterranea* Skuja', *Toxicon*, 42(5), pp. 533–538. doi: 10.1016/S0041-0101(03)00233-2.

Newcombe, G. (2009) 'Global Water Research Coalition: International Guidance Manual for the Management of Toxic Cyanobacteria', p. 415.

Nguyen, A. V., Schulze, H. J. and Ralston, J. (1997) 'Elementary steps in particle—bubble attachment', *International Journal of Mineral Processing*, 51(1–4), pp. 183–195. doi: 10.1017/CBO9781107707092.011.

Noel, B. *et al.* (1995) *EPA Water Treatment Manual - Filtration*. Environmental Protection Agency, Ireland. Available at: [https://www.epa.ie/pubs/advice/drinkingwater/EPA\\_water\\_treatment\\_manual\\_filtration1.pdf](https://www.epa.ie/pubs/advice/drinkingwater/EPA_water_treatment_manual_filtration1.pdf).

O'Neil, J. M. *et al.* (2012) 'The rise of harmful cyanobacteria blooms: The potential roles of eutrophication and climate change', *Harmful Algae*. Elsevier B.V., 14, pp. 313–334. doi: 10.1016/j.hal.2011.10.027.

Oliveira, J. S. (2002) *Análise Sedimentar Em Zonas Costeiras: Subsídio Ao Diagnóstico Ambiental Da Lagoa Do Peri – Ilha De Santa Catarina-Sc, Brasil*. Universidade de Santa Catarina.

Onodera, H. *et al.* (1997) 'Confirmation of anatoxin-a(s), in the cyanobacterium *Anabaena lemmermannii*, as the cause of bird kills in Danish lakes', *Toxicon*. doi: 10.1016/S0041-0101(97)00038-X.

Osswald, J. *et al.* (2007) 'Toxicology and detection methods of the alkaloid neurotoxin produced by cyanobacteria, anatoxin-a', *Environment International*, 33(8), pp. 1070–1089. doi: 10.1016/j.envint.2007.06.003.

Paerl, H. W. and Paul, V. J. (2012) 'Climate change: Links to global expansion of harmful cyanobacteria', *Water Research*. Elsevier Ltd, 46(5), pp. 1349–1363. doi: 10.1016/j.watres.2011.08.002.

Poon, C. P. C. (1997) 'Electroflotation for groundwater decontamination', in *Journal of Hazardous Materials*. doi: 10.1016/S0304-3894(97)00013-7.

Preece, E. P. *et al.* (2017) 'A review of microcystin detections in Estuarine and Marine waters: Environmental implications and human health risk', *Harmful Algae*. Elsevier B.V., 61, pp. 31–45. doi: 10.1016/j.hal.2016.11.006.

- Rhodes, C. P. *et al.* (2007) 'Effect of Temperature on the Electrolysis of Water in Concentrated Alkali Hydroxide Solutions', *Solar Energy*, 15729(2006), pp. 15729–15729.
- Ribau Teixeira, M. and Rosa, M. J. (2006) 'Neurotoxic and hepatotoxic cyanotoxins removal by nanofiltration', *Water Research*. doi: 10.1016/j.watres.2006.05.035.
- Robinson, W. R. (no date) *Chemistry: 17.7 Electrolysis*, Rice University. Available at: <https://opentextbc.ca/chemistry/chapter/17-7-electrolysis/> (Accessed: 19 February 2019).
- Romero, L. G. *et al.* (2014) 'Removal of cyanobacteria and cyanotoxins during lake bank filtration at Lagoa do Peri, Brazil', *Clean Technologies and Environmental Policy*, 16(6), pp. 1133–1143. doi: 10.1007/s10098-014-0715-x.
- Schöntag, J. M. and Sens, M. L. (2015) 'Effective production of rapid filters with polystyrene granules as a media filter', *Water Science and Technology: Water Supply*, 15(5), pp. 1088–1098. doi: 10.2166/ws.2015.072.
- Shen, F. *et al.* (2003) 'Electrochemical removal of fluoride ions from industrial wastewater', *Chemical Engineering Science*. doi: 10.1016/S0009-2509(02)00639-5.
- Sillanpa, M. and Shestakova, M. (2017) *Electrochemical Water Treatment Methods - Fundamentals, Methods and Full Scale Applications*. Butterworth-Heinemann. doi: 10.1016/B978-0-12-811462-9.00002-5.
- Srinivasan, V. and Subbaiyan, M. (1989) 'Electroflotation Studies on Cu, Ni, Zn, and Cd with Ammonium Dodecyl Dithiocarbamate', *Separation Science and Technology*, 24(1–2), pp. 145–150. doi: 10.1080/01496398908049757.
- Stewart, I., Seawright, A. A. and Shaw, G. R. (2008) 'Cyanobacterial poisoning in livestock, wild mammals and birds – an overview', in *In: Hudnell H.K. (eds) Cyanobacterial Harmful Algal Blooms: State of the Science and Research Needs. Advances in Experimental Medicine and Biology, vol 619*. Springer, New York, NY, pp. 613–637. doi: 10.1007/978-0-387-75865-7\_28.
- Stirling, D. J. and Quilliam, M. A. (2001) 'First report of the cyanobacterial toxin cylindrospermopsin in New Zealand', *Toxicon*. doi: 10.1016/S0041-0101(00)00266-X.
- Svrcek, C. and Smith, D. W. (2004) 'Cyanobacteria toxins and the current state of knowledge on water treatment options: a review', *Journal of Environmental Engineering and Science*, 3(3), pp. 155–185. doi: 10.1139/s04-010.
- Sylvéus, A. (2012) *Diagnóstico das cianobactérias na Lagoa do Peri, Florianópolis, SC e a legislação sobre água para consumo humano*. Universidade de Santa Catarina. doi: 10.1007/s40732-018-0320-1.

Tsai, L.-S., Hernlem, B. and Huxsoll, C. C. (2002) ‘Disinfection and Solids Removal of Poultry Chiller Water by Electroflotation’, *Journal of Food Science*, 67(6), pp. 2160–2164. doi: 10.1111/j.1365-2621.2002.tb09520.x.

TU Delft (2007) ‘Granular Filtration’, *MWH’s Water Treatment*, pp. 727–818. doi: 10.1002/9781118131473.ch11.

Vercesi, G. *et al.* (no date) ‘Characterization of DSA-type oxygen evolving electrodes. Choice of base metal’, *Elsevier*. Available at: <https://www.sciencedirect.com/science/article/pii/004060319180257J> (Accessed: 29 December 2018).

Verrelli, D. I., Koh, P. T. L. and Nguyen, A. V. (2011) ‘Particle-bubble interaction and attachment in flotation’, *Chemical Engineering Science*. Elsevier, 66(23), pp. 5910–5921. doi: 10.1016/j.ces.2011.08.016.

Vuori, E. *et al.* (1997) ‘Removal of nodularin from brackish water with reverse osmosis or vacuum distillation’, *Water Research*. doi: 10.1016/S0043-1354(97)00127-9.

Wakeman, R. J. (2011) *FLOTATION, A-to-Z Guide to Thermodynamics, Heat & Mass Transfer, and Fluids Engineering*. doi: 10.1615/AtoZ.f.flotation.

Westrick, J. A. *et al.* (2010) ‘A review of cyanobacteria and cyanotoxins removal/inactivation in drinking water treatment’, *Analytical and Bioanalytical Chemistry*, 397(5), pp. 1705–1714. doi: 10.1007/s00216-010-3709-5.

Wood, S. *et al.* (2007) ‘First report of homoanatoxin-a and associated dog neurotoxicosis in New Zealand’, *Toxicon*, 50 (2), pp. 292–301. doi: 10.1016/j.toxicon.2007.03.025.

World Health Organization (no date) *Chemical hazards in drinking-water: Microcystin-LR*. Available at: [https://www.who.int/water\\_sanitation\\_health/water-quality/guidelines/chemicals/microcystin/en/](https://www.who.int/water_sanitation_health/water-quality/guidelines/chemicals/microcystin/en/) (Accessed: 26 December 2018).

Xing, Y. *et al.* (2017) ‘Recent experimental advances for understanding bubble-particle attachment in flotation’, *Advances in Colloid and Interface Science*. Elsevier, 246(May), pp. 105–132. doi: 10.1016/j.cis.2017.05.019.

Yang, Z., Kong, F. and Zhang, M. (2016) ‘Groundwater contamination by microcystin from toxic cyanobacteria blooms in Lake Chaohu, China’, *Environmental Monitoring and Assessment*. Environmental Monitoring and Assessment, 188(5). doi: 10.1007/s10661-016-5289-0.

## APPENDIX A – Parameters

### Data from Experiment 1

Raw water

<b>Turbidity (NTU)</b>	<b>Colour (HU)</b>	<b>pH</b>	<b>Conductivity (µS/cm)</b>	<b>Temperature (°C)</b>
7,65	152	8,8	70,8	28

Raw water with NaCl

<b>Turbidity (NTU)</b>	<b>Colour (HU)</b>	<b>pH</b>	<b>Conductivity (µS/cm)</b>	<b>Temperature (°C)</b>
7,98	152	8,04	198,8	31,2

Results after EF

<b>Hour</b>	<b>Turbidity (NTU)</b>	<b>Colour (HU)</b>	<b>pH</b>	<b>Conductivity (µS/cm)</b>	<b>Temperature (°C)</b>
1	15,8	175	9,96	183,4	32
2	15,5	178	9,89	184,4	34,4
3	15,4	175	9,97	183,8	32,1
4	14,6	168	10,02	185	34,8
5	15,7	188	10,01	181,6	36,3
6	15,6	182	9,97	183,6	33,4

## Results after integrated process

Hour	Turbidity (NTU)	Colour (HU)	pH	Conductivity ( $\mu\text{S/cm}$ )	Temperature ( $^{\circ}\text{C}$ )
1	9,2	111	9,88	171,9	29,9
2	8,59	103	9,94	179,9	32
3	7,95	93	9,91	175	31
4	7,36	91	9,87	176,5	32
5	7,02	88	9,73	174,2	33
6	6,87	92	9,73	177	31,8

## Data from Experiment 2

Raw water

Turbidity (NTU)	Colour (HU)	pH	Conductivity ( $\mu\text{S/cm}$ )	Temperature ( $^{\circ}\text{C}$ )
7,77	140	8,82	81,4	Not measured

Raw water with NaCl

Turbidity (NTU)	Colour (HU)	pH	Conductivity ( $\mu\text{S/cm}$ )	Temperature ( $^{\circ}\text{C}$ )
5,61	117	8,01	149,6	27,2

Results after EF

Hour	Turbidity (NTU)	Colour (HU)	pH	Conductivity ( $\mu\text{S/cm}$ )	Temperature ( $^{\circ}\text{C}$ )
1	9,5	154	9,29	139,8	29,8
2	9,41	142	9,71	145,2	30,1
3	7,7	132	9,72	141,6	32
4	8,78	140	9,84	148	32,9
5	8,07	127	9,73	148,3	31,4
6	7,92	124	9,81	163,7	28,4

Results after integrated process

Hour	Turbidity (NTU)	Colour (HU)	pH	Conductivity ( $\mu\text{S/cm}$ )	Temperature ( $^{\circ}\text{C}$ )
1	3,55	54	9,2	130	28,3
2	2,89	47	8,71	131,2	28,4
3	2,85	50	9,11	134,8	29,5
4	3,11	52	9,56	132,9	30,2
5	2,69	46	9,49	130,8	29,3
6	2,98	47	9,72	129,6	27,4

### Data from Experiment 3

Raw water

<b>Turbidity (NTU)</b>	<b>Colour (HU)</b>	<b>pH</b>	<b>Conductivity (<math>\mu</math>S/cm)</b>	<b>Temperature (<math>^{\circ}</math>C)</b>
4,45	108	7,24	72,2	28,8

Raw water with NaCl

<b>Turbidity (NTU)</b>	<b>Colour (HU)</b>	<b>pH</b>	<b>Conductivity (<math>\mu</math>S/cm)</b>	<b>Temperature (<math>^{\circ}</math>C)</b>
4,58	106	7,45	289	28,3

Results after EF

<b>Hour</b>	<b>Turbidity (NTU)</b>	<b>Colour (HU)</b>	<b>pH</b>	<b>Conductivity (<math>\mu</math>S/cm)</b>	<b>Temperature (<math>^{\circ}</math>C)</b>
1	5,21	118	7,95	262	32,9
2	4,79	106	8,25	267	34,3
3	4,61	133	8,28	270	35,4
4	5,7	118	8,22	268	33,5
5	5,12	109	8,22	208	33,3
6	4,68	104	8,23	269	32,3

## Results after integrated process

Hour	Turbidity (NTU)	Colour (HU)	pH	Conductivity ( $\mu\text{S/cm}$ )	Temperature ( $^{\circ}\text{C}$ )
1	4,51	101	6,85	229	31,3
2	3,92	94	8,06	258	32,3
3	3,67	83	8,1	267	33,1
4	4,06	93	8,08	269	32,8
5	4,12	92	8,21	269	32,3
6	3,95	88	8,23	267	31,2

## Data from Experiment 4

### Raw water

Turbidity (NTU)	Colour (HU)	pH	Conductivity ( $\mu\text{S/cm}$ )	Temperature ( $^{\circ}\text{C}$ )
4,9	106	7,48	108,7	28,2

### Raw water with NaCl

Turbidity (NTU)	Colour (HU)	pH	Conductivity ( $\mu\text{S/cm}$ )	Temperature ( $^{\circ}\text{C}$ )
4,37	105	7,14	171,3	29,7

Results after EF

<b>Hour</b>	<b>Turbidity (NTU)</b>	<b>Colour (HU)</b>	<b>pH</b>	<b>Conductivity (<math>\mu</math>S/cm)</b>	<b>Temperature (<math>^{\circ}</math>C)</b>
1	3,46	77	8,2	141,1	35,2
2	5,7	99	8,05	140,9	35,2
3	3,76	85	8,05	141,6	34,4
4	3,7	88	8,1	142,2	33,6
5	3,62	87	8,1	141,6	32,8
6	3,66	89	8,1	140,6	32,3

Results after integrated process

<b>Hour</b>	<b>Turbidity (NTU)</b>	<b>Colour (HU)</b>	<b>pH</b>	<b>Conductivity (<math>\mu</math>S/cm)</b>	<b>Temperature (<math>^{\circ}</math>C)</b>
1	2,97	69	7,87	136,7	33,4
2	3,25	81	7,99	140,1	33,6
3	3,01	72	8	140,8	33,3
4	2,92	73	8,01	140,5	32,8
5	2,92	77	8,09	140,8	32
6	2,88	80	8,13	141,3	31,2

## Data from experiment 5

Raw water

<b>Turbidity (NTU)</b>	<b>Colour (HU)</b>	<b>pH</b>	<b>Conductivity (<math>\mu\text{S/cm}</math>)</b>	<b>Temperature (<math>^{\circ}\text{C}</math>)</b>
5,2	96	7,82	73,8	26

Raw water with NaCl

<b>Turbidity (NTU)</b>	<b>Colour (HU)</b>	<b>pH</b>	<b>Conductivity (<math>\mu\text{S/cm}</math>)</b>	<b>Temperature (<math>^{\circ}\text{C}</math>)</b>
5,24	99	7,21	281	27,8

Results after EF

<b>Hour</b>	<b>Turbidity (NTU)</b>	<b>Colour (HU)</b>	<b>pH</b>	<b>Conductivity (<math>\mu\text{S/cm}</math>)</b>	<b>Temperature (<math>^{\circ}\text{C}</math>)</b>
1	19	180	9,62	258	30
2	19,6	184	9,8	256	29,6
3	20,2	201	9,78	257	29,1
4	22,2	217	9,96	253	29
5	25,3	242	10,26	251	29,2
6	24	244	10,3	246	29,9

### Results after integrated process

Hour	Turbidity (NTU)	Colour (HU)	pH	Conductivity ( $\mu\text{S/cm}$ )	Temperature ( $^{\circ}\text{C}$ )
1	6,23	64	9,96	251	29,3
2	6,19	72	9,73	249	28,5
3	6,3	79	9,67	246	28,3
4	6,66	77	9,67	243	27,8
5	7,44	90	9,87	241	27,6
6	9,67	116	10,07	233	28,6

### Data from experiment 6

#### Raw water

Turbidity (NTU)	Colour (HU)	pH	Conductivity ( $\mu\text{S/cm}$ )	Temperature ( $^{\circ}\text{C}$ )
4,47	95	7,26	73,5	26,2

#### Raw water with NaCl

Turbidity (NTU)	Colour (HU)	pH	Conductivity ( $\mu\text{S/cm}$ )	Temperature ( $^{\circ}\text{C}$ )
4,21	97	7,08	153,5	26,3

Results after EF

<b>Time (Hour)</b>	<b>Turbidity (NTU)</b>	<b>Colour (HU)</b>	<b>pH</b>	<b>Conductivity (<math>\mu\text{S}/\text{cm}</math>)</b>	<b>Temperature (<math>^{\circ}\text{C}</math>)</b>
1	25,1	158	9,43	138,5	27,4
2	13,9	177	9,14	141,6	27,2
3	15,8	164	9,26	138,6	26,9
4	18,8	188	9,04	137,2	26,3
5	14,5	152	9,02	135,4	27
6	15,4	152	9,18	135,8	27,2

Results after integrated process

<b>Time (Hour)</b>	<b>Turbidity (NTU)</b>	<b>Colour (HU)</b>	<b>pH</b>	<b>Conductivity (<math>\mu\text{S}/\text{cm}</math>)</b>	<b>Temperature (<math>^{\circ}\text{C}</math>)</b>
1	5,13	61	9,03	139,2	27,3
2	4,07	62	9,5	136,4	26,7
3	4,73	65	9,53	137,5	26,5
4	4,43	64	9,36	137,8	26,1
5	4,37	54	9,43	137,2	26,8
6	4,44	54	9,47	136,3	26,6

### Data from Experiment I

Minutes	Turbidity (NTU)	Colour (HU)	pH	Conductivity ( $\mu\text{S}/\text{cm}$ )	Temperature ( $^{\circ}\text{C}$ )
0	4,37	105	7,14	171,3	29,7
30	10,4	121	10,26	165	29,3
60	12,2	144	9,96	154,4	29,8

### Data from Experiment II

Minutes	Turbidity (NTU)	Colour (HU)	pH	Conductivity ( $\mu\text{S}/\text{cm}$ )	Temperature ( $^{\circ}\text{C}$ )
0	4,37	105	7,14	171,3	29,7
25	5,46	103	115,8	5,79	28,1

### Data from experiments on retention time and sample outlet

Without NaCl (outlet 1)

Minutes	Turbidity (NTU)	Colour (HU)	pH	Conductivity ( $\mu\text{S}/\text{cm}$ )	Temperature ( $^{\circ}\text{C}$ )
0	7,61	118	7,37	80,3	29,3
30	11,6	120	10,27	67,9	30,9
60	9,09	81	10,4	70,3	30,9

Without NaCl (outlet 2)

Minutes	Turbidity (NTU)	Colour (HU)	pH	Conductivity ( $\mu\text{S}/\text{cm}$ )	Temperature ( $^{\circ}\text{C}$ )
0	7,61	118	7,37	80,3	29,3
30	12,4	130	10,21	69,8	30,8
60	9,23	85	10,36	68,2	30,5

With NaCl (outlet 1)

<b>Minutes</b>	<b>Turbidity (NTU)</b>	<b>Colour (HU)</b>	<b>pH</b>	<b>Conductivity (<math>\mu</math>S/cm)</b>	<b>Temperature (<math>^{\circ}</math>C)</b>
0	7,61	118	7,37	126,5	29,3
30	17,4	160	10,51	130,6	31,5
60	16	128	10,81	153,5	33,5

With NaCl (outlet 2)

<b>Minutes</b>	<b>Turbidity (NTU)</b>	<b>Colour (HU)</b>	<b>pH</b>	<b>Conductivity (<math>\mu</math>S/cm)</b>	<b>Temperature (<math>^{\circ}</math>C)</b>
0	7,61	118	7,37	126,5	29,3
30	17,9	166	10,61	133,2	32,5
60	19,9	135	10,82	146,4	33,2

## APPENDIX B – Cyanobacteria cell density

	<b>Experiment 1</b>		<b>Experiment 2</b>	
	Cells/ml	Cells/ml	Cells/ml	Cells/ml
Hour	EF	Filtration	EF	Filtration
0	102900	102900	107600	107600
1	19000	21000	62000	50000
2	21500	11700	45500	46200
3	19100	12400	37400	31000
4	18500	12500	32700	25300
5	17000	8200	27100	15100
6	7900	3400	23300	17900

	<b>Experiment 3</b>		<b>Experiment 4</b>	
	Cells/ml	Cells/ml	Cells/ml	Cells/ml
Hour	EF	Filtration	EF	Filtration
0	73600	73600	83700	83700
1	73400	44000	65000	44000
2	63900	48700	67900	56400
3	47000	37200	53800	42000
4	49300	38600	58300	41200
5	42400	48600	33400	23800
6	52500	29200	42200	21400

	<b>Experiment 5</b>		<b>Experiment 6</b>	
	Cells/ml	Cells/ml	Cells/ml	Cells/ml
Hour	EF	Filtration	EF	Filtration
0	66100	66100	53300	53300
1	13900	13100	19300	13600
2	6500	8400	18800	11400
3	6900	4500	17100	8300
4	7200	5200	16900	9700
5	8200	8300	16600	9300
6	7600	3000	15900	5600

---

## **APPENDIX C – Water column height, piezometer and effluent rate**

### Water column height

	<b>Exp.1</b>	<b>Exp..2</b>	<b>Exp.3</b>	<b>Exp.4</b>	<b>Exp.5</b>	<b>Exp.6</b>
Hour	cm	cm	cm	cm	cm	cm
0	0	0	0	0	0	0
1	3,9	2,4	1,1	1,1	7,6	6,3
2	10,1	18,4	1,1	1,1	18,8	14,1
3	16,9	28,8	1,1	1,1	29,7	25,6
4	24,1	28,4	1,1	1,1	33,6	33,1
5	29,1	41,1	1,1	1,1	36,6	41,6
6	34,6	53,8	1,1	1,1	40,6	48,1

### Head loss in piezometer for Experiment 1

	<b>Piezo 2</b>	<b>Piezo 3</b>	<b>Piezo 5</b>
Hour	mWC	mWC	mWC
0	0	0	0
1	0	0	0
2	0	0	0
3	0	0	0
4	0,002	0,004	0,006
5	0,002	0,004	0,007
6	0,003	0,0065	0,0104

### Head loss in piezometer for Experiment 2

	<b>Piezo 2</b>	<b>Piezo 3</b>	<b>Piezo 5</b>
Hour	mWC	mWC	mWC
0	0	0	0
1	0	0	0,001
2	0,002	0,002	0,002
3	0,003	0,005	0,006
4	0,002	0,003	0,003
5	0,004	0,006	0,007
6	0,006	0,008	0,01

---

### Head loss in piezometer for Experiment 3

	<b>Piezo 2</b>	<b>Piezo 3</b>	<b>Piezo 5</b>
Hour	mWC	mWC	mWC
0	0	0	0
1	0,001	0,001	0,001
2	0,001	0,001	0,001
3	0,001	0,001	0,001
4	0,001	0,001	0,001
5	0,001	0,001	0,001
6	0,001	0,001	0,001

---

#### Head loss in piezometer for Experiment 4

	<b>Piezo 2</b>	<b>Piezo 3</b>	<b>Piezo 5</b>
Hour	mWC	mWC	mWC
0	0	0	0
1	0	0	0
2	0,001	0,001	0,001
3	0,001	0,001	0,001
4	0,001	0,001	0,001
5	0,001	0,001	0,001
6	0,001	0,001	0,001

---

#### Head loss in piezometer for Experiment 5

	<b>Piezo 2</b>	<b>Piezo 3</b>	<b>Piezo 5</b>
Hour	mWC	mWC	mWC
0	0	0	0
1	0,002	0,002	0,002
2	0,002	0,002	0,003
3	0,004	0,006	0,008
4	0,004	0,006	0,008
5	0,003	0,011	0,013
6	0,004	0,012	0,014

---

### Head loss in piezometer for Experiment 6

	<b>Piezo 2</b>	<b>Piezo 3</b>	<b>Piezo 5</b>
Hour	mWC	mWC	mWC
0	0	0	0
1	0,001	0,001	0,001
2	0,001	0,001	0,001
3	0,001	0,003	0,005
4	0,001	0,006	0,01
5	0,002	0,009	0,015
6	0,003	0,017	0,027

### Effluent rates

	<b>Exp.1</b>	<b>Exp..2</b>	<b>Exp.3</b>	<b>Exp.4</b>	<b>Exp.5</b>	<b>Exp.6</b>
Hour	ml/s	ml/s	ml/s	ml/s	ml/s	ml/s
1	6,0	4,7	6,3	6,3	8,5	8,6
2	6,0	4,7	6,3	6,3	8,6	8,7
3	5,8	4,8	6,3	6,3	8,7	8,7
4	5,7	4,5	6,3	6,3	8,3	8,5
5	5,3	4,1	6,3	6,3	7,5	8,3
6	5,3	4,1	6,3	6,3	5,2	8,5

## APPENDIX D – Backwash turbidity

Backwash turbidity

	Exp.1	Exp..2	Exp.3	Exp.4	Exp.5	Exp.6
Minutes	NTU	NTU	NTU	NTU	NTU	NTU
0	128	44,2	6,96	4,13	70,9	25
1	16,7	6,07	20,8	24,3	53,1	21,9
2	5,71	6,82	6,53	8,77	20,1	4,19
3	4,85	2,27	5,65	3,85	3,17	2,11
4	4,46	3,03	4,54	3,57	4,99	2,47
5	4,36	3,61	3,57	3,14	3,73	2,58
6	3,79	2,98	4,14	3,22	4,33	2,28
7	3,84	2,81	4,07	3,23	3,69	2,27
8	4,67	3,39	3,85	2,9	4,18	2,61
9	4,08	2,13	4,01	2,99	3,75	2,33
10	4,95	2,08	3,97	3	3,18	2,4